SEISMIC RESISTANCE OF A HYBRID SHEARWALL SYSTEM

Vom Fachbereich 13 - Bauingenieurwesen
der Technischen Universität Darmstadt
zur Erlangung der Würde eines
Doktor Ingenieurs
(Dr.-Ing.)

genehmigte
DISSERTATION

vorgelegt von
N. Mohammad Shirali (M. Sc.)
aus Bander-e-turkman, Iran

Darmstadt 2002
D 17

Referent: Prof. Dr.–Ing. Jörg Lange
Korreferent: Prof. Ir. Jack G. Bouwkamp

Tag der Einreichung: 15.03.2002
Tag der mündlichen Prüfung: 29.05.2002

ABSTRACT

SEISMIC RESISTANCE OF A HYBRID SHEARWALL SYSTEM

Shirali, N. Mohammad, Ph. D. in Structural Engineering, May, 2002, 125 Pages

Keywords: Hybrid structure, Shear wall , Earthquake design, Interface connection, Shear strength, Cyclic loads, Finite element method, Nonlinear response, Concrete, Steel, Composite

Earthquake design of buildings involves the creation of a structural system capable of resisting the seismic forces in a ductile manner. Postearthquake observations have shown that the failure of many reinforced concrete buildings has been due to the inability of the lower-story columns to resist the earthquake imposed loads. Failure of these members are often related to an inappropriate layout of the reinforcement in the upper and lower regions of these columns (insufficient column-tie sizing and spacing, leading to tie failure as well as buckling of the longitudinal reinforcement). Considering these observations, a new hybrid structural system for both moment resistant frame and shearwall buildings, which was proposed by Bouwkamp 1990, has since been studied at the Darmstadt University of Technology. The system involves the use of prefabricated composite columns consisting of steel tubular thin-walled sections filled with concrete and typical reinforced concrete beam-slab floors. In case of shear walls, the composite columns are used as edge members of the concrete shear walls. In principle, the steel tubular column section replaces effectively the longitudinal column reinforcement and provides the confinement for the (core) concrete.

Realizing that the connection between the composite columns and concrete beam-slab floor as well as between the shear-wall edge members and concrete wall are critical, the connection design at the interface of the different elements has been a major subject of study. Earlier research on the design and seismic response of hybrid moment resistant frames have shown that this system can be used effectively for the aseismic design of ductile moment resistant frames. The present study has focussed on the use of this system for shear wall type buildings.

Ten alternative interface designs, reflecting a one-third scale model of the edge region of the first story shear wall of an 8-story building, have been developed and tested. The model shear wall was designed with a double-layered 10 x 10 cm mesh having ϕ 8 mm bars vertically and ϕ 6mm bars horizontally. Horizontal anchor bars between composite column and concrete wall extended through holes in the steel column section, were spaced at 10 cm o.c. and directly connected to the wall reinforcement. Also, an interface arrangement with inclined (45-degree) anchor bars as well as headed shear studs welded to the steel tube section were investigated. All specimen were tested under cyclic alternating displacement-controlled loads.

Main results in terms of force-displacement, shear force- shear distortion and force-slip relation are presented and discussed.

A non-linear FE computer program, ANSYS 5.7 has been used to study the inelastic cyclic response under shear of the different interface connections (IFC) tested. Two models have been developed to capture the interface behavior between edge column and RC wall panel. Firstly, a model with non-linear springs, interconnecting the common interface nodal points of the wall panel and steel tube have been introduced. The non-linear spring-characteristics were taken from the empirically derived mechanical model idealising the force-slip relationship at the interface. Secondly, a simple truss-like model capable of capturing the interface behavior has been derived. A comparison between experimental and numerical results show an excellent agreement and clearly support the validity of the both models developed in this study for predicting the non-linear response of the hybrid shear wall system under earthquake load conditions.

KURZFASSUNG

HYBRIDES SCHUBWAND SYSTEM ZUR ANWENDUNG IN ERDBEBENGEBIETEN

Shirali, N. Mohammad, Dr.-Ing. in Bauingenieurwesen, Mai, 2002, 125 Seite

Schlüsselwörter: Hybrides Tragwerk, Schubwand, Erdbebenbemessung, Anschlussbereich, Schubkapazität, Zyklischenbelastung, Finite Elemente Methode, Nichtlineare Verhalten, Beton, Stahl, Verbund

Die Erdbebenbemessung eines Gebäudes bezieht die Konstruktion einer Bauwerksstruktur ein, die seismischen Kräften in einer duktilen Weise widerstehen kann. Nachbebenuntersuchungen haben gezeigt, dass Einstürze häufig durch Versagen der Stützen in den unteren Geschossen des Stahlbetonrahmens verursacht wurden. Weiterhin sind lokale Schäden an Randstützen in Stahlbetonschubwänden bemerkt worden. Ursache dafür ist hauptsächlich mangelnde Umschnürung des Betonkernes (Abstand) und das Knicken der Längsbewehrung, wie auch mangelhafte Qualitätsüberwachung und Baustelleninspektion.

In Betracht dieser Schadensbeobachtungen, um den Erdbebenwiderstand von Stahlbetonschubwänden und Stahlbetonrahmen zu verbessern, wurde, ein neues hybrides System für die oben genannten Systeme von Bouwkamp 1990 vorgeschlagen. Diese Systeme wurden seitdem an der Technische Universität Darmstadt experimentell untersucht. Dieses hybride Systeme wird durch betongefüllte rechteckige Stahlhohlprofile als Verbundstützen gekennzeichnet, welche die volle Umschnürung des Betonkernes und der Längsbewehrung herstellt. Verbundstützen, gebildet aus ausbetonierten rechteckigen Stahlhohlprofilen, werden in typischer Stahlbauweise erstellt. Der Rest des Gebäudes, insbesondere die Decken werden konventionell hergestellt. Die hybride Schubwand besteht aus Verbundstützen als Randstützen und einer Stahlbetonwand, die miteinander durch eine Anschlussbewehrung verbunden sind. Die Kombination von Beton und Stahlhohlprofil und die volle Umschnürung des Kernbetons durch das Stahlhohlprofil erhöht die Tragfähigkeit, die Steifigkeit und die Duktilität der Verbundrandstütze im hybriden Schubwandsystem.

Die Schlüsseleigenschaft für die Entwicklung dieses Wandsystems ist das Verhalten der Verbindung zwischen der Verbundrandstütze und dem Stahlbetonpaneel. Eine frühere Forschung auf dem Gebiet der Bemessung des seismischen Verhaltens der hybriden Stahlbetonrahmen hat gezeigt, dass dieses System effektiv für erdbebengefährdete Regionen benutzt werden kann. Die vorliegende Untersuchung hat sich auf den Gebrauch von Hybriden Schubwandsystemen (HSW) und einen wirkungsvollen und ökonomischen Einsatz dieses System in erdbebengefährdeten Gebieten konzentriert.

Zur Entwicklung einer optimalen Entwurfslösung für den Anschluss zwischen der Stahlbetonwand und der Verbundstütze sind zehn alternative Entwürfe entwickelt und getestet worden. Zu diesem Zweck ist ein 8-stöckiges Gebäude mit einer hybriden Schubwand als horizontallasttragendes Element entworfen worden. Als Versuchskörper wurde der Verbindungsteil des ersten Stockwerkes des Schubwandmodells im Maßstab 1:3 angenommen und entworfen. Die Bemessung des ausgewählten Versuchsmodells ergab eine kreuzweise Bewehrung mit 6 mm dicken Horizontalstäben und 8 mm dicken Vertikalstäben auf beiden Seiten (zwei Schichten) der Wandscheiben. Als Parameter wurden der Durchmesser und die Anordnung der Bewehrung untersucht. Es wurden folgende vier verschiedenen Modellvarianten untersucht:

1) Anschlussbewehrungen als durchgesteckte Bewehrung senkrecht zur Verbundfuge
2) durchgesteckte Bewehrung senkrecht zur Verbundfuge mit zusätzlich angeschweißten Kopfbolzen am Stahlhohlprofil
3) durchgesteckte Bewehrung mit 45 Grad Neigung zur Verbundfuge
4) angeschweißte Bewehrung am Stahlhohlprofil senkrecht zur Verbundfuge

Die Versuche wurden statisch-zyklisch, weggesteuert durchgeführt.

Das Verhalten der Versuchskörper wurde in bezug auf Kraft-Verschiebungs-Beziehungen, Kraft-Schub-Verformungs-Beziehungen und Kraft-Schlupf-Beziehungen angegeben und analysiert.

Das nichtlineare FE –Programm ANSYS 5.7 wurde benutzt, um zyklisches nichtlineares Verhalten der unterschiedlichen Anschlusslösungen unter zyklischer Schublast zu untersuchen. Zwei Modelle wurde entwickelt, um das Verhalten des Anschlusses zwischen den Randstützen und dem Stahlbetonpaneel zu prüfen. Erst wurde ein Modell mit nichtlinearen Federn im Anschlussbereich abgebildet. Die nichtlinearen Feder-Eigenschaften wurden aus einem mechanischen Modell für eine idealisierte Kraft-Schlupf-Beziehung, die aus experimentellen Ergebnissen abgeleitet wurde, entwickelt. Als zweites wurde ein einfaches Fachwerk Modell verwendet, dass in der Lage ist, das Anschlussverhalten abzubilden. Ein Vergleich zwischen den experimentellen und numerischen Resultaten zeigt eine ausgezeichnete Übereinstimmung und bestätigt deutlich die Gültigkeit der beiden Modelle, die in dieser Studie für die Voraussagen des nichtlinearen Verhaltens des hybriden Schubwandsystems unter Erdbebenbelastung verwendet wurde.

ACKNOWLEDGEMENTS

The work described in this thesis was carried out during my research assistantship in the Institute of Steel Construction and Fracture Mechanics at Darmstadt University of Technology under supervision of Prof. Dr.-Ing. Jörg Lange and Prof. Ir. Jack G. Bouwkamp.

The author wishes to express his sincere thanks to Prof. Ir. Jack G. Bouwkamp for his invaluable comments and extensive critical discussions and suggestions throughout the research work.

The author would like also to express his sincere thanks to Prof. Dr.-Ing. Jörg Lange for his guidance, encouragement, critical suggesstions and his painstaking reading of the manuscript during this work. His invaluable support are greatly appreciated.

Acknowledgements are also due to Prof. Dr.-Ing. Eckehard Fehling from University of Gesamthochschule Kassel for his helpful discussion and invaluable support during all the stages of the work.

Sincere thanks are also due to Prof. Dr.-Ing T. Seeger, head of Material Mechanics Laboratory at Darmstadt University of Technology, for his readiness to help and his assistance. Sincere thanks are also due to Dr.-Ing. habil U. Akbay for his interest.

The efforts of all colleagues, laboratory and administrative staff members of the Institute of steel construction are greatly appreciated. Especially, I would like to thank Dr.-Ing. Almut Suppes and Mrs. Hedy Lang for their help and encouragement during this work.

My deepest gratitude goes to my family and friends who have always encouraged and supported me throughout my education.

N. M. Shirali

TABEL OF CONTENTS

LIST OF FIGURES

LIST OF TABLES

NOTATIONS

Latin upper case symbols

A	Cross-section area
A_a	Cross sectional areas of the structural steel
A_c	Gross cross-sectional area of concrete
A_e	Minimum cross sectional area in any horizontal plane of a structural wall in the first story of a structural wall
A_i	Effective cross sectional area in any horizontal plane in the first story of a structural wall
A_s	Cross sectional areas of the reinforcement
A_{vf}	Shear-friction reinforcement across the shear plane
E_a	Modulus of elasticity of the structural steel
E_c	Modulus of elasticity of the concrete
E_s	Modulus of elasticity of the reinforcement
$\overline{F}$	Normalized force value
F_b	Seismic base shear force
F_R	Experimental reference force value
F_t	Top floor load
F_x, F_i, F_n	Lateral force applied at level x, i or n
G	Shear modulus
H	Total height of the building
H_w	Height of a wall
I	Occupancy importance factor
I_1	First invariant of the stress tensor, σ_{ij}
I_a	Moments of the inertia of the cross sectional areas of the structural steel
I_c	Moments of the inertia of the cross sectional areas of the concrete
I_s	Moments of the inertia of the cross sectional areas of the reinforcement
J_2 , J_3	Second and third invariants of the deviatoric stress tensor, s_{ij}

K	Experimental initial stiffness for the straight and diagonal-bar reinforcing arrangements
K_{d1} and K_{d2}	Exponents describing the design spectrum for vibration periods greater than T_C and T_D
L	Length
M_{Sd}	Design bending moment at the base of the wall
M_{Rd}	Design flexural resistance at the base of the wall
M_x	Overturning moment at level x of the building
N	Axial force
N	Total number of stories above the base of the building
$N_{pl, Rd}$	Design value of ultimate plastic axial force resistance
N_{Rd}	Design value of axial force resistance
N_{sd}	Design value of acting axial force
Q	Behavior factor
R_w	Nonlinear response modification factor ranging from 4 to 12
S	Subsoil factor (1.0 to 2.0)
$\overline{S}$	Normalized slip value
$S_d(T_1)$	Ordinate of the design spectrum at the fundamental period T_1 of the building
$S_e(T)$	Ordinate of the elastic response spectrum
S_R	Experimental reference slip value
T	Natural period of vibration of the building
T_B, T_C, T_D	Design-spectral parameters
T_1	Fundamental period of vibration of the building
V	Shear force
V_{cd}	Shear resistance of concrete compression zone
V_{dd}	Dowel resistance of bars
V_{fd}	Friction resistance
V_{id}	Shear resistance of inclined bars
$V_{(M_{Rd})}$	Shear force corresponding at the state of the design flexural failure of the critical wall region

Vn	Shear strength
V_{Rd}	Design value of shear resistance
V_{sd}	Design shear force
V'_{Sd}	Shear force obtained from the analysis
V_{wd}	Contribution of the reinforcement to the shear resistance
V_x	Shear force at any story x of the building
W	Total weight of the building
W_j, W_i , W_x	Weight at jth, ith or xth level
Z	Zoning factor for regional seismicity

Latin lower case symbols

b_w	Width of the web of a beam, thickness of the boundary element of a wall
b_{wo}	Thickness of the web of a wall
d_b	Diameter of the reinforcing bar
d_{bh}	Diameter of the horizontal bar
d_{bv}	Diameter of the vertical bar
d_{bw}	Diameter of the hoop reinforcement in beams and columns
d_e	Length of the structural wall in the first story oriented parallel to the applied forces
f	Strength of a material
f_1	High compressive stress point on the compressive meridian
f_2	High compressive stress point on the tensile meridian
f_{bc}	Biaxial compressive strength
f_c	Unaxial compresive strength
f_{cd}	Design value of concrete compressive strength
f_{ck}	Characteristic strength for concrete
f_t	Tensile strength of the reinforcement

f_t	Uniaxial tensile strength
f_y	Yield stress of the steel
f_{yd}	Design value of yield stress of the steel
f_{yk}	Characteristic value of yield stress of the steel
$f_{yd,h}$	Design yield strength of the horizontal web reinforcement
$f_{yd,v}$	Design value of the yield strength of the vertical web reinforcement
h	Height, depth
h_c	Width of a column in the direction of a beam framing into the column
h_{cr}	Critical height of a reinforced concrete wall
h_N	Total height of the building in feet
h_s	Clear storey height
h_w	Depth of a beam
h_x, h_i , h_n	Height above ground of the levels x, i or n
k	Coefficient, factor
l	Length
l_b	Anchorage length of reinforcement
l_c	Length of a wall area with confining reinforcement
l_{cr}	Length of a critical region
l_w	Length of a wall
l_{wi}	Length of the structural wall in the first story in the direction parallel to the applied forces
q	Behavior factor
r_c	Compressive meridians
r_t	Tensile meridians
s	Local sub-soil condition
s_h	Spacing of horizontal web reinforcement in a wall
s_v	Spacing of vertical web reinforcement in a wall
t	Thickness
z	Lever arm of internal forces
z_j, z_i	Heights of masses above level of application

Greek symbols

α	Angle, coefficient, factor, ratio
α	Ratio of the peak ground acceleration to the acceleration of gravity
α_s	Shear ratio
β_0	Spectral acceleration amplification factor for 5 % viscous damping
ε	Strain, coefficient, factor
ε	Magnification factor depending on the ductility class
ε_C	Compressive strain in the concrete
ε_s	Tensile strain in the steel
δ_I	Floor displacements due to a set of lateral forces f_i at floor levels i=1,2,...., N in an N-story building
$f(\xi, r, \theta)$	Haigh-Westergaard stress space
γ	Partial safety factor
γ	Unit weight of the concrete
γ_{Rd}	Design value of the over strength ratio of steel
γ_{Rd}	Global factor
λ	Factor accounting for the available shear resistance of plain concrete after cyclic degradation in a beam-column joint
μ	Coefficient of the friction
ν	Poisson's ratio
ρ	Reinforcement ratio
ρ_h	Reinforcement ratio of the horizontal web bars
ρ_v	Reinforcement ratio of the vertical web bars
τ	Shear stress
τ_{Rd}	Basic design shear strength of members
σ	Moments reversal factor used in capacity design
$\sigma_1, \sigma_2, \sigma_3$	Principle stresses

1 INTRODUCTION

1.1 General

The subject of earthquake resistance design of structures has a long history. Hence, it has been recognized that to design a safe and economic structure in seismic regions, the structural engineer needs to use to select an appropriate structural system. In multi-story buildings, reinforced concrete (RC) structural walls provide an efficient bracing system against lateral forces. Buildings with shearwalls perform favorably in comparison with more flexible framed structures as far as damage to non-structural elements is concerned.

Recognizing the usefulness of structural walls, many experimental and analytical studies have been carried out worldwide during the past four decades to better understand the seismic behavior of these walls. As a result, substantial advances in the seismic design of RC structural walls have been achieved as reflected in current codes. Postearthquake investigations, however, have shown that significant damage has still occurred in RC buildings, primarily due to poor design details or / and construction. Damage to shear walls occurred often in the edge columns (flanges) of such walls due to a lack of confinement of the concrete core and buckling of the longitudinal steel in these edge elements.

In order to improve the earthquake resistance of such RC shear wall buildings, a new hybrid structural-wall system has been proposed and studied at the Darmstadt University of Technology (TUD). This system is characterized by concrete-filled square or rectangular steel tubes serving as composite edge-member columns and a typical concrete shear wall. The tubular steel sections provide full confinement of the core concrete and longitudinal column reinforcing steel and allow deleting the typical, but often inadequate, stirrup reinforcement. The use of steel sections with filled-in concrete will improve the performance (ductile behavior) of the edge members. In hybrid shearwalls with well-confined boundary elements, some amount of web damage can occur without necessarily limiting the flexural

capacity of the wall. The present research covers the development of an experimental test program and the evaluation of the experimental findings. Recommendations for an effective and economic design of hybrid shearwall systems (HSW), suitable for use in regions of high-seismic risk, have been presented. A significant aspect of the hybrid wall system is the design and performance of the interface connection reinforcement between the composite edge member column and concrete wall.

The composite columns made of concrete filled steel tubes (CFST), are erected in a typical steel construction manner. These concrete filled columns are prefabricated with the interface-connection reinforcement for the walls, or possibly the beams, extended through holes in the steel tubular walls. Typically, the girders and slab system are formed and constructed as a typical reinforced concrete floor system. Also, the use of steel beams connected to the composite concrete-filled steel columns, together with a composite slab could be an alternative. The composite columns can be fabricated in segments with nominal lengths of 1 ½ or 2 ½ stories for the first- and upper- floor regions. At intermediate floor levels the prefabricated columns could typically have a length of 2 stories.

In the fabrication/construction process, holes for the interface connection reinforcement, are drilled first in the tubular column wall. The necessary reinforcement is then placed before casting of the concrete. First, if necessary, a steel reinforcement cage will be placed inside the hollow column section. Then, the interface connection reinforcement to connect the edge column to the RC wall panel or beams will be placed through the predrilled holes. As an alternative interface connection, shear studs used in combination with the reinforcing bars could be welded to the wall of the tubular steel column. Finally, the concrete will be poured to fill the column section. The fabrication process can be carried out on-site or in a construction yard.

1.2 Objectives

The main objective of this research program was aimed at evaluating experimentally the cyclic force – slip behavior at the interface connection under cyclic displacement controlled load reversals and to predict analytically the nonlinear static and dynamic response of such hybrid shear walls under earthquake loading.

Accordingly, an experimental program for testing 1/3-scale hybrid shearwall specimens was undertaken to obtain information on the behavior of the interface connection reinforcement (IFCR) between the RC wall panel and edge members. Different design solutions were studied to develop an optimal interface connection (IFC).

Secondly, considering various solutions, an idealized numerical model of the composite system, capable of predicting the cyclic force-slip behavior of the interface connection, has been developed and its accuracy assessed in comparison with the experimental test data.

1.3 Scope

In order to assess the seismic behavior of the various IFCR layouts between tube and wall panel, ten 1/3-scale wall elements with one-sided composite steel-tube columns (edge members) have been studied under cyclic displacement controlled loads. The specimens studied, represented a part of a 1/3-scale hybrid shearwall of a hybrid building system.

This report is divided into eight chapters. The opening chapter addresses the usefulness of structural shear walls as lateral load resisting elements for buildings in seismic zones and gives a brief description of the proposed hybrid wall system.

The second chapter describes both the principle aspects of RC shearwall design, as given in two codes, namely, the European Seismic Code 8 (EC8) and the USA Uniform Building Code (UBC-94), and the design considerations of the hybrid structural wall members. Also, the design of the composite tubular steel section filled with concrete, as a boundary

element of the hybrid shear wall, is briefly discussed. The seismic design of a 8-story high, hybrid shearwall structure is presented. The structure has been designed in detail using simplified equivalent static lateral-load analysis procedures as defined in the EC8 and UBC94 code provisions. In this process, code-defined approximate fundamental periods and appropriate earthquake design spectra have been used, to determine the seismic base shear force and the lateral force distribution over the height of the building.

In the third chapter, the experimental program has been described. The design and construction of the test specimens and details of the wall reinforcements and interface connections are presented. Material properties, test procedures and the instrumentation layout are given.

The experimental results are presented in chapter 4. In particular, the overall force – displacement, the shear force - shear distortion behavior of the different test specimens and the force – slip relationship at the interface between the composite edge column and shear wall are given and discussed.

Considering the experimental results presented in chapter 4, chapter 5 covers the development of an idealized nonlinear force – slip relationship of the interface connection for subsequent correlative studies (chapter 7).

A nonlinear FE computer program has been used in chapter 6 to evaluate the overall cyclic response of the hybrid shear walls for different interface connections (IFC) of the hybrid shear wall system. Nonlinear material models for both reinforcing steel and concrete that are capable of reproducing the hysteretic response of the hybrid shear wall are presented.

In chapter 7, the accuracy of the mathematical model to predict the cyclic nonlinear behavior of the hybrid shear walls, with both straight and inclined interface reinforcement, has been assessed by comparing the analytical results with the experimental force-slip results of the test specimens.

Finally, chapter 8 covers the summary, conclusions and recommendations for further research and design improvement.

2 SEISMIC DESIGN OF HYBRID SHEARWALL

2.1 General

Structural codes are legal documents which provide guidelines for the design, detailing and construction of structures. Field observations in addition to experimental and analytical research have been the main source in the development of seismic code requirements. Code provisions can be seen as a minimum demand for structures with a more or less conventional and regular configuration. Most seismic building codes permit the determination of the design lateral forces using either a static lateral force procedure or a dynamic force analysis method.

Worldwide, the simple equivalent lateral force method combined with the capacity design concept is the most commonly used method to evaluate the earthquake design forces. For the preliminary seismic design of a prototype building used in this study, the simple static lateral force procedures defined in the European and US Seismic codes (respectively the 1998 Eurocode 8 and the 1994 Uniform Building Code), have been used. The use of these codes is justified as the prototype structure is regular in layout as defined in the both codes. These two seismic design codes are used in order to show the current design method practiced in Europe and the USA. A brief description of the principal requirements of each code with respect to the seismic design of RC shear walls have been summarized. An eight story prototype building with hybrid shearwalls to resist the horizontally induced seismic loads has been designed according to Eurocode 8. A comparison with UBC code requirements is presented.

2.2 Design considerations

Basically, the two codes reflect a design philosophy by which the structures should be able to resist minor earthquakes without damage, moderate earthquakes without structural damage but possibly with some nonstructural damage, and major earthquakes without collapse but with both structural and nonstructural damage. The basic reason to permit substantial

building damage under major earthquake exposure lies in the high construction cost of a structure designed to resist seismic forces without damage.

As current codes have not yet codified design procedures for the proposed hybrid wall system, procedures specified for RC shear walls have been used. For the design of the composite edge members, design rules for composite columns have to be followed. The interface connection reinforcement, necessary to develop a monolithic hybrid wall system, is designed in accordance with the shear friction design concept given in Eurocode 8 [18] and UBC 94 [44].

These codes involve the following procedures for the design of the building:

1. Determination of the base shear force considering the seismicity zone, the earthquake design spectrum and fundamental period of vibration of the building and the structural system ductility.
2. Determination of the dynamic forces over the height of the building by assuming a basically triangular distribution of the base shear force.
3. Analyse the member forces of the building combining both vertical gravity loads and horizontal forces.
4. Proportioning and detailing of the members and connections considering critical member-force combinations.

In this study the hybrid shear wall is designed as a RC panel with composite edge member columns. In order to achieve a monolithic behavior of the hybrid walls, different interface connection designs between the boundary columns and concrete shear wall have been developed and tested as part of this study. The interface connection detailing is based on the shear friction design method. It is assumed that all forces at the interface connection are carried by the concrete reinforcing bars or/and other connectors (shear studs).

In the following sections, a summary of the shear wall design requirements using the EC2 [19], EC4 [17] and EC8 [18] codes are presented.

2.3 Design procedure according to Eurocode

Eurocode 8 is an European seismic code issued by the Commission of the European Communities for the design and construction of buildings in seismic regions. The general purpose of the code is to protect human lives and limit structural damages under earthquakes. The capacity design criteria based on the ultimate limit state of structural systems and the serviceability limit state of such systems are considered in this code. EC8 classifies two distinct types of failure for RC walls, namely, flexural and shear failure. The behavior factor to be used in the analysis procedure reflects the expected ductility of the system as reflected by the anticipated type of failure. Based on these failure modes, design expressions are given. A brief description of the design procedures for shear wall is listed in the following sections.

2.3.1 Determination of base shear force

The seismic base shear force F_b is defined as:

$$F_b = S_d(T_1) \cdot W \qquad 2.1$$

where, S_d (T_1) is the ordinate of the design spectrum at the fundamental period T_1 of the building and W is the total weight of the building.

Design spectrum S_d (T), as based on the elastic response spectrum shown in Figure 2.1, is normalized by the acceleration of the gravity, and is defined by the following expressions:

$$0 \le T \le T_B: \qquad S_d(T) = \alpha \cdot s \cdot \left[1 + \frac{T}{T_B} \cdot \left(\frac{\beta_0}{q} - 1\right)\right] \qquad 2.2$$

$$T_B \le T \le T_C: \qquad S_d(T) = \alpha \cdot s \cdot \frac{\beta_0}{q} \qquad 2.3$$

$$T_C \le T \le T_D: \qquad S_d(T) = \alpha \cdot s \cdot \frac{\beta_0}{q}\left[\frac{T_C}{T}\right]^{K_{d1}} \quad \text{or} \quad S_d(T) \ge 0.20\alpha \qquad 2.4$$

$$T_D \le T: \qquad S_d(T) = \alpha \cdot s \cdot \frac{\beta_0}{q}\left[\frac{T_C}{T}\right]^{K_{d1}} \cdot \left[\frac{T_D}{T}\right]^{K_{d2}} \quad \text{or} \quad S_d(T) \ge 0.20\alpha \qquad 2.5$$

where, α is the ratio of the peak ground acceleration to the acceleration of gravity ($\alpha = a_g/g$) ,

s local sub-soil condition,

T_B, T_C, T_D design-spectral parameters,

K_{d1} and K_{d2} are exponents describing the design spectrum for vibration Periods greater than T_C and T_D, respectively – see Table 2.1,

β_0 is the spectral acceleration amplification factor for 5 % viscous damping and

q behavior factor.

The specific values of the several parameters pertinent to the different sub-soil classes are shown in Table 2.1.

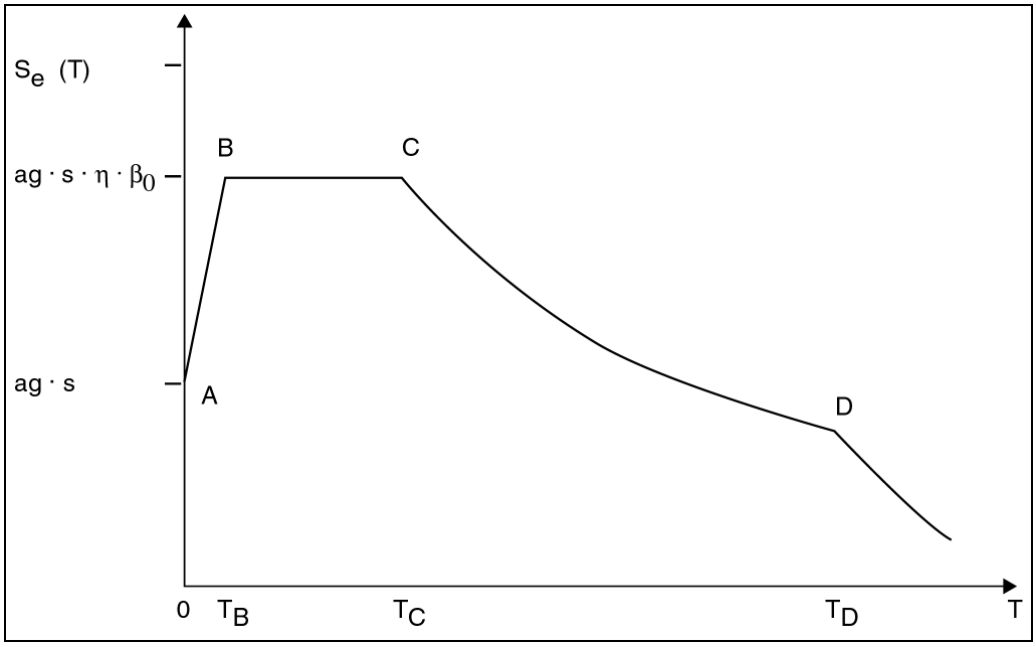

Figure 2.1: Elastic response spectrum

Table 2.1: Values of the parameters defining the design spectrum

Sub-soil class	S	β_0	K_1	K_2	T_B	T_C	T_D	K_{d1}	K_{d2}
A	1.0	2.5	1.0	2.0	0.10	0.40	3.0	2/3	5/3
B	1.0	2.5	1.0	2.0	0.15	0.60	3.0	2/3	5/3
C	0.9	2.5	1.0	2.0	0.20	0.80	3.0	2/3	5/3

The natural period of vibration of the building, T, can be approximated by:

$$T = C_t \left[H^{3/4}\right] \qquad 2.6$$

where, H is the total height of the building in meters and

C_t for a building with RC structural walls is 0.05 or, alternatively $0.075 / \sqrt{A_c}$, with A_C being $= \sum A_i \left[0.2 + (l_{wi} / H)^2\right]$, where A_i is the effective cross sectional area in any horizontal plane in the first story of a structural wall and

l_{wi} the length of the structural wall in the first story in the direction parallel to the applied forces.

Alternatively, the period of the structure may be determined from Rayleigh's formula as

$$T = 2\,\pi \sqrt{\sum_{i=1}^{N} W_i \delta_i^2 / g \sum_{i=1}^{N} f_i \delta_i} \qquad 2.7$$

Where the W_i is the weight at the ith level , and δ_i are the floor displacements due to a set of lateral forces f_i at floor levels i=1,2,....,N in an N-story building.

2.3.2 **Distribution of the base shear force**

The base shear force determined from eq. 2.1 is distributed vertically as a set of lateral forces Fi at any floor level i of the building in accordance with the following formula (2.8). The resulting lateral force distribution along the height of the building is triangular in form, linearly increasing from the base, and corresponds approximately to the dynamic forces under the fundamental mode response.

$$Fi = F_b \cdot \frac{W_i z_i}{\sum_{j=1}^{N} W_j z_j} \qquad 2.8$$

Where

F_b = base shear

N = total number of stories above the base of the building

F_i = lateral force applied at level i

z_j, z_i = heights of masses above level of application

W_j, W_i = mass at jth or ith level

2.3.3 **Analysis of the structure**

The shear force V_x at any story x is given by the following formula as the sum of the lateral seismic forces above the specified story, namely,

$$V_x = \sum_{i=x+1}^{N} F_i \qquad 2.9$$

Consequently, the overturning moment M_x at level x of the building is given by

$$M_x = \sum_{i=x+1}^{N} F_i (z_i - z_x) \qquad 2.10$$

2.3.4 **Design requirements of hybrid shear wall**

The design of earthquake resistant hybrid shear walls is aimed at providing a structural system with adequate energy dissipation and a sustained capacity to resist both horizontal and vertical loads. In general, the designer needs to know the maximum possible shear and moment values which can be expected considering the pattern of seismic forces. The designer should be able to determine the shear and flexural capacities in the critical wall regions in order to predict, given the different load combinations, if either flexural or shear failure can be expected. In order to develop a ductile system, it is desired to provide structural walls with a shear capacity greater than the maximum shear associated with the available moment capacity. Hence, the wall design may call for a shear load capacity twice as large as the shear force related directly with the flexural capacity of the walls.

The different design provisions in EC8 for RC slender and squat walls consider the different modes of failures as reflected in the different "ductility classes" used in earthquake resistant concrete design. Slender walls are defined as walls with a height to length ratio greater than 2 and squat walls as walls with a corresponding ratio less than or equal to 2. The basic two types of the failure, namely, flexural failure and shear failure are shown in Figure 2.2.

Depending on the intended hysteretic energy dissipating capacity of concrete shear walls, three ductility classes (DC), namely, low, medium and high can be selected. This selection affects both the overall dynamic forces as reflected by the base shear force F_b – which is influenced by the behavior factor q – and the detailed design requirements associated with the different "ductility classes". In the following sections, design procedures for RC walls and composite columns are summarized.

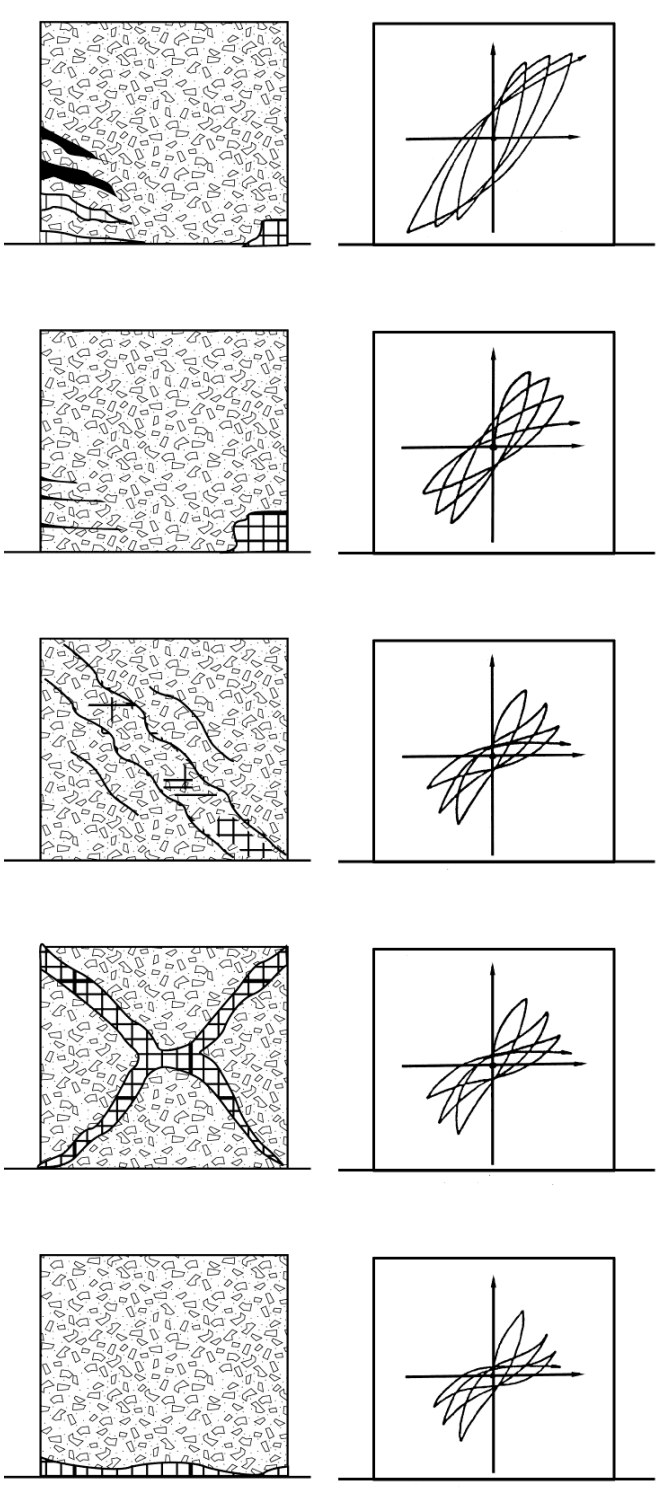

Failure mode
Flexural, ductile
Flexural, brittle
Shear, web diagonal failure in compression
Shear, web diagonal failure in tension
Shear, horizontal sliding

Figure 2.2: Failure modes of the RC wall with expected response

2.3.4.1 **Design of the wall panel**

For slender walls, with the typical flexural mode of failure, the design shear force V_{sd} can be expressed as:

$$V_{Sd} = \varepsilon \cdot V'_{Sd} \qquad 2.11$$

Where, V'_{Sd} is the shear force obtained from the analysis, and

ε is the magnification factor depending on the ductility class and calculated as:

$$\varepsilon = q \cdot \sqrt{(\frac{\gamma_{Rd}}{q} \cdot \frac{M_{rd}}{M_{Sd}}) + 0.1(\frac{S_e(T_c)}{S_e(T_1)})^2} \leq q \qquad 2.12$$

Where, γ_{Rd} is a global factor, intended to counterbalance the chosen partial safety factor of steel and to cover partial hardening effects as well as uncertainties of the models involved; it may taken equal to 1.25 in case of a high ductility class design,

M_{Sd} is the design bending moment at the base of the wall,

M_{Rd} is the design flexural resistance at the base of the wall,

$S_e(T)$ is the ordinate of the elastic response spectrum,

T_1 is the fundamental period of vibration of the building,

T_c is the upper limit period of the constant spectral acceleration branch, and

q is the behavior factor.

For squat walls, which typically fail in shear, there is no need to consider a dynamic amplification which would modify the wall bending moments and shear forces obtained from the analysis. However, because the energy-dissipation capacity of a shear failure mode in squat walls is not well defined, the design requirement calls for an increase in the shear force obtained from the force analysis, namely,

$$V_{Sd} = \gamma_{Rd} \cdot (M_{Rd} / M_{Sd}) \cdot V'_{Sd} \quad \leq q \cdot V'_{Sd} \qquad 2.13$$

In general, the distinction between the two types of failure may be made on the basis of the ratio:

$$\upsilon = \frac{V_{Rd}}{\gamma_{Rd} \cdot V_{(M_{Rd})}} \qquad 2.14$$

Where V_{Rd} is the minimum value of the design strength at shear failure mode (diagonal compression, diagonal tension or shear sliding),

$V_{(M_{Rd})}$ is the shear force corresponding at the state of the design flexural failure of the critical wall region,

γ_{Rd} is a global factor expressing the uncertainties of both the models predicting the shear and flexural strength and the shear - ratio value needed in order to translate M_{Rd} into $V_{(MRd)}$ values. For a high ductility class γ_{Rd} can be taken equal to 1.4.

In correspondence to the different anticipated modes of failure, different q-factors can be selected in the force analysis process. In the preliminary design of the wall reinforcement it is necessary to assume a realistic υ-value to assure the intended mode of failure. For slender walls (height-to-length ratio larger than 2.0) designed for ductility classes H (high) or M (medium) and intended to experience a flexural mode of failure, a υ-value of more than 1.0 should be assumed. In case of squat walls (height-to-length ratio less than 0.75) designed for one of the above ductility classes, a υ-value of less than 0.50 should be assumed if the wall is to experience shear failure. For the walls with height-to-length ratio between 0.75 and 2.0, a υ-value between 0.5 and 1 are assumed with a mixed type of wall failure (flexural and shear failure).

In assessing the potential development of a flexural or shear mode of failure, the reinforcing layout in the “critical” region of the wall should be considered. This region extends

over part of the lower portion of the shear wall with a height of about equal to the length of the wall or 1/6 of the height of the building.

In evaluating the shear capacity of the wall, the shear resistance of both the concrete and reinforcing steel has to be considered for several different modes of failure. For the concrete, both the diagonal compression and tension failure the following inequality should satisfy, namely:

For diagonal compression failure of the web,

$$V_{Sd} \leq V_{Rd2} \qquad 2.15$$

In this expression V_{Rd2} may be calculated:

for the critical region as:

$$V_{Rd2} = 0{,}4 \cdot (0.7 - f_{ck}/200) \cdot f_{cd} \cdot b_{w0} \cdot z \qquad 2.16$$

and for the zone outside of the critical region as:

$$V_{Rd2} = 0{,}5 \cdot (0.7 - f_{ck}/200) \cdot f_{cd} \cdot b_{w0} \cdot z \qquad 2.17$$

where

z is the internal lever arm, which may be taken equal to $0{,}8.l_w$,

b_{w0} is the web thickness of the wall, and

f_{ck} is the characteristic strength for concrete in MPa, but limited to 40 MPa.

For diagonal tension failure of the web,

$$V_{Sd} \leq V_{Rd3} \qquad 2.18$$

In which the shear resistance V_{Rd3} is defined as:

$$V_{Rd3} = V_{cd} + V_{wd} \qquad 2.19$$

where, V_{cd} is the contribution of the concrete, with a distinction made for the critical region with normal tensile or compressive forces and V_{wd} is the contribution of the reinforcement.

As the diagonal tension failure is affected by both the horizontal and vertical reinforcement – acting in a simplified truss model in equilibrium with the concrete providing the diagonal compressive strut elements – the web reinforcing bars together with the concrete should satisfy the following conditions:

- horizontal web reinforcing bars (fully anchored to the wall boundary elements):

$$V_{Sd} \leq \rho_h \cdot f_{yd,h} \cdot b_{w0} \cdot z + V_{cd} \qquad 2.20$$

where,

ρ_h is the reinforcement ratio of the horizontal web bars ($\rho_h = A_h / b_{w0} \cdot s_h$),

$f_{yd,h}$ is the design yield strength of the horizontal web reinforcement,

z is the internal lever arm (c.o.c. distance of boundary elements), and

V_{cd} is the shear resistance due to mechanisms others than axial resistance of the reinforcement and concrete-to-concrete friction.

In case of axial tension in the critical region V_{cd} is equal to zero; in case of axial compression in the critical region :

$$V_{cd} = \tau_{Rd} \cdot (1.2 + 40\rho) \cdot b_{w0} \cdot z \qquad 2.21$$

where, τ_{Rd} is the basic design shear strength, and

ρ the reinforcement ratio ($\rho = A_s / b_{w0}.z$) 2.22

vertical web reinforcement (properly anchored and spliced along the height of the wall):

$$V_{Sd} \leq \rho_v \cdot f_{yd,v} \cdot b_{w0} \cdot z + V_{cd} + \min N_{Sd} \qquad 2.23$$

where,

ρ_v is the reinforcement ratio of the vertical web bars ($\rho_v = A_v / b_{w0}.s_v$),

$f_{yd,v}$ the design value of the yield strength of the vertical web reinforcement, and

N_{sd} the compressive force, taken positive.

As a minimal measure against lateral instability, the thickness b_{w0} of the web should not be less than stipulated in the following:

$$b_{w0} = \min\{150mm; q \cdot l_w / 60; h_s / 20\} \quad 2.24$$

The web reinforcement should form two identical orthogonal grids of bars with the same bond characteristics. The minimum amount of reinforcement in both directions, to prevent premature web shear cracking of the walls, should not be less than $\rho_{h,\min} = \rho_{v,\min} = 0.002$.

The following detailing provisions of the web reinforcement should be taken into account:

Horizontal bars:

$$\rho_h = A_h / b_{w0} \cdot s_h \geq 0.002 \quad 2.25$$

$$d_{bh} \geq 8mm \text{ and } \leq b_{w0} / 8 \quad 2.26$$

$$s_h \leq 20 \cdot d_{bh} \text{ or } 200 \text{ mm} \quad \text{(for walls with high ductility class)} \quad 2.27$$

where, d_{bh} is the diameter of the horizontal bar and s_h is the spacing distance of the horizontal bars.

Vertical bars:

$$\rho_v = A_v / b_{w0} \cdot s_v \geq 0.002 \quad 2.28$$

$$d_{bv} \geq 8mm \text{ and } \leq b_{w0} / 8 \quad 2.29$$

$$s_v \leq 20 \cdot d_{bv} \text{ or } 200 \text{ mm} \quad \text{(for wall with high ductility class)} \quad 2.30$$

where, d_{bv} is the diameter of the vertical bar and s_v is the spacing distance of the vertical bars.

2.3.4.2 **Design of the composite edge column**

Composite columns as boundary elements are designed in accordance to Eurocode 4 and are assumed to carry the total factored vertical loads from gravity and the overturning moment due to the earthquake loads. Axial load strength $N_{pl.Rd}$ of composite rectangular column under compression is:

$$N_{pl.Rd} = A_a f_{yd} + A_c f_{cd} + A_s f_{sd} \qquad 2.31$$

Where

A_a, A_c, A_s are the cross sectional areas of the structural steel, the concrete and the reinforcement, and

f_{yd}, f_{cd}, and f_{sd} are the design strengths of the respective materials.

The design strengths of the materials are obtained by dividing characteristic strength by the corresponding partial safety factors, namely,

$f_{yd} = f_y / \gamma_{Ma}$	for structural steel	γ_{Ma}	= 1.10
$f_{cd} = f_{ck} / \gamma_c$	for concrete	γ_c	= 1.50
$f_{sd} = f_{sk} / \gamma_s$	for reinforcement	γ_s	= 1.15

For columns under tension, the tensile strength of concrete is neglected. Hence, the axial tensile strength of the composite column can be expressed as:

$$N_{pl.Rd} = A_a f_{yd} + A_s f_{sd} \qquad 2.32$$

According to EC 4, the effective flexural stiffness of the composite column may be expressed as the sum of the flexural stiffnesses of the different components, namely,

$$(EI)_e = E_a I_a + 0.8 E_{cd} I_c + E_s I_s \qquad 2.33$$

where, I_a ,I_c ,I_s are, respectively, the moments of the inertia of the cross sectional areas of the structural steel, the concrete (with the area in tension assumed to be uncracked) and the reinforcement,

E_a, E_s are the moduli of elasticity of the structural steel and the reinforce ment, and 0.8 $E_{cd}I_c$ is the effective flexural stiffness of the concrete section with $E_{cd} = E_{cm}$ /1.35, in which E_{cm} is the secant modulus of the concrete.

In order to prevent local buckling of the concrete-filled steel tube, the depth to thickness ratio should satisfy the following expression:

$$h / t \le 52\varepsilon \tag{2.34}$$

where, h is the greater overall dimensions of the section, and

$$\varepsilon = \sqrt{\frac{235}{f_y}} \tag{2.35}$$

2.3.4.3 **Interface connection design**

When shear-friction reinforcement is perpendicular to the shear plane, the shear strength Vn can be computed as,

$$V_n = A_{vf}\, f_y\, \mu \tag{2.36}$$

Where A_{vf} is shear-friction reinforcement across the shear plane, f_y is the yield strength of reinforcement and μ is effectively a coefficient of friction. In case reinforcing steel or headed studs are positioned normal to the shear-friction plane the coefficient of friction is equal to 0.7λ. The factor λ is equal to1.0 for normal weight concrete.

When shear-friction reinforcement is inclined to the shear plane such that the shear force produces tension in shear-friction reinforcement, the shear strength can be computed as,

$$V_n = A_{vf}\, f_y \left(\mu \sin\alpha_1 + \cos\alpha_1\right) \tag{2.37}$$

Where α_1 is the angle between the shear-friction reinforcement and shear plane.

2.4 Design procedure according to UBC 1994

The Uniform Building Code (UBC) is the common building code in the US and covers the design requirements pertinent to the structural safety of buildings. The earthquake resistant design requirements of this code are aimed primarily to safeguard against major structural failures and loss of life. The minimum seismic design forces stipulated by this code are determined in accordance with a seismic-equivalent static lateral force procedure, which has also been incorporated in Eurocode 8. A short summary of the design analysis is given in the following sections.

2.4.1 Determination of base shear force

A critical design quantity in seismic design is the base shear force resulting from the earthquake induced dynamic motion of the building. Reflecting the anticipated earthquake intensity or "effective peak ground acceleration", expressed by a "zoning" factor Z, the "importance" of the building, a spectral coefficient based on the earthquake design spectrum as influenced by the local soil condition, and the expected ductility of the building, the total base shear force can effectively be expressed as a percentage of the building weight, namely,

$$V = \frac{ZIC}{R_W} W \qquad 2.38$$

In which

$$C = \frac{1.25S}{T^{2/3}} \quad \text{but not exceeding } 2.75, \text{ and} \qquad 2.39$$

I the occupancy importance factor (1.00 or 1.25),

S the subsoil factor (1.0 to 2.0),

Z the zoning factor for regional seismicity ranging in value from 0.075 to 0.40,

W the weight of the building and applicable portions of other loads (live loads), and

R_w nonlinear response modification factor ranging from 4 to 12, and

T natural period of vibration of the building, approximated as:

$$T = C_t \left[h_N^{3/4} \right] \qquad 2.40$$

Where,

h_N is the total height of the building in feet, and

C_t = 0.02, or alternatively, for RC walls $C_t = 0.1\sqrt{A_c}$, with A_c calculated as:

$A_c = \sum A_e \left[0.2 + (d_e / h_N)^2 \right]$, where

A_e is the minimum cross sectional area in any horizontal plane of a structural wall in the first story of a structural wall, and

d_e the length of the structural wall in the first story oriented parallel to the applied forces.

Alternatively, the period of the structure may be determined from Rayleigh's formula as given in Eq. 2.7.

2.4.2 **Distribution of the base shear force**

Other than a specified force F_t at the top of the building, reflecting the influence of higher modes of vibration of the building under seismic ground excitation, the total remaining total force ($V - F_t$) is distributed vertically as dynamic loads F_x any level (x) of the building in accordance with the following formula. The resulting distribution along the height of the building reflects basically the response of the building according to the fundamental mode.

$$F_x = \frac{(V - F_t)W_x h_x}{\sum_{i=1}^{N} W_i h_i} \qquad 2.41$$

Where, F_t is the top floor load, with Ft = 0 for T ≤ 0.7 Sec, or

$F_t = 0.07.T.V < 0.25\ V$ for T > 0.7 Sec,

V	base shear
N	total number of stories above the base of the building
F_x, F_i, F_n	lateral force applied at level x, i or n
h_x, h_i , h_n	height above ground of the levels x, i or n, and
W_x, W_i	weight of the mass at xth or ith level

2.4.3 **Analysis of the structure**

The shear force V_x at any story x is given by the following formula as the sum of the lateral seismic forces above that story, namely,

$$V_x = F_t + \sum_{i=x}^{N} F_i \qquad 2.42$$

Consequently, the overturning moment M_x at level x of the building is given by

$$M_x = F_t (h_n - h_x) + \sum_{i=x}^{N} F_i (h_i - h_x) \qquad 2.43$$

Story drift or interstory displacement shall not exceed $0.04/R_w$ times the story height, nor 0.005 times the story height for the building less than 65 ft. Drift leads to second-order effects, and is the main source of both human discomfort under normal service conditions and non-structural damages under earthquake conditions.

2.5 Building description

A 6-bay by 4-bay, 8-storey high hybrid shearwall building with rectangular floor plan dimensions of 36 m by 20 m and a height of 28 m has been designed to resist both gravity and earthquake loads. The building – designed as an office building - has a typical storey height of 3.5 m, except for the first floor which has a height of 4.5 m. While the vertical loads are assumed to be carried by the columns, the lateral loads are resisted by four parallel hybrid shear walls placed parallel to each of the principal directions. The walls in the longitudinal direction of the building are 6 m long and 28 m high with a thickness of 0.25 m; in transverse direction the walls are 5 m long and 28 m high and have a thickness of 0.30 m. The building is symmetric in both directions, thus minimizing unfavourable torsional effects which can be developed during an earthquake. Wall aspect ratios in longitudinal and transverse directions are 4.6 and 5.6 respectively. Columns and shearwalls have constant cross sections over the height of the building; beams and slabs also have the same dimensions at each storey level. The plan and elevation of the building as well as the cross-section and elevation of a hybrid shear wall in the longitudinal direction are shown in figures 2.3-2.5.

2.6 Earthquake analysis and design of prototype building according to Eurocode 8

The building is assumed to be located in seismic zone 3 and founded on hard rock (sub-soil class A). The normal live load is taken as 5 kN/m^2 . For the preliminary design the equivalent lateral load procedure has been used. Subsequently, a 3-D computer model has been analyzed using both the ETABS and SAP2000.

Considering the earthquake zoning and sub-soil condition as well as the design ductility of the building, the following spectral parameters define the design spectrum according to Eq. 2.4:

α=0.33, S=1.0, β_0 =2.5, T_c=0.4, and q=5.

The fundamental period T1 of the building, according to Eq. 2.6, is calculated as 0.6 sec. and the corresponding spectral design factor S_d (T_1), according to Eq. 2.4, is calculated as 0.126. With a total weight of the building W (including partially contributing live loads) of 59976 kN and the spectral design factor of 0.126, the seismic base shear force F_b, according to Eq. 2.1, has been calculated to be 7557 kN. The results of the calculations based on procedures explained in sections 2.3.1 to 2.3.3 for the whole building and a single shear wall in the longitudinal direction are listed in Tables 2.2 and 2.3, respectively.

Table 2.2: Force distribution in longitudinal direction of the building.

Storey	Height	Lateral load	Story shear	Moment
	(m)	kN	KN	KN.m
Roof level	28.0	1364	0.00	0.00
ST-7	24.5	1548	1364	4774
ST-6	21.0	1327	2912	14967
ST-5	17.5	1106	4239	29804
ST-4	14.0	885	5345	48513
ST-3	10.5	664	6230	70317
ST-2	7.0	442	6894	94444
ST-1	3.5	221	7336	120119
Basement	0.0		7557	148569
Summation		7557		

Table 2.3: Force distribution for single shear-wall in longitudinal direction.

Storey	Height	Lateral load	Story shear	Moment
	(m)	KN	kN	KN.m
Roof level	28.0	389	0.00	0.00
ST-7	24.5	375	389	1362
ST-6	21.0	321	764	4036
ST-5	17.5	268	1085	7836
ST-4	14.0	214	1353	12573
ST-3	10.5	161	1567	18060
ST-2	7.0	107	1728	24110
ST-1	3.5	54	1835	30535
Basement	0.0		1889	37147
Summation		1889		

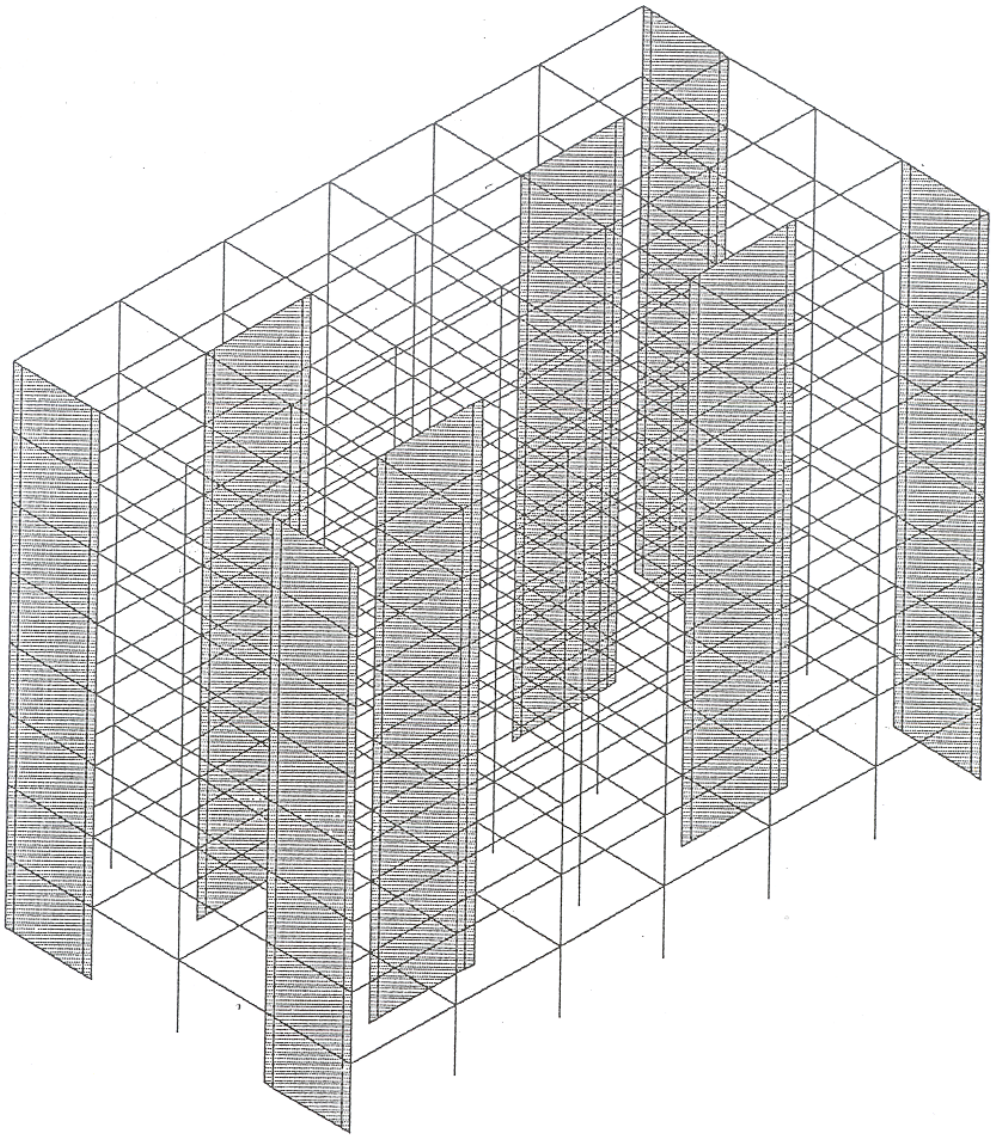

Figure 2.3: 3D view of building

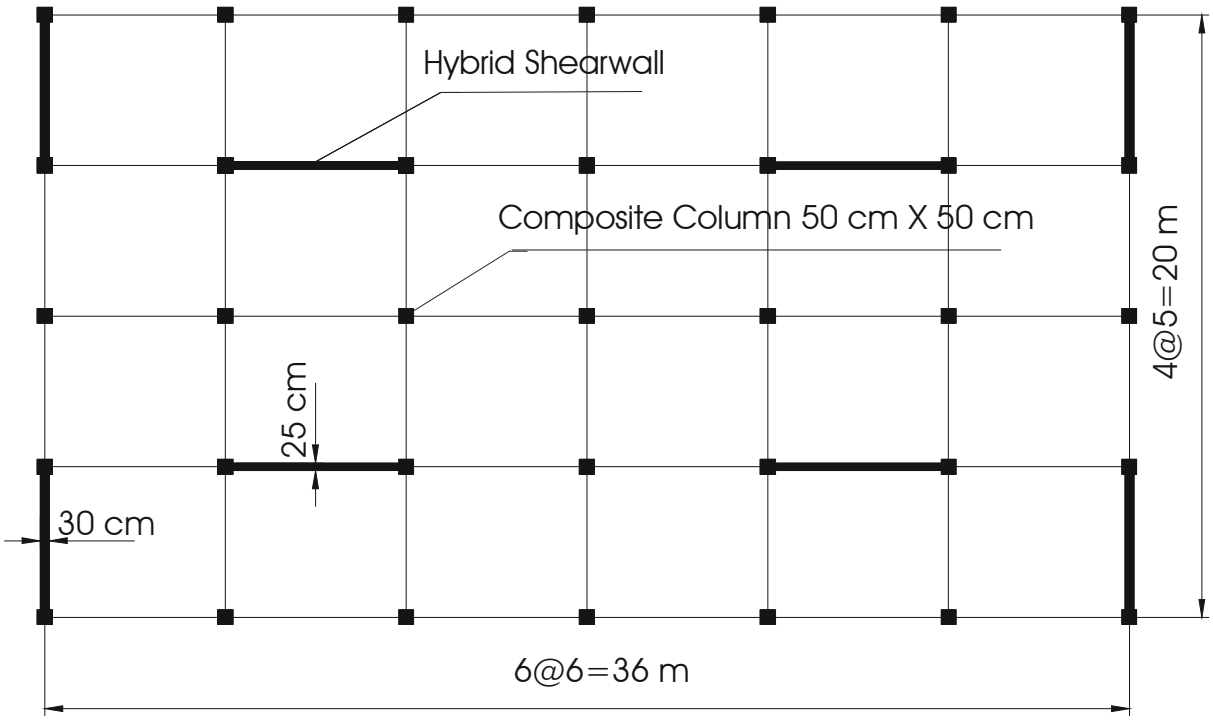

Figure 2.4: Plan view of building

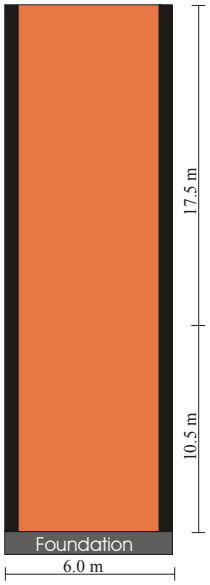

Figure 2.5: Elevation view of selected hybrid shearwall

2.6.1 **Design of the hybrid shear-wall**

The hybrid shear wall in the longitudinal direction has been designed based on the procedures described in section 2.3. For the preliminary design, a 0.25 m thick RC wall panel with a 0.40 m square composite edge element had been selected. The following material properties have been used for the calculations:

Material properties:

Concrete:
C30, characteristics strength, f_{ck} = 30000 kN/m^2, unit weight of the concrete, γ = 25 kN/m^2 , modulus of elasticity of concrete, $E_c = 3.2*10^7$ kN/m^2 and Poisson's ratio ν = 0.20.

Reinforcing steel:
Yield strength, f_{sk} =500000 kN/m^2, modulus of elasticity of steel, $E_s = 2.0*10^8$ kN/m^2 .

Steel tube section:
Yield strength, f_{sk} =240000 kN/m^2 , modulus of elasticity of steel, $E_s = 2.1*10^8$ kN/m^2 .

The above material values lead to the following resistant values in accordance with the EC8 stipulated procedures as explained in section 2.3.

Design of RC wall panel:

Considering that the base shear force with the load combination factor of 1.4 leads to a base shear force of 1.4 x 1889 kN = 2645 kN. The design shear force V_{sd} for the wall, using Eq. 2.11 with an amplification factor of $\varepsilon = 1.98$, is thus calculated as $V_{Sd} = 5273.23$ kN.

Checking the diagonal compression failure of the web, the shear resistance V_{Rd2} is calculated from Eqs. 2.16 and 2.17 for both inside and outside of the critical region as 5280 kN (inside the critical region) and 5293 kN (outside the critical region), respectively. Both values satisfy the inequality in Eq. 2.15 with V_{Sd} = 5273.23 kN.

For checking the diagonal tension failure of the web it is necessary to evaluate the contribution of the concrete and reinforcement in consideration of Eqs. 2.20 - 2.30 with particular emphasis of the wall reinforcement, both horizontal and vertical. Considering the design base shear force of 5273 kN and the material and dimensional parameters $f_{yd,v}$ = 435 N/mm^2, b_{w0}= 250 mm, Z= 0.8l_w = 4800 mm and τ_{Rd} = 0.34 N/mm^2, the reinforcement ratios were found to be $\rho_h = \rho_v = \rho = 0.0094$. Accordingly, the prototype shearwall contains a reinforcing layout of two curtains of 16 mm vertical and horizontal reinforcing bars spaced at 200 mm. Correspondingly, the shear resistance V_{Rd3} is found to be 5549.81 kN according to Eq. 2.19, with a contribution of the concrete of 643.01 kN and of the reinforcement of 4906.80 kN.

These results satisfy the inequality requirement ($V_{Sd} \leq V_{Rd3}$) of Eq. 2.18.

2.6.2 **Design of composite columns:**

The axial compressive and tensile strength $N_{pl.Rd}$ of the composite edge columns are calculated, using Eqs. 2.31 and 2.32, as 10149 kN and 5083 kN, respectively. The effective flexural stiffness of the composite column is determined from Eq. 2.33 as 3399 kNm^2. In checking the local buckling of the steel tube wall, the width to thickness ratio of the wall is 32, satisfying Eq. 2.34.

2.7 **Analysis of prototype building according to UBC94**

In order to make a comparison of the design forces of the prototype building considering both EC8 and UBC94 specifications, this section presents the analysis of the base shear force and associated dynamic forces according to UBC94. The building is located in a US seismic Zone 3, which has an acceleration response spectrum with an effective peak ground acceleration of 0.30g. However, to permit a direct comparison with the EC8 analysis, in which a spectrum with an effective spectral peak ground acceleration of 0.33g ($\alpha = 0.33$) had been assumed, the spectrum used for the UBC analysis has also been defined as having an effective peak ground acceleration of 0.33g (Z = 0.33). In both cases the site condition has been assumed to be hard rock (S = 1.0). The normal live load is taken the same, namely 5 kN/m^2. The period of the structure (T1), according to Eq. 2.40 is of course the same as for EC8, namely 0.6 sec. According to UBC94, for shear wall type buildings a system ductility factor (Rw) has been defined. The building importance (I) has been rated the same as for the EC8 calculations.

For calculating the base design force (V) according to UBC94 – see Eq. 2.38 - the following factors, reflecting the code defined design earthquake and building characteristics noted above have been used, namely, Z=0.33, I=1.0 , S=1.0 and R_w=8. Accordingly, with a total building weight of 59976 kN, the base shear force was calculated as 4354 kN. The results of the calculations for the entire building and for a single shear wall in the longitudinal direction, are listed in Tables 2.4 and 2.5, respectively.

Table 2.4: Force distribution for the building in longitudinal direction.

	H	F_i	V_x	M_x
Storey	Height	Lateral load	Storey shear	Bending moment
	(m)	kN	KN	KN.m
Roof level	28	786		0.00
ST-7	24.5	892	785.93	2750.76
ST-6	21	765	1678.01	8623.78
ST-5	17.5	637.20	2442.64	17173.03
ST-4	14	509.76	3079.84	27952.48
ST-3	10.5	382.32	3589.60	40516.08
ST-2	7	254.88	3971.92	54417.79
ST-1	3.5	127.44	4226.80	69211.57
Basement			4354.24	84451.40
Summation		4354.24		

Table 2.5: Force distribution for a single shear-wall in longitudinal direction.

	H	F_i	V_x	M_x
Storey	Height	Lateral load	Storey shear	Bending Moment
	(m)	KN	kN	KN.m
Roof level	28	224		0,00
ST-7	24.5	216	224	784.69
ST-6	21	185	440	2325.70
ST-5	17.5	154	625	4514.98
ST-4	14	123	779	7244.48
ST-3	10.5	92	1088.56	10406.17
ST-2	7	62	995.95	13891.99
ST-1	3.5	31	1057.69	17593.90
Basement			1088.56	21403.86
Summation		1087		

2.8 **Comparison of the EC8 and UBC94**

A comparison of the base shear forces according to the two design codes shows a distinct difference, namely 7557 kN (EC8) versus 4354 kN (UBC94). The reasons for these different values result in part from a relatively small difference between the elastic response spectral factors for T1 = 0.6 sec, namely, 0.630g for EC8 (being S_d (T) x q) and 0.585g for UBC94 (being Z x C). A far greater difference results from the difference in the structural ductility (behavior or performance) factor used in the two codes, namely, a "behavior factor" q of 5 for EC8 and a "structural system ductility factor" Rw of 8. As these factors basically reduce the elastic base-shear force coefficient – in percentage of total building weight W – these factors become 0.630/5 = 0.126 for EC8 and 0.585/8 = 0.073 for UBC94. This in turn results in the base shear force design values of 7557kN and 4354 kN, respectively.

In designing the wall reinforcement in accordance to both codes, the design according to EC8 leads to a less economic design (more steel) than in case of a design according to UBC94. The larger code specified base shear force from EC8 results in a stronger, more heavy reinforced wall which will remain elastic under increasing earthquake forces, as compared to the wall designed in accordance with UBC94 specifications. The steel in the latter wall will yield at an earlier force level and will potentially exhibit an earlier more effective energy dissipation. In principle, the EC8 design is conservative, as compared to the UBC94 design solution.

3 EXPERIMENTAL PROGRAM

3.1 General

In developing an optimum design solution for the interface connection between the wall panel and the composite edge member, several alternative interface designs have been developed and tested. For this purpose, a prototype building as explained in the previous chapter, has been designed according to the provisions of Eurocodes EC2, EC4 and EC8.

The experimental program was divided into two series of tests. In all tests, a cyclic displacement-controlled axial force was applied to the composite edge member causing a shear transfer along the interface connection into the wall panel. The first series of tests was carried out to evaluate the overall behavior of the hybrid wall, considering the cyclic shear resistance of both the interface connection and the concrete shear wall. In the second series of tests, the test setup was altered to study specifically the shear behavior of the different interface connections.

In fact, the results of the first test series showed in all cases a shear failure of the concrete wall panel rather than a failure of the interface connections. Although these results clearly showed that the interface design solutions were superior to the shear resistance of the walls, it was not possible to make a comparative evaluation of the different interface designs. Hence, the specific objective of the second series of tests was an assessment of the hysteretic characteristics of the different types of interface connections. For that purpose, the test set up was altered to allow a restraint of the wall panels. This arrangement increased effectively the panel capacity and allowed an increase of the test loads in order to cause failure in the interface connections and to allow a comparative evaluation of the different interface designs.

3.2 Selection of test specimen

Considering the test objectives and test capabilities at the TUD Institute for Steel Construction and Material Mechanics, it was necessary to use a scale model. Considering the necessity to obtain results which reflect the full-scale behavior, the choice of the scale factor is determined as a compromise between the specimen fabrication costs and test capacity limitations. In that respect, bond and yield characteristic of the reinforcing bars and aggregate interlocking in the cracked region are factors influencing the scaling factor of the model.

The critical shear wall region is assumed to be the first three stories of the specific test building., resulting in a shear wall with a length to width ratio of about 1.5. Ideally, the tests should be carried out on such three-story high test structures. However, because economic considerations and test limitations did not permit the study of such large size wall specimen, it was necessary to develop smaller specimen. Such specimen should reflect a representative portion of the critical three-story high wall section. Hence, it was decided to design the full shear wall in this lower region - considering both overturning moments and shear forces – and study only a small portion of this wall, containing both edge beam and shear wall.

As the test specimen had to allow studying different shearwall-to-edge member interface design solutions, and the results should be representative of the cyclic response of full-size shearwalls, a reduction in scale to not less than one-third of the actual wall was considered acceptable. In that case, common readily available reinforcing bars, which would model properly the tensile force resistance of the reinforcement and bond stresses, could be used. The one-third scale model of the three-story high shear wall over the first three floors of the full-scale structure is shown in Fig. 3.1. Because space and test-capacity limitations did not allow testing the entire shearwall model, it was decided to study only the edge portion of the first-story shear wall as identified in Fig. 3.1 and shown in perspective in Fig. 3.2.

In order to study several design solutions of the reinforcement along the column-wall interface and in the wall connection region, it was decided to test a total of 12 specimens. Because of cost restrictions, it was decided not to model the floors as edge elements on either side of the test specimen, but rather introduce additional reinforcement along the free edges of the wall in order to resist the overturning moment of the test specimen caused by the horizontal cyclic test load acting along the column-wall interface. Structurally, this was considered acceptable because of the basic shear loading of the wall specimen. Each specimen consisted of a tubular steel column with cross-sectional dimensions of 160 mm x160 mm and a wall thickness of 5.6 mm, attached, by interface connection (IFC) reinforcement, to the RC wall panel which had a thickness of 85 mm.

In the real structure the shear walls, which are designed to resist the shear only (not considering overturning moments), were reinforced at both faces with 18 mm bars in both directions spaced at 30 cm. Considering the 1:3 model scale, the RC walls in the test specimens were to be reinforced at both faces with 6 mm diameter bars in both the vertical and horizontal directions, placed in a 10 cm spacing arrangement. However, in the test specimen walls, 6 mm bars were only used in the vertical direction (perpendicular to the edge column). In the horizontal direction (parallel to the edge column) 8 mm diameter bars were used instead. This heavier reinforcement was introduced to prevent possible premature diagonal cracking of the wall of the test specimen. In fact, squat walls have a tendency to experience premature cracking along the diagonal instead of multiple diagonal cracking of the entire wall. With additional horizontal reinforcement cracking along the diagonal can be prevented [33]

The experimental program considers the following basic types of interface connections (IFCs):

1) Horizontal reinforcement extended from the steel composite tubular edge member and connected directly to the horizontal panel reinforcement, with or without additional intermediate horizontal IFC reinforcement.

2) Diagonal reinforcement (45°) extended from the steel composite tubular edge member and connected to the horizontal panel reinforcement, with or without additional intermediate diagonal IFC reinforcement.

3) Horizontal panel reinforcement welded directly to the tubular wall of the steel tubular composite edge column.

4) Shear studs welded to the steel tubular wall at intervals equal to the horizontal panel reinforcement. In addition, horizontal connection reinforcement extended through the wall of the tubular section and was connected to the typical horizontal panel reinforcement.

A summary of the reinforcing layouts for the several test specimens covering the different IFC design solutions is presented in Table 3.1. A total of l0 test specimens, subdivided in two test series, has been studied under cyclic shear along the interface plane between composite column and concrete shear wall. It should be noted that the orientation of the horizontal and vertical bars reflects the position of the wall element in the test frame (with the edge member placed in a horizontal position). Although the basic reinforcement of the model concrete shear wall was designed as a two-layered mesh of 6 mm bars at 10 cm intervals in both horizontal and vertical directions, in the test specimens the horizontal bars – running parallel to the edge beam – have been increased to 8 mm to prevent premature cracking of the squat wall along the diagonal of the test specimen wall. In order to provide for a dowel-type shear transfer along the interface, the interface connection reinforcement consists basically of 8 mm bars spaced at 10 cm or 6 mm bars spaced effectively at 5 cm.

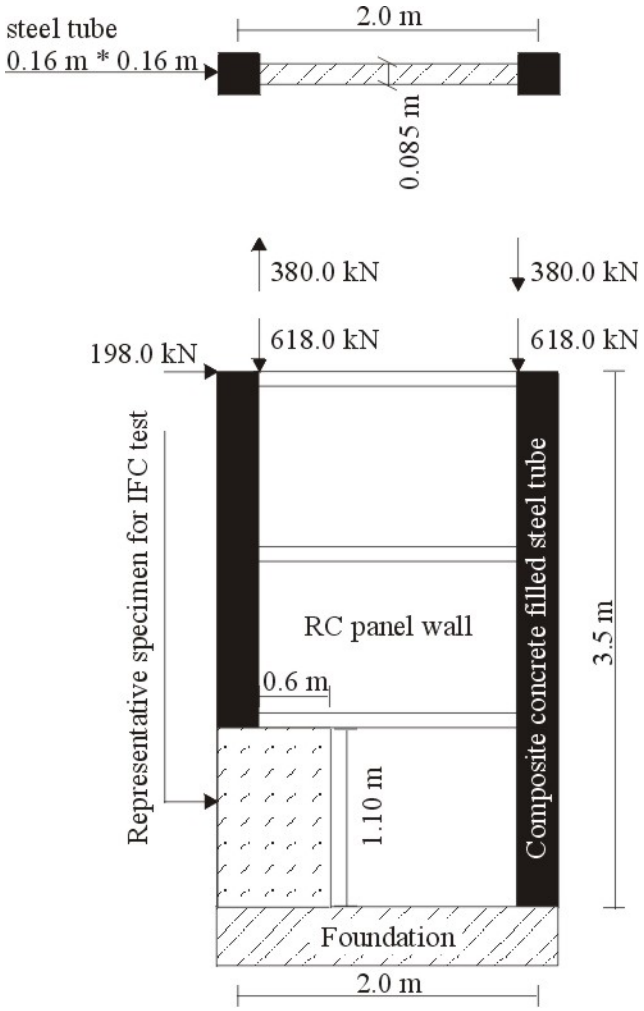

Figure 3.1: 1/3 Scale of hybrid shearwall (HSW)

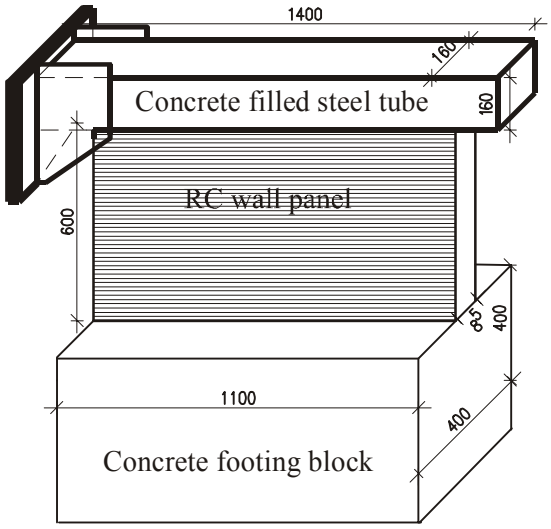

Figure 3.2: General view of test specimen

Table 3.1. Hybrid Shear wall System – Basic Reinforcement of Test Specimens

	Nr.	Test specimen	Panel reinforcement		Interface connection reinforcement
			H. Bars	V. Bars	
Serie 1	1	HSW-1	Φ8	Φ6	Straight anchor bars (Φ8) @ 10 cm
	2	HSW-2	Φ8	Φ6	Diagonal anchor bars (Φ8) @ 10 cm
	3	HSW-3	Φ8	Φ6	Straight anchor bars (Φ6) @ 10 cm plus diagonal anchor bars (Φ6) @ 10 cm
	4	HSW-4	Φ8	Φ6	Straight anchor bars (Φ6) @ 10 cm plus (Φ9.52) with 12 cm long shear studs @ 10 cm
	5	HSW-5	Φ8	Φ6	Open stirrups with straight anchor bars (Φ8) @ 10 cm welded to steel tube wall
Serie 2	6	HSW-6	Φ8	Φ6	Straight anchor bars (Φ8) @ 10 cm
	7	HSW-7	Φ8	Φ6	Straight anchor bars (Φ6) @ 5 cm
	8	HSW-8	Φ8	Φ6	Straight anchor bars (Φ6) @ 10 cm plus (Φ9.52) with 12 cm long shear studs @ 10 cm
	9	HSW-9	Φ8	Φ6	Diagonal anchor bars (Φ8) @ 10 cm
	10	HSW-10	Φ8	Φ6	Diagonal anchor bars (Φ6) @ 5 cm

HSW = Hybrid Shear Wall.

3.3 Test specimen design

The primary objective of this experimental program was the development of the most favorable design of the interface connection unter cyclic seismic-induced loading. Hence, several alternative connection designs were tested. Detailed considerations for the different interface connection solutions are presented in the following sub-sections. The design for the IFC is based on shear-friction method of design (UBC 1994).

3.3.1 Interface connection with reinforcing bars

Reinforcing bars at the IFC are typically placed in pairs as in the RC wall panel. These bars are placed either perpendicular or angular (45 degree) to the interface surface between the composite column and concrete shear wall and have hooks inside the edge column to provide sufficient anchorage (Figure 3.3-3.7). Transverse holes in the tubular wall for the IFC reinforcement at the edge column can be arranged in sets of 2 with a spacing distance equal to the spacing distance of the horizontal wall reinforcement meshes. In case of both perpendicular and diagonal reinforcement a second set of holes at a reduced transverse distance will be necessary to accommodate the diagonal bars. Spacing of the holes along the interface connection is equal to the full- or half-spacing distance of the typical wall reinforcement.

Considering the alternating shear forces along the interface, straight bars transfer the shear by dowel action. In case of inclined bars, which are placed under 45° with the interface in both forcing directions, the shear forces tend to produce tension in the reinforcement. The dowel strength across the IFC can be developed by the shear strength across the bars and the flexure resistance of the reinforcing bars. Under those circumstances, the required amount of reinforcing steel at the IFC should be larger than in the RC wall section where the concrete carries part of shear forces. Hence, either a larger bar size, spaced at the same

distance as the reinforcing steel in the RC wall panel, or the same bar size as the reinforcing bars of the RC wall, but with a closer spacing distance, should be used. In comparison to the straight bars, the diagonal bar size for the IFC reinforcement can be reduced because of tension-compression force transfer rather than the dowel action under shear force transfer. The following specimens are designed with straight or/and diagonal reinforcing bars: HSW1, HSW2, and HSW3 of Series 1 and HSW6, HSW7, HSW9 and HSW10.

3.3.2 Interface connection with reinforcing bars and shear studs

In these connections, straight bars having the same bar size (6 mm) and spacing distances as in the RC wall panel have been used. These bars, which extended 30 cm outside the edge column, were hooked and placed through holes drilled in the column wall. Subsequently, concrete was placed inside the tubular section. In addition, shear studs with a diameter of 9.52 mm were welded at the same level as the reinforcing bars extending from the composite concrete-filled steel tube (Figure 3.8). In this case the applied shear force is mainly resisted by dowel action of the bars and shear studs. The shear stud diameter should not be too large in comparison to the straight-bar diameter and the thickness of the steel tube. Otherwise, because of the higher relative stiffness of the studs with respect to the reinforcing bars, the studs will resist a larger portion of the interface shear load than the bars and may exhibit a shear failure of the studs or a tearing of the tubular wall. In case of such failure, the load resisting capacity of the IFC decreases significantly and may lead to a failure of the reinforcing bars. This alternative solution, which is simple to fabricate, has been studied in specimen HSW4 and HSW8.

3.3.3 Interface connection with reinforcing bars welded to composite edge columns

A possible third design alternative is the welding of the RC wall panel horizontal reinforcement to the edge columns (Figure 3.9). In that case the 8 mm diameter hairpin type of connection bars are welded to the steel tubular wall and lapped to the 6 mm horizontal wall panel reinforcement. This design solution is studied in specimen HSW5.

3.4 Construction of specimens

The hybrid shearwall test specimens were constructed in a precast concrete workshop. After inserting the connection bars through predrilled holes inside the steel tube section concrete was poured inside the column. After connecting the extended bars to the panel reinforcement, the plywood formwork for the wall was placed in position and the concrete was poured. The concrete was poured with the column and wall in a (normal) vertical position. Each time two specimens were poured from the same batch. The specimens were cured for 3 days while covered by plastic sheets. Prior to testing, each wall element was whitewashed for ease in crack identification. In the following sub-sections material properties are presented.

3.4.1 Concrete

The concrete to be used in this study was specified as C30/35 according to Eurocode 2 with characteristic mean values for the cylinder strength f_{ck} of 30 N/mm^2 and the secant modulus E_{cm} of 32 kN/mm^2, respectively. The following concrete mix was used for the construction of the specimens: normal-strength Portland cement 350 kg/m^3, water 180 liter/m^3 and aggregate 1790 kg/m^3 with a maximum aggregate size of 8 mm. In order to obtain the necessary workability, special additives had to be used, to reach a slump value of

120 mm. For each batch of concrete, three concrete cubes (15 *15 cm) were made to measure the concrete compressive strength and three cylinders with dimensions of (15 * 30 cm) were made to measure the modulus of elasticity of the concrete.

The results of of the compressive strength and modulus of elasticity tests are summarized in Table 3.2. The respective tests were carried out a few days before testing the specific test specimens. At that time the concrete had an age of 40 - 90 days. The test results, which showed quite non-uniform results, were found to vary between compressive strength values of 21.78 and 46.30 N/mm^2 and moduli of elasticity E_c between 20500 and 28600 N/mm^2. The summary of theoretical and experimental values of the pertinent concrete properties of the 5 batches of concrete are given in table 3.2.

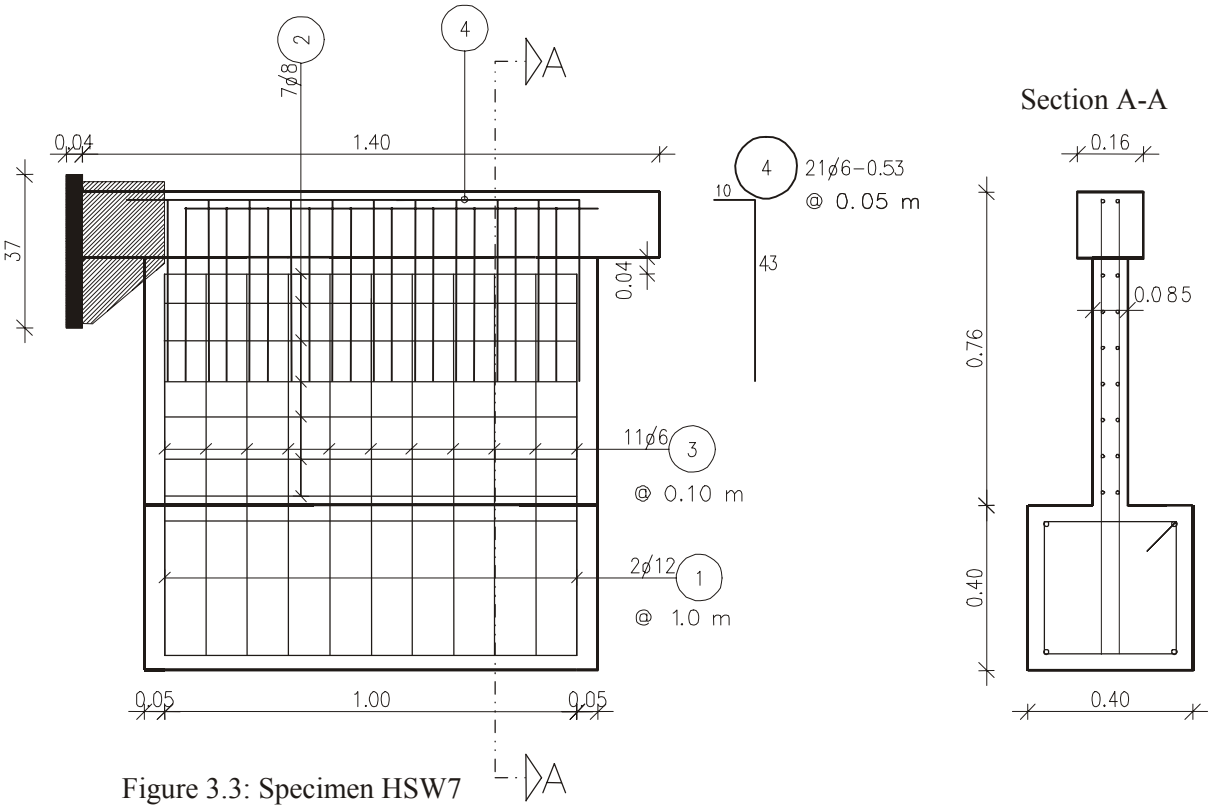

Figure 3.3: Specimen HSW7

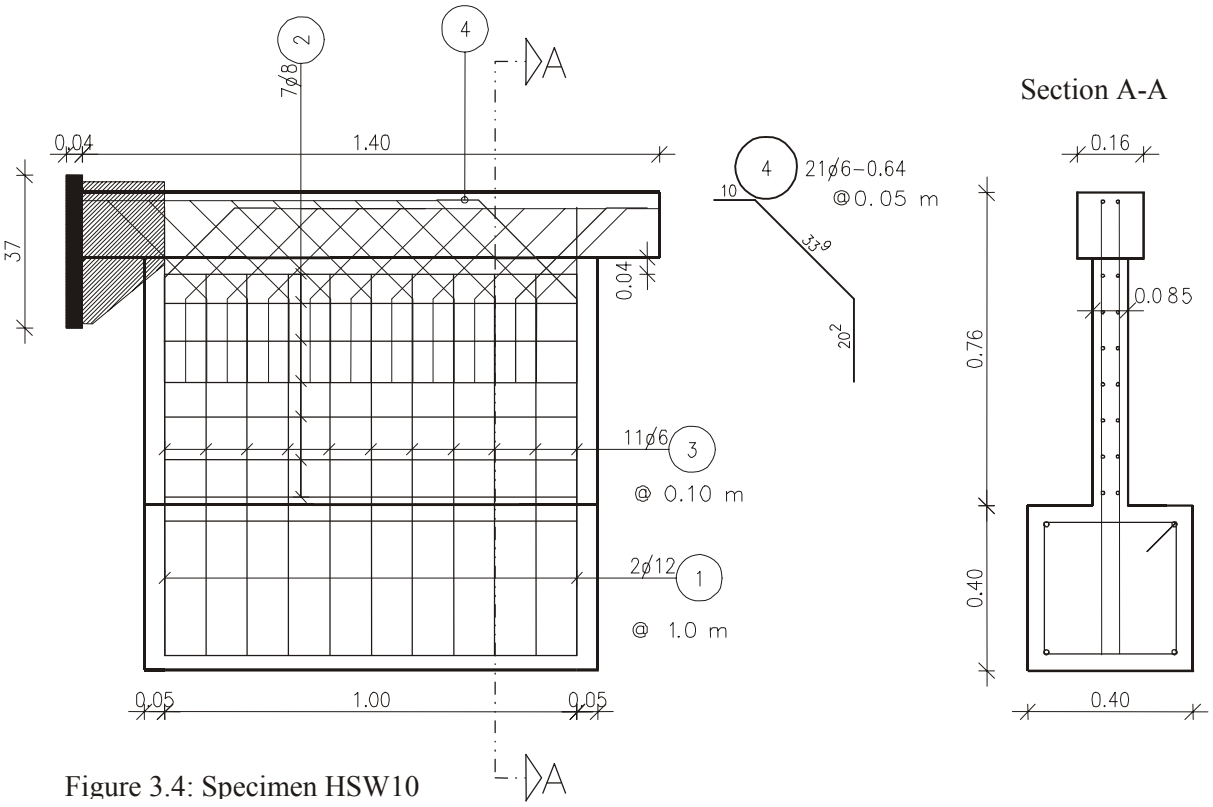

Figure 3.4: Specimen HSW10

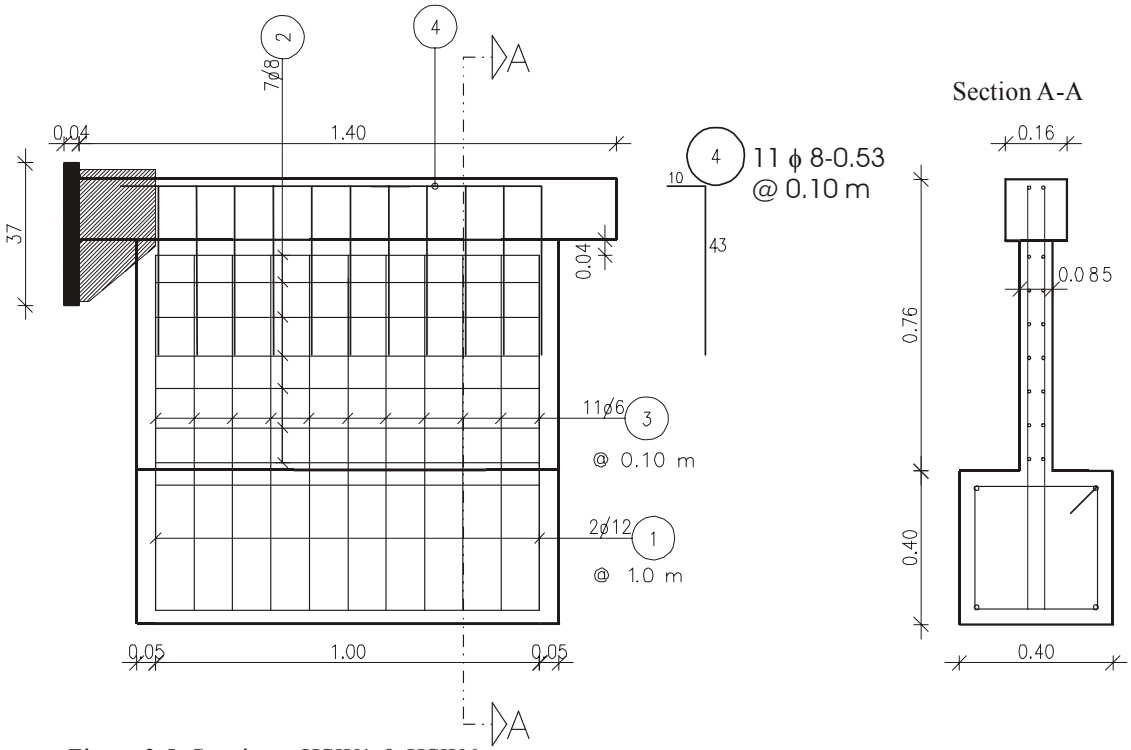

Figure 3.5: Specimen HSW1 & HSW6

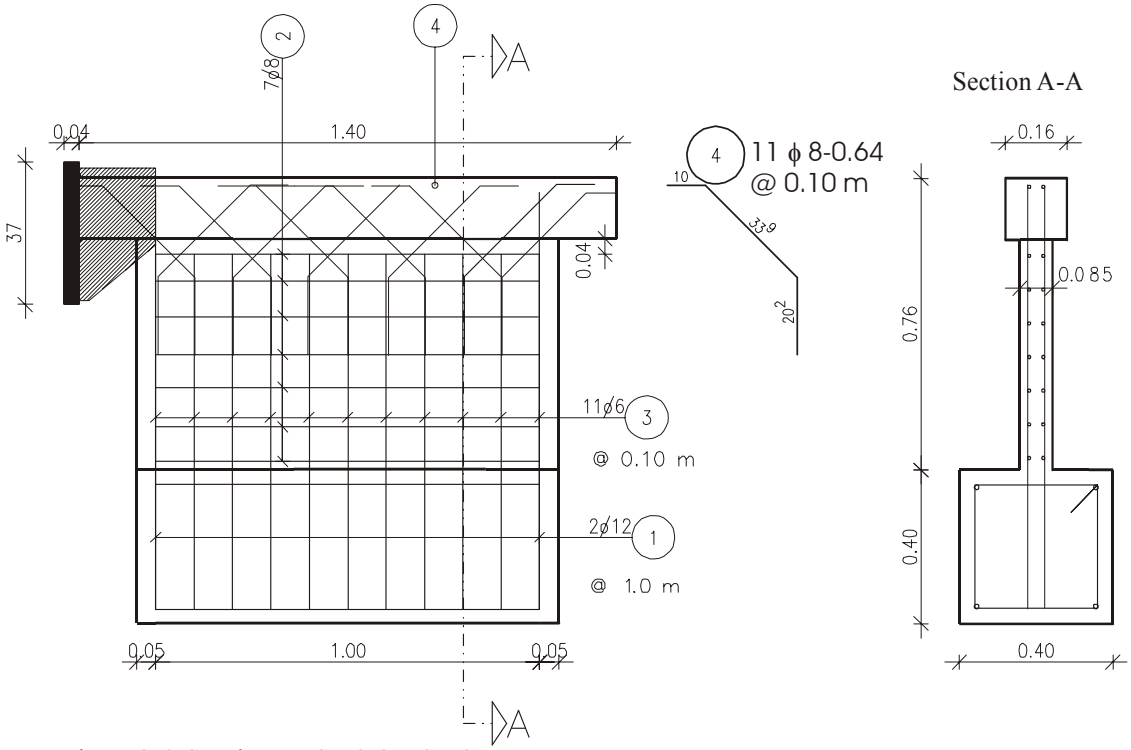

Figure 3.6: Specimen HSW2 & HSW9

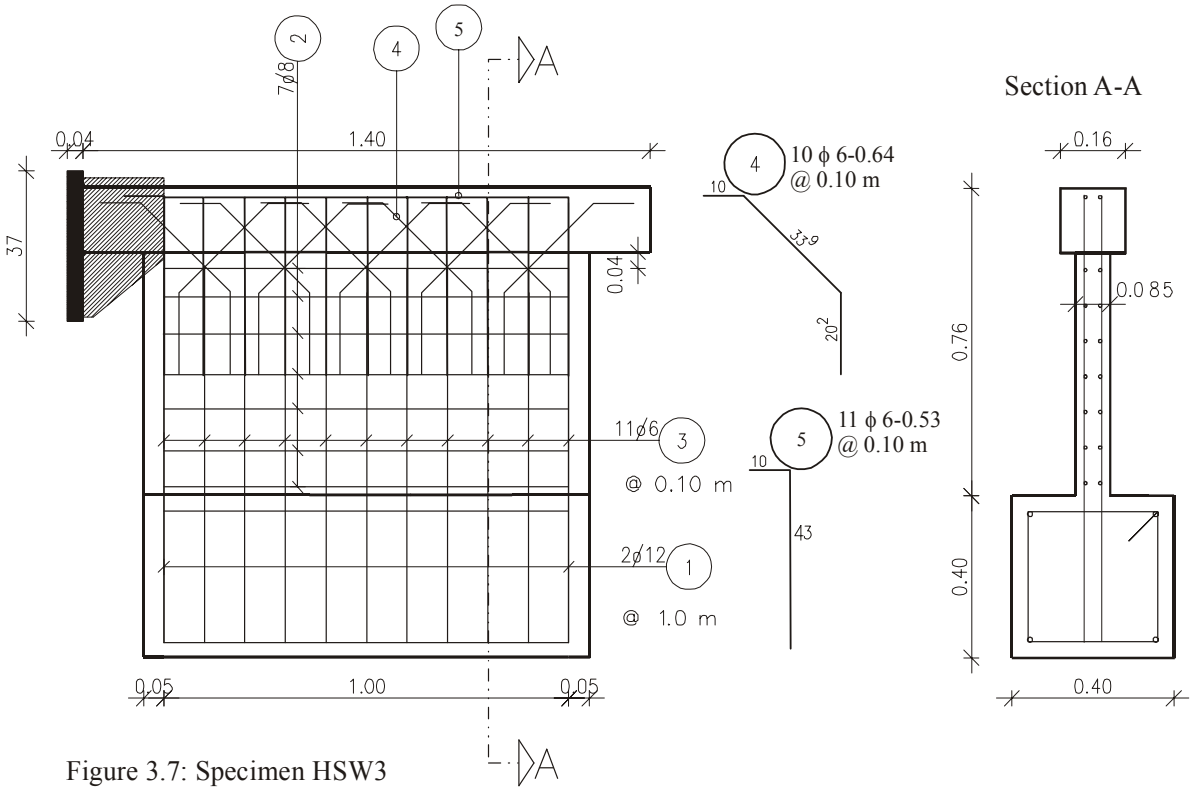

Figure 3.7: Specimen HSW3

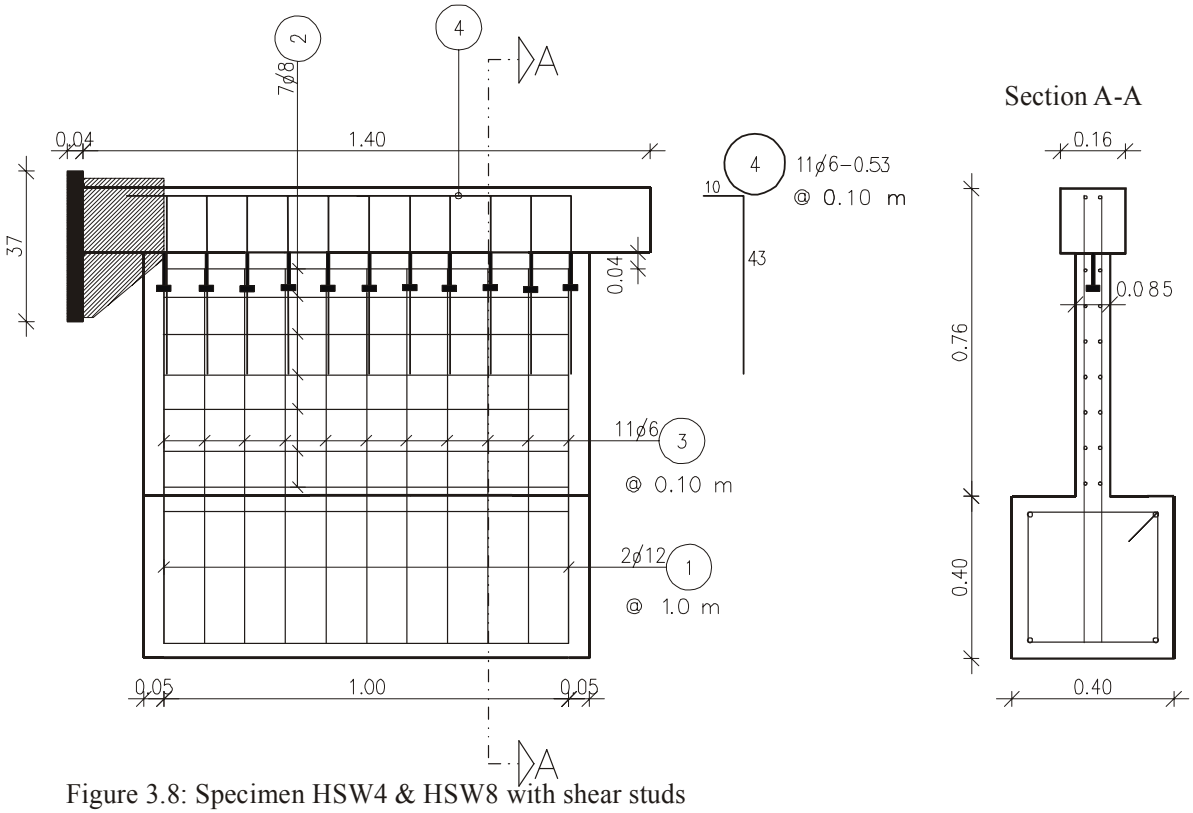

Figure 3.8: Specimen HSW4 & HSW8 with shear studs

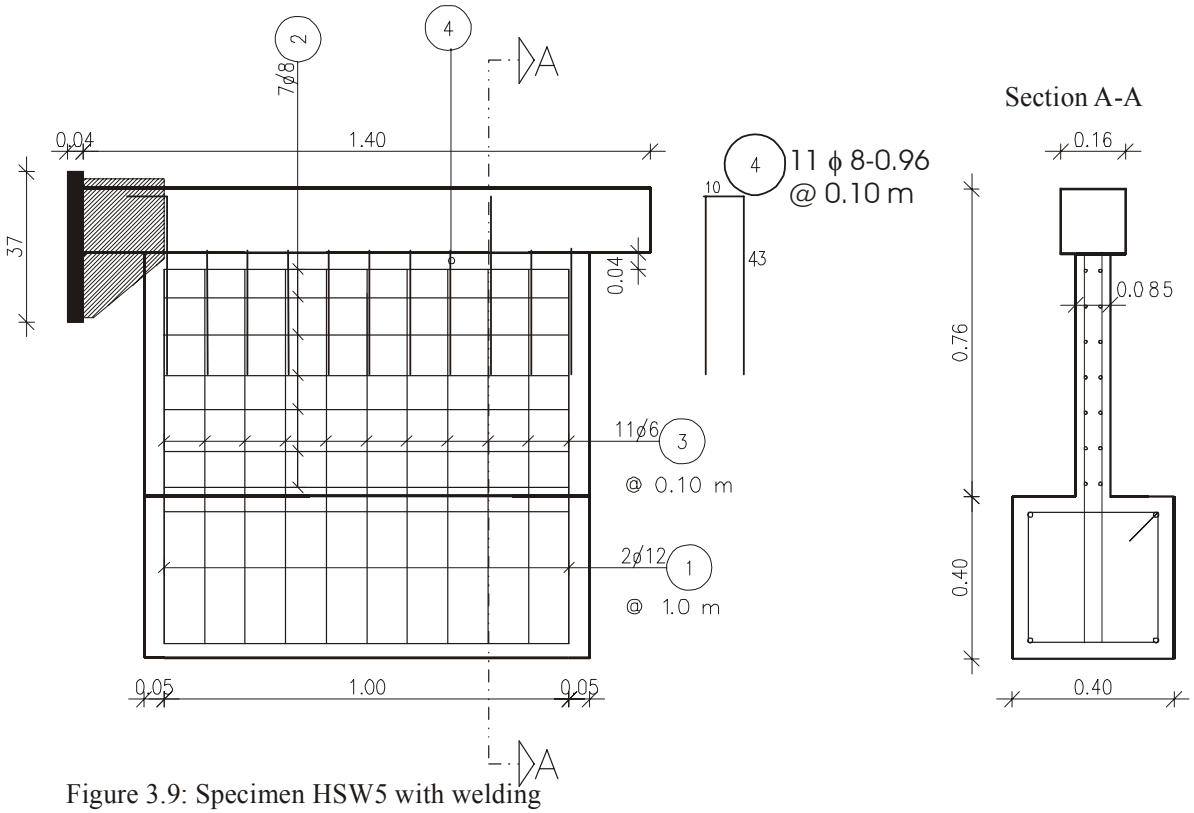

Figure 3.9: Specimen HSW5 with welding

Table 3.2. Concrete properties of test specimens

Nr.	Test Specimen	Concrete Property (N/mm^2)	
		Theoretical	Measured
1	HSW-1	30,00	38,30
2	HSW-2	30,00	28,78
3	HSW-3	30,00	38,30
4	HSW-4	30,00	21,78
5	HSW-5	30,00	33,26
6	HSW-6	30,00	46,30
7	HSW-7	30,00	46,30
8	HSW-8	30,00	21,78
9	HSW-9	30,00	33,26
10	HSW-10	30,00	28,78

3.4.2 **Reinforcing steel**

The yield strength of the reinforcing steel having a steel grade of BSt 500 averaged at about 500 N/mm^2. All reinforcement used in the hybrid shearwall test specimens was taken from the same mill.

3.4.3 **Tubular steel section**

Based on the original design of the 8-story high hybrid shear-wall structure, the decision to use a 1/3 scale model to study the interface behavior resulted in test specimens with a square steel tubular section of 160 mm x 160 mm and a wall thickness of 5.6 mm. The hot

rolled steel tubes used for the fabrication of the test specimens had a yield strength of nominally 240 N/mm2.

3.5 **Test setup**

In order to evaluate the cyclic shear-load resistance of the interface connection between column and wall panel, it was decided to use a displacement-controlled double-acting load cylinder connected to the edge column with a forcing action directly along the interface. An overall view of the test setup as used for both series of tests is presented in Fig. 3.9, and shows the reaction frame, test specimen and double-acting actuator. The difference between the two test series is the external support condition of the wall edges of the test specimen. In the first series of tests the edges of the wall panel were left free to deform to allow for an unrestricted shear distortion of the wall (Figure 3.10). In the second series of tests the edges of the wall were supported rigidly up to the mid-height of the test panel, thus limiting the shear distortion and reducing bending effects in the wall panel (Figure 3.11).

The overall test setup, with the edge member in a horizontal position, was dictated by the available test frame and actuator capacity. The one-third scale model test specimen, with a length of 110 cm and a height of 68 cm (being a portion of the shearwall width, measured to the edge-member center line), represents part of the first-story shearwall. The wall thickness was set at 8.5 cm (or basically 1/3 of the proto-type wall thickness of 25 cm).

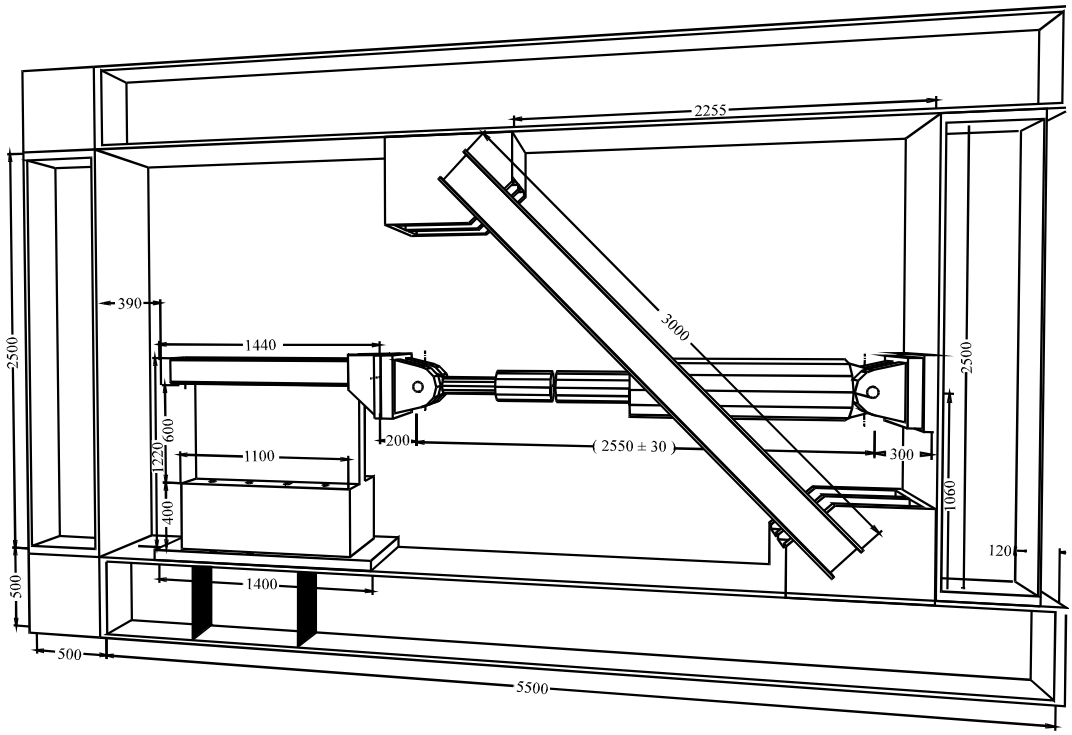

Figure 3.10: Test setup

In order to anchor the test specimen to the test frame, a concrete anchoring block with overall dimensions of 40 cm x 40 cm x 110 cm was cast integrally with the test wall. This block was anchored with HS bolts to the upper flange of the lower beam of the test frame. Considering that under horizontal displacement-controlled cyclic loading, a certain rocking of the test specimen may occur due to deformations of the upper flange of the lower steel beam of the test frame, vertical web stiffeners were added to stiffen the upper flange directly below the test specimen.

3.6 **Instrumentation**

The instrumentation of the specimens was designed to obtain under increasing displacement-controlled cyclic loads information about not only the axial force distribution along the edge column, in order to evaluate the shear-force transfer along the interface, but also the slip along the interface between column and panel as well as the bending and shear deformation of the concrete wall.

Strain gages (D30-D41, see Fig. 3.10) to record the axial forces were placed at three sections along the length of the column. In each section four gages were placed, two on each side wall near the top and bottom of the section. In order to measure the relative slip between the column and RC-wall panel, three LV displacement transducers (LVDT) were placed on one side of the wall only. The position of these LVDTs coincided with the instrumented sections of the tubular edge column. The bending and shear deformations of the concrete panel were measured by transducers placed vertically and horizontally (against a reference frame) and along the panel diagonals. Transducers at the bottom on both sides of the specimen measure the movement attributed to the support.

Basically, the different interface connections were designed with the intend that the resistance of the connections would be larger than the capacity of the shear wall. However, in the first series of tests the shear wall failed prematurely before any significant slip along the interface could be detected. In fact, the shear wall failed due to bending and shear in the lower part of the wall. In order to prevent such failure and obtain a better assessment of the interface connections, it was decided in the second series of tests to restrain the shear distortion of the lower part of the wall and reduce the overturning moment in the lower region. This latter setup is shown in Fig. 3.11.

Considerin the instrumentation specifically, other than the typical test control transducers for the displacement control and loadcell output, LVDT displacement transducers W10 through W22 were used to record the shear panel deformations (W10 – 13), the interface

slip (W14 – 16 with a gage length of 7 cm), and the bending deformations (W17 - 22, vertically). The displacement potentiometers W23 - W26 were used to measure possible base rocking motions. Furthermore, straingages (D30 - D41) were placed at the three previously noted sections along the length of the steel column tube. Finally, displacement potentiometers (SZ 2 and 3) were used to measure the overall shear distortions of the shear wall.

3.7 **Test Sequence**

The tests were performed under displacement controlled cyclic loading until complete failure of the specimens were observed. A typical displacement-controlled loading history is shown in Figure 3.12. Specifically, the alternating displacements in sets of three cycles were increased in 0.5 mm intervals from +/- 0.5 to 3.0 mm and in 1.0 mm intervals from +/- 4.0 to +/- 5.0. Hereafter, the displacements were applied in single cycles with an 1.0 mm interval reduction to a displacement of +/- 2.0 mm. Subsequently, the displacements were increased again as single cycles with an interval of 1.0 mm up to a displacement of +/- 5.0 mm. Finally, the test specimen was subjected in sets of two cycles to displacements of +/- 6.0, 7.0, 8.0, 9.0, 10.0, 12.0, 14.0, 16.0 mm etc., up to failure.

The displacement history of three or two cycles allowed in principle an assessment of the deteriorating behavior under repeated displacements. The cyclic displacement reduction after the specimen had been subjected to cycles of up to +/- 5.0 mm, was introduced to evaluate the extend of permanent damage up to that level of distortion.

Front view

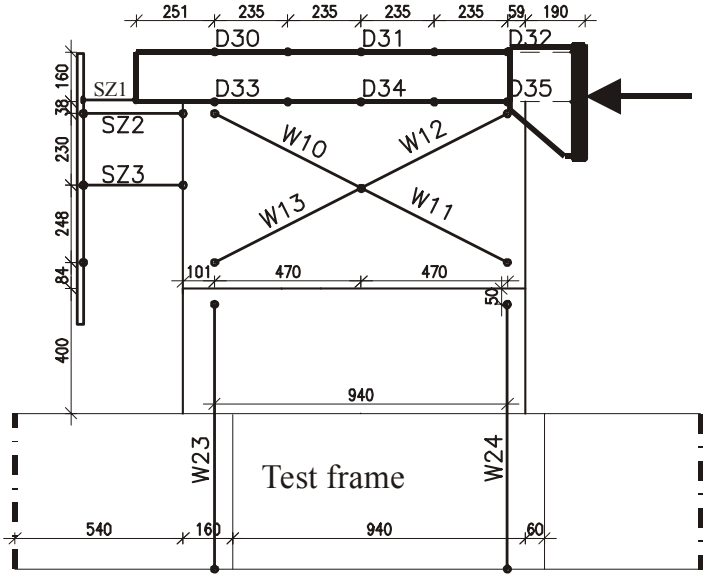

Back view

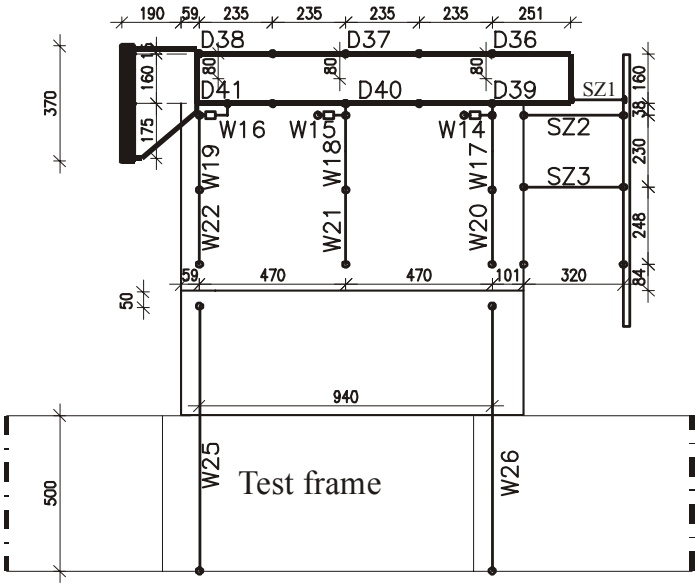

Figure 3.11: Instrumentation of test specimen for test serie 1

Front view

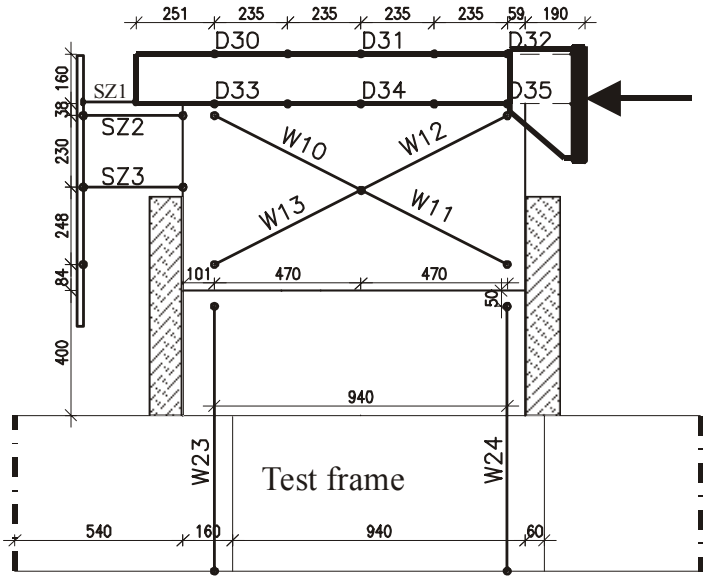

Back view

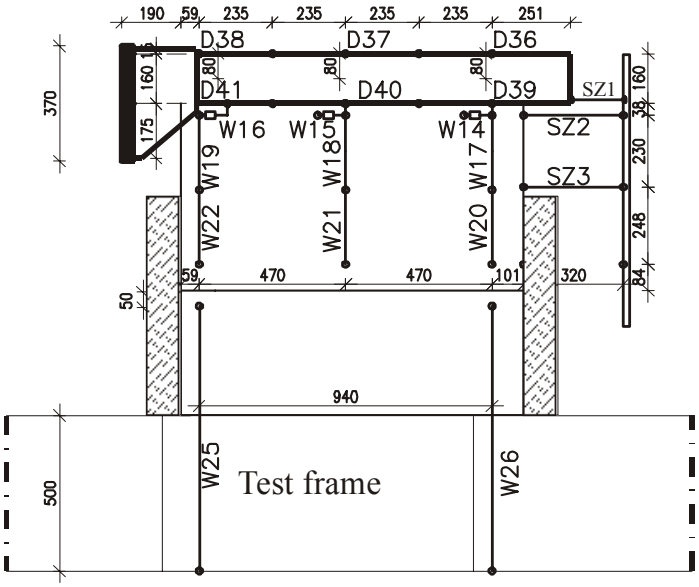

Figure 3.12: Instrumentation of test specimen for test serie 2

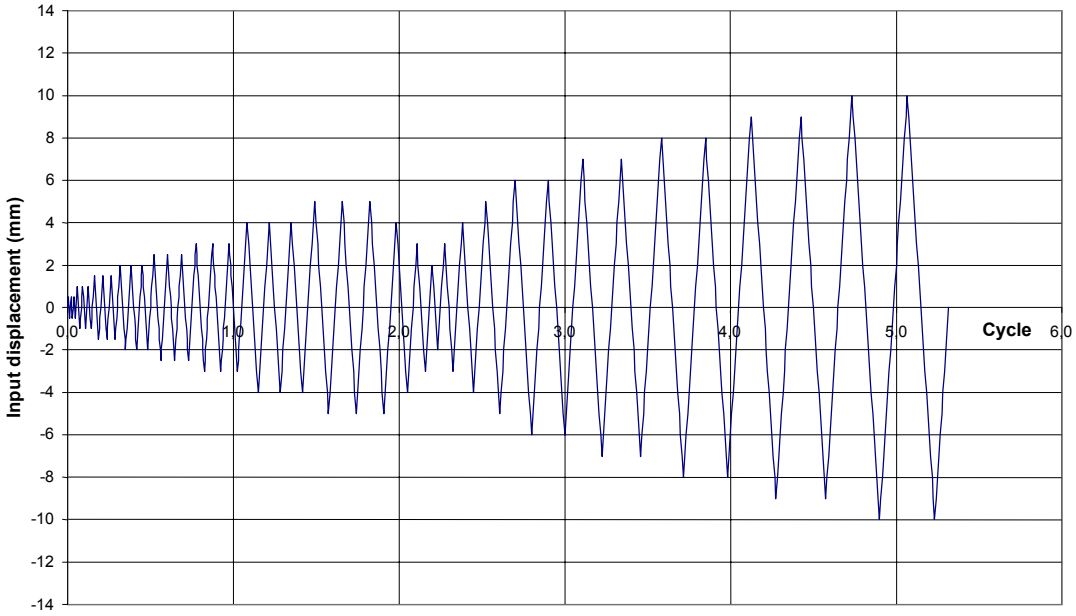

Figure 3.13: Loading History

4 TEST RESULTS AND DISCUSSIONS

4.1 General

For the purpose of this study, characteristic test results, covering the load - displacement, shear force - shear distortion and shear force – interface slip relationship as well as the shear force distribution along the length of the interface have been evaluated.

The purpose of the straingage layout along the length of the column section was an evaluation of the shear-force transfer along the interface between composite column and concrete panel. Results showed under low force and displacement levels a force-transfer concentration near the loaded end of the column of about 1.4. However, under increasing displacement levels and repeated loading cycles, the shear force distribution became more uniform. Because the purpose of these measurements was limited to the relative force distribution during testing, detailed test results are not presented in this report.

Test results on the force-displacement, shear distortion and interface slipping have been evaluated and are presented in detail in the following sections. A qualitative assesment of the cyclic response of the several specimens has been made from a direct comparison of the various response parameters. In evaluating the test results, particular emphasis is paid to the force - slip relationship indicative of the behavior of the interface connections.

4.2 Force – Displacement

4.2.1 Test serie 1

The hysteretic force displacement relationships for the specimens (HSW1-HSW5), showing the actuator force versus the displacement at SZ1, are presented in Figs. 4.1 - 4.5. A first observation of the different graphs shows a very high degree of pinching, typical for

the crack development in concrete under cyclic shear loads. In fact, in all specimens first diagonal hairline cracking occured at a cyclic load of about 50 to 100 kN corresponding to a displacement of about 0.5 to 1 mm. Before reaching the maximum resistance, cracking was observed over a larger area of the wall panel. However, after having reached the maximum resistance, failure was initiated by the appearence of widening cracks at the bottom part of the wall panel beginning from the mid-height of the panel (bending) towards the middle region at the bottom of the panel (shear). Under this continuing cyclic exposure, the concrete cover at both sides of the panel was crushed and spalling of the concrete cover was observed. Also, in this test phase the widening of the main cracks caused the vertical reinforcement in the bottom part of the panel to rupture progressively from the outer edges towards the middle of the panel. The failure was thus a flexure - shear failure originated by concrete crushing and tearing of the vertical reinforcement of the wall panel. Maximum forces and displacements reached during the experiments are tabulated in Table 4.1.

Considering the several graphs, it is obvious that before the specimens reached their maximum load resistance, repeating the cyclic displacements at the same displacement magnitude did not significantly reduce the cyclic load resistance (stable loops). However, at and after the maximum resistance had been reached, subsequent repeated cycling at the same displacement level exhibited invariably a significant reduction of the force resistance and illustrates the progressive failure of one of the cracks. This phenomenon – of basically stable loops before raching the maximum load resistance and the subsequent reduction of the resistance under repeated cycling at the same displacement level at or after the maximum resistance had been reached – is clearly illustrated in Fig. 4.5.

Comparing the behavior of the different test specimens, it should be noted that the relative low resistance of HSW1, and to a certain extent also HSW2, were in part due to the fact that the concrete in the center region of the panels had been poorly compacted. Other than for HSW1, it is of interest to note that the the maximum resistance in each of the 4 other specimens occured at total shear displacements between 5 and 6 mm, reflecting basically similar cracking pattern of the concrete wall panels. This could be expected as the rein-

forcement in the wall panel was the same for all specimens. In as far as the observed behavior failed to provide information about the resistant and displacement capacities of the different interface connections, it was decided to study the remaining test specimens with restrained side edges. In that case it could be expected that the shear load capacity would be increased and an assessment of the interface design solutions could be made. The restraint on both sides of the test specimens has been introduced by restraining the panel through the introduction of steel blocks along the lower half of the wall panel.

4.2.2 **Test serie 2**

The actuator force-displacement response, showing the force versus interface displacement for the several specimens of the 2nd test series is given in Figs. 4.6 thr. 4.10. The pertinent test results, covering in fact the force and displacement capacities of the specimens at the interface, are presented in Table 4.1. Considering the graphical test data, the cyclic response shows, similarly to the results of the 1st test series, a considerable pinching of the histeretic loops. In comparison with the test results from the 1st series of tests, the restrained test setup did invariable lead to increased horizontal load resistances. At the same time, the recorded cyclic-load displacements were a combination of the shear distortions (slippage) of the interface connection between edge-column and concrete panel, combined with a shear distortion of the concrete panel.

As in the 1st test series, also in the 2nd series of tests the graphs show a significant pinching effect. In comparison with the earlier results, also, the repeated cycles up to failure show little deterioration. However, from the moment that the maximum resistance has been reached, the load resistance under repeated displacement cycles reduces significantly.

Comparing the response of the different specimens, in order to assess the efficiency of the different interface designs, the response of the specimens with straight anchor bars is less effective than those with diagonal bars. In fact, considering the deterioration under repeated

alternating cyclic displacements after the maximum resistance had been reached, the first three specimens (HSW6,HSW7and HSW8) with straight anchorage bars, as compared to the two with diagonal bars, show a distinct loss of resistance. Specifically, specimen HSW6, which had experiencied little loss of resistance up to a 3-cycle alternating displacement of +/- 4.0 mm, exhibited after 3-cycles at +/- 5.0 mm a drop in resistance of 30% (after 5.5 cycles the resistance had even dropped to 50%). The same basic phenomenon was observed for specimen HSW7. In this case, after having observed virtually no-loss of resistance up to a 3-cycle alternating displacement of +/- 3 mm, a loss of 30% was observed after 3 cycles at +/- 4 mm (increasing to 40% in the next half cycle). Also, specimen HSW8 showed a similar deteriorating behavior as specimens 6 and 7. Specifically, after the loss of resistance under a 3-cycle displacement of +/- 4.0 mm had still been minimal, at +/- 5.0 mm, a loss of resistance of about 25% after 3 cycles occurred. This loss increased to about 40% after 4.5 cycles.

In comparison, the other two specimens (HSW 9 and 10) with diagonal anchorage bars, exhibited both a relatively gradual drop in resistance after the maximum resistance had been reached and, under increased displacements, relatively little deterioration under repeated alternating cyclic deformations. In fact, after having reached the maximum resistance under cyclic displacements at about +/- 4.0 mm, both specimens showed - up to cyclic displacements of +/- 6.0 mm – only a limited loss of resistance. Comparing these results with those of specimens 6,7 and 8, it can be observed that under cyclic displacements of +/- 6 mm the interface shear force resistance of specimens 6,7 and 8 had dropped significantly to about 30 % of the maximum capacities (which were reached at cyclic displacements of +/- 4.0 mm for specimens 6 and 7, and +/- 5.0 mm for specimen 8). Comparing the results of specimens HSW9 and 10 directly, specimen 10, with two layers of 6 mm 45°-diagonal anchorage bars arranged at an interval of 5.0 cm, shows a better response than specimen 9, with 8 mm 45° anchorage bars spaced at 10.0 cm.

Considering the results of both test series, the interface design of diagonally arranged 6 mm anchoring bars, spaced at 5.0 cm and penetrating into the composite column, as used in

Specimen 10, seems to offer the best interface solution. In case welding on site would be possible, welded hairpin bent 8 mm bars spaced at 10 cm, as basically in case of Specimen 5, offer an even more effective interface design.

The mode of failure of the specimens differed according to the arrangement of the reinforcing bars at interface connection. All the test specimens in the first serie experienced a shear mode of failure. During the first cycles of loading, hair line inclined cracks formed which is distributed uniformly in the RC panel. Under increased reversed cyclic displacements, significant cracks were initiated at lower parts of RC panel, in which the opening of such a crack reached about 5-8 mm leaded to shear mode of failure, as presented in Figures 4.11-4.14.

The specimens in the second series were mainly failed at interface connections as shown in Figures 4.15-4.18. For the specimens with straight reinforcing bars, after initial hair line cracks in RC panel at first stages of loading, the concrete at interface connection region spalled off (destroyed) and interface reinforcing bars were buckled. In case of diagonaly reinforced bars at IFC, after the initial diagonal cracking of concrete, the horizontal forces were mainly taken by the diagonal bars, thus the behavior of these specimens were governed by reinforcing bars. Hence, the specimens with diagonal reinforcement layout as compared to specimens with straight bars having the same bar size led to an increased ultimate capacity at IFC. Therefoere, the diagonal reinforcing bars restrained the expansion of cracks at the IFC region, and failure occured in central region of the RC panel.

Table 4.1. Summary of test results

	Nr.	Tension			Compression					Calculated	
Serie	Specimen Number	Ultimate lateral force (Vu)	Displacement at Max. Vu	Ultimate Displacement	Ultimate lateral force (Vu)	Displacement at Max. Vu	Ultimate Displacement	Side Support	Type of Failure	Shear Strength at IFC	Shear Str. of wall panel
		kN	mm	mm	kN	mm	mm			kN	kN
Serie 1	HSW1	231	3.5	7	-203	-4.5	-7	No	WP[1]	327.3	436.8
	HSW2	283	5	8	-290	-6	-8	No	WP	562	378
	HSW3	368	5	8	-315	-5	-8	No	WP	469.4	436.8
	HSW4	353	6	8	-305	-5	-8	No	WP	374.7	329.4
	HSW5	440	5	10	-435	-5	-10	No	WP	528	407
Serie 2	HSW6	320	4	7	-330	-4	-7	Yes	IFC[2]	327	480
	HSW7	390	4	18	-440	-3	-18	Yes	IFC	350	480
	HSW8	422	5	15	-384	-4	-13	Yes	IFC	375	329
	HSW9	420	4.5	8	-435	-6	-8	Yes	WP	562	407
	HSW10	445	4	8	-520	-5	-8	Yes	WP	601	378

1) Wall Panel

2) Interface Connection

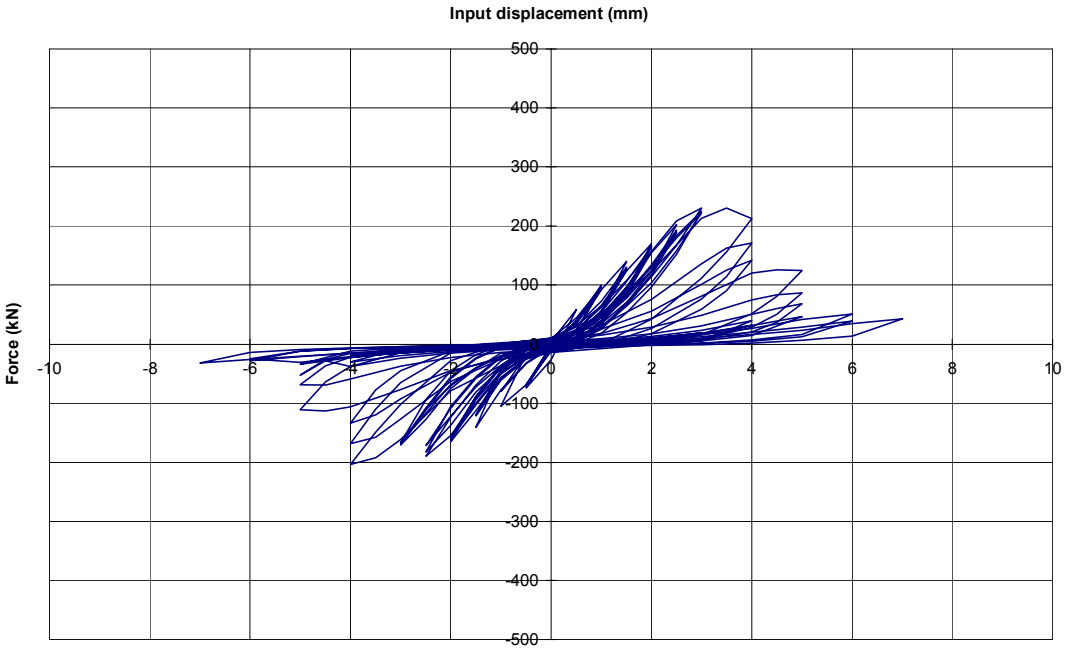

Figure 4.1: Force - displacement diagram for HSW-1

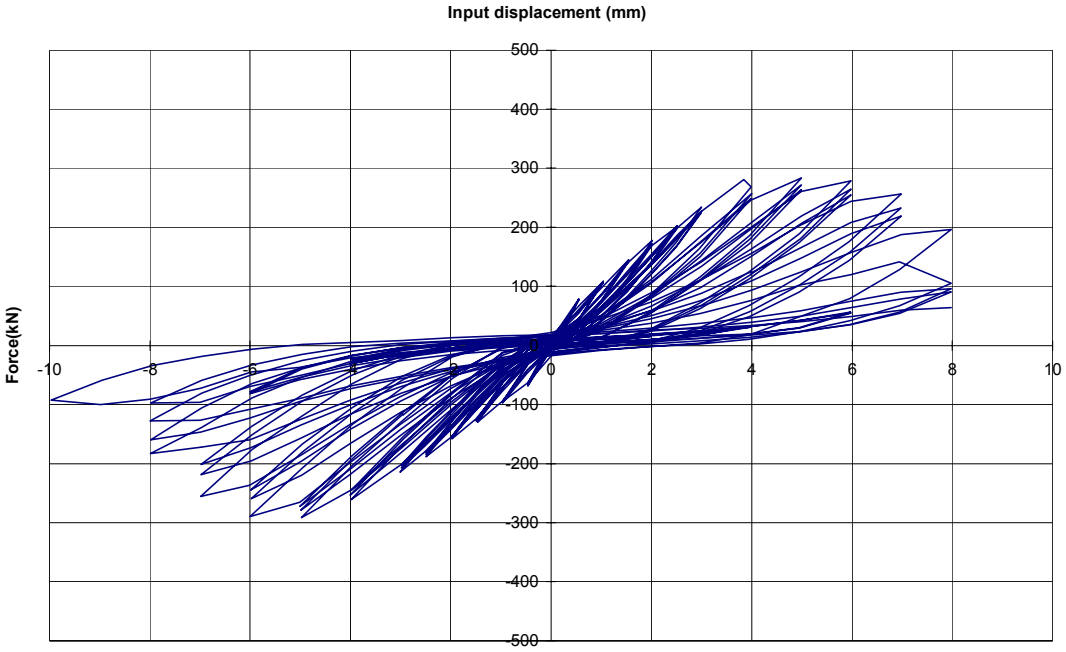

Figure 4.2: Force - displacement diagram for HSW-2

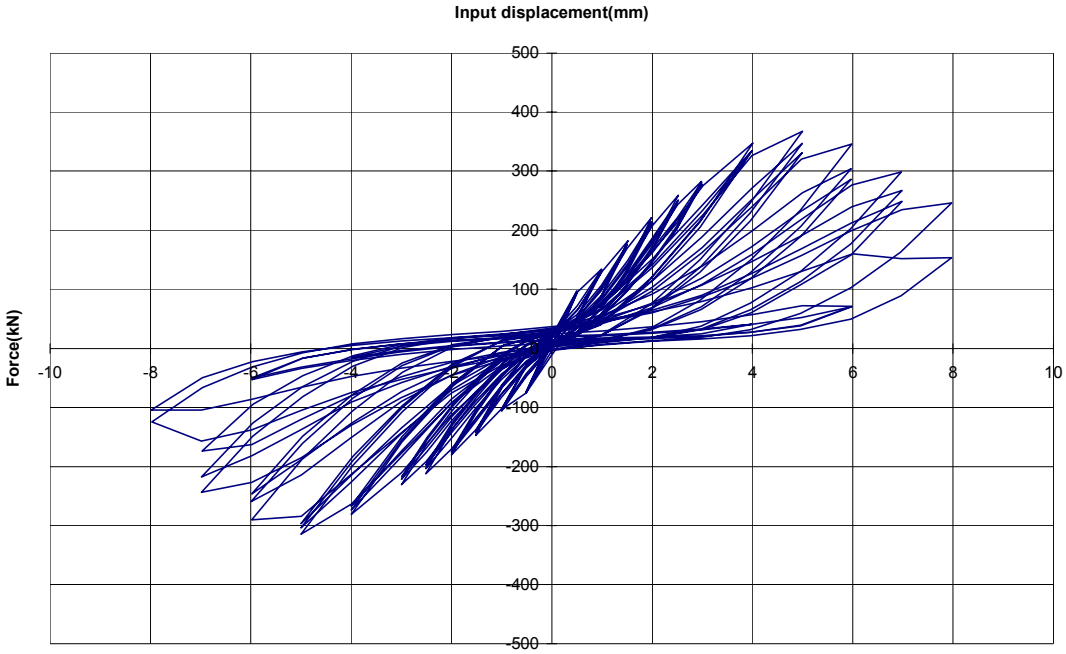

Figure 4.3: Force- displacement diagram for HSW-3

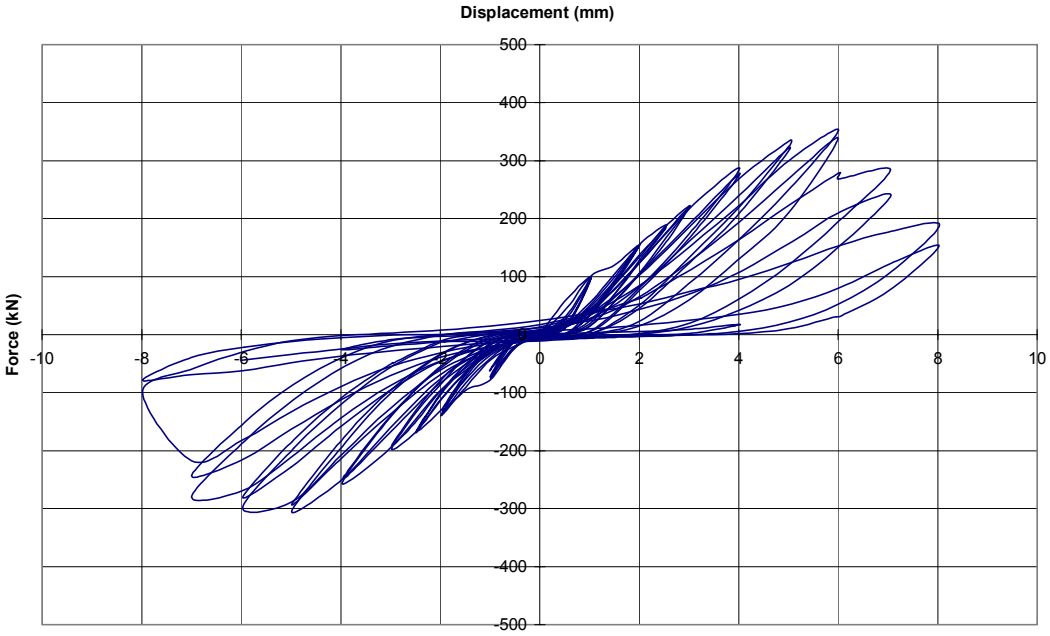

Figure 4.4: Force - Displacement diagram for HSW-4

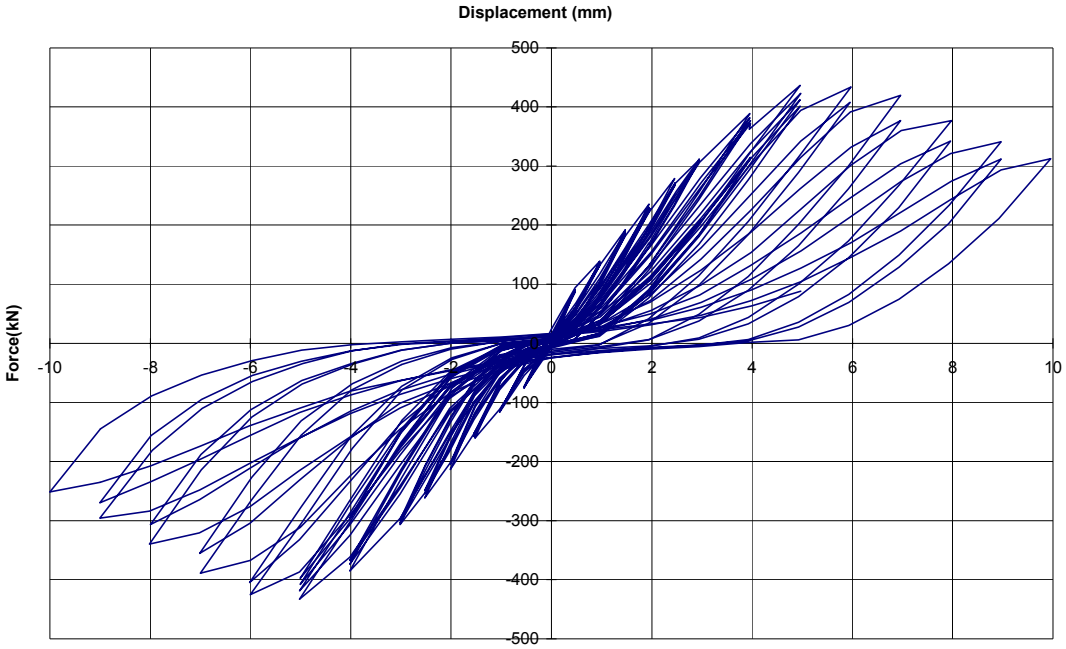

Figure 4.5: Force - Displacement diagram for HSW-5

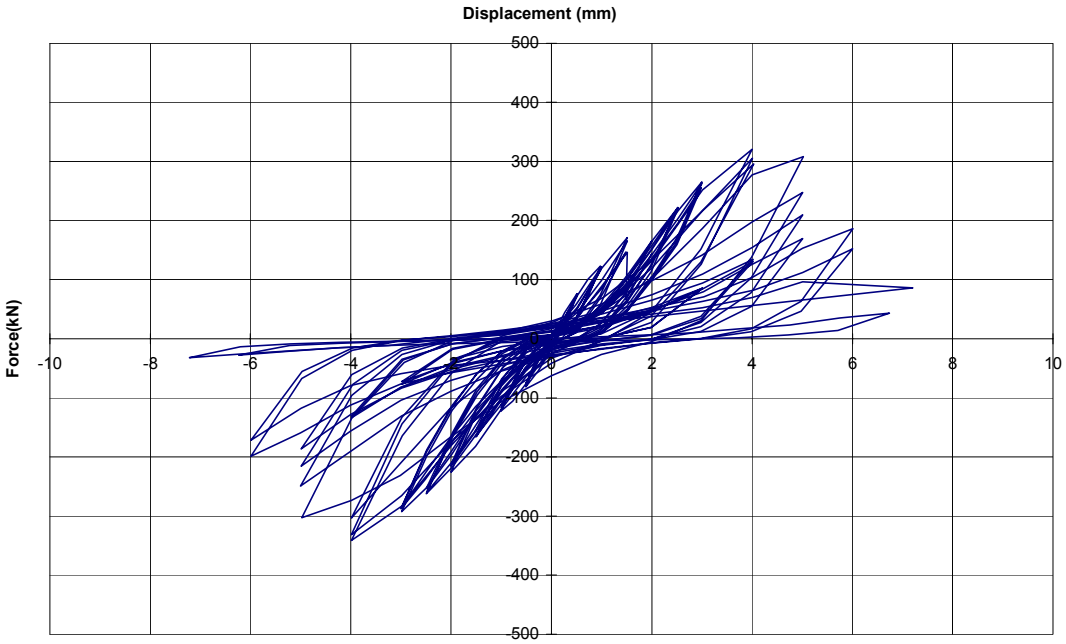

Figure 4.6: Force - Displacement diagram for HSW-6

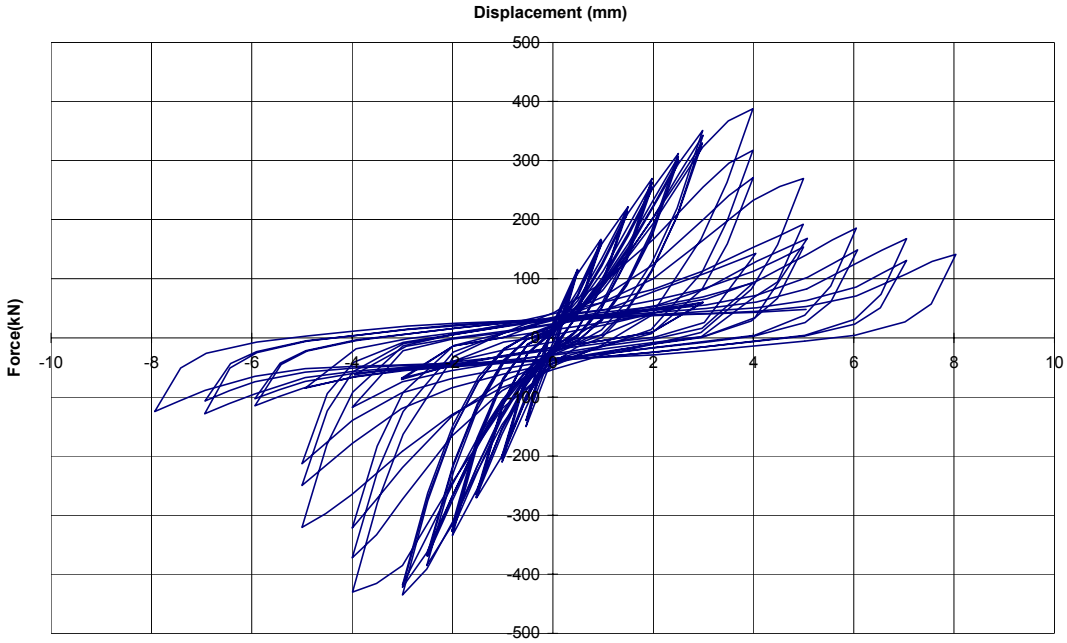

Figure 4.7: Force - Displacement diagram for HSW-7

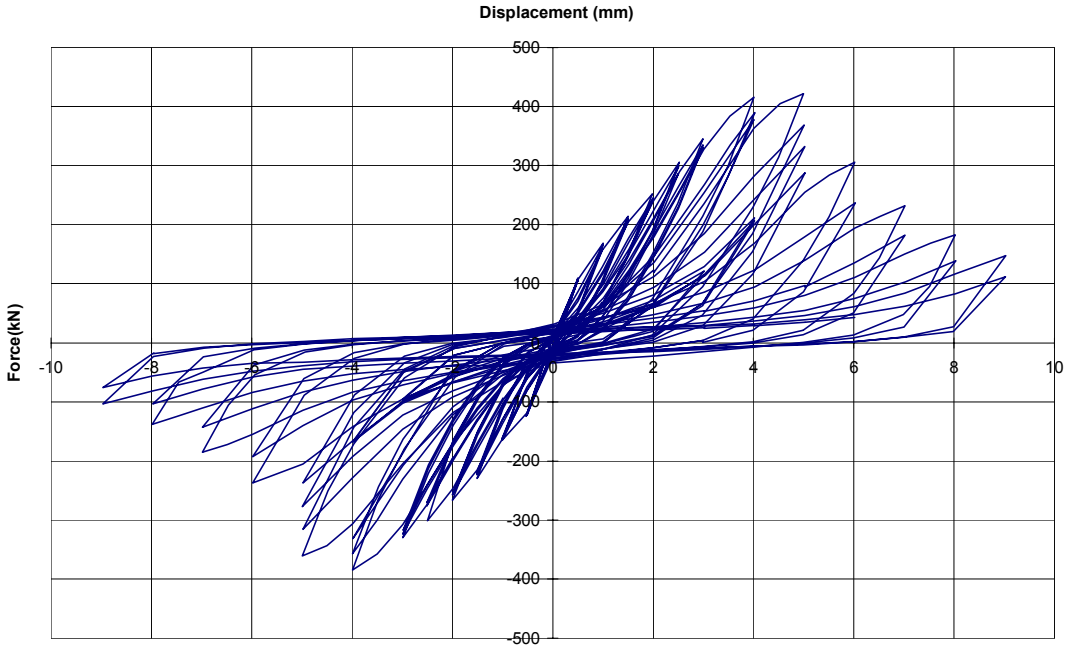

Figure 4.8: Force - Displacement diagram for HSW-8

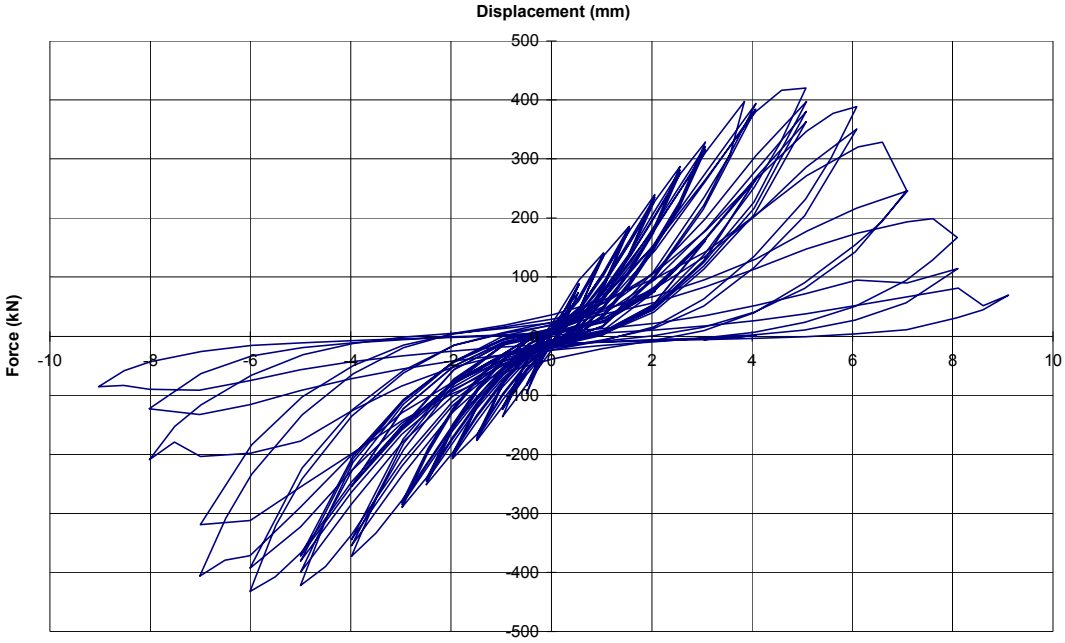

Figure 4.9: Force - Displacement diagram for HSW-9

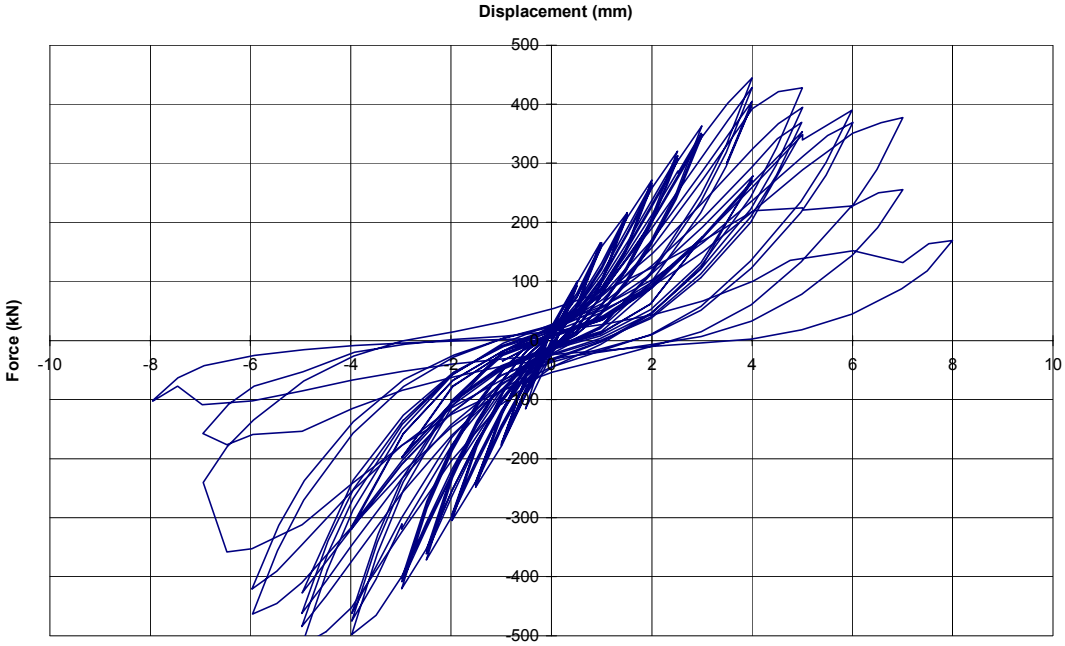

Figure 4.10: Force - Displacement diagram for HSW-10

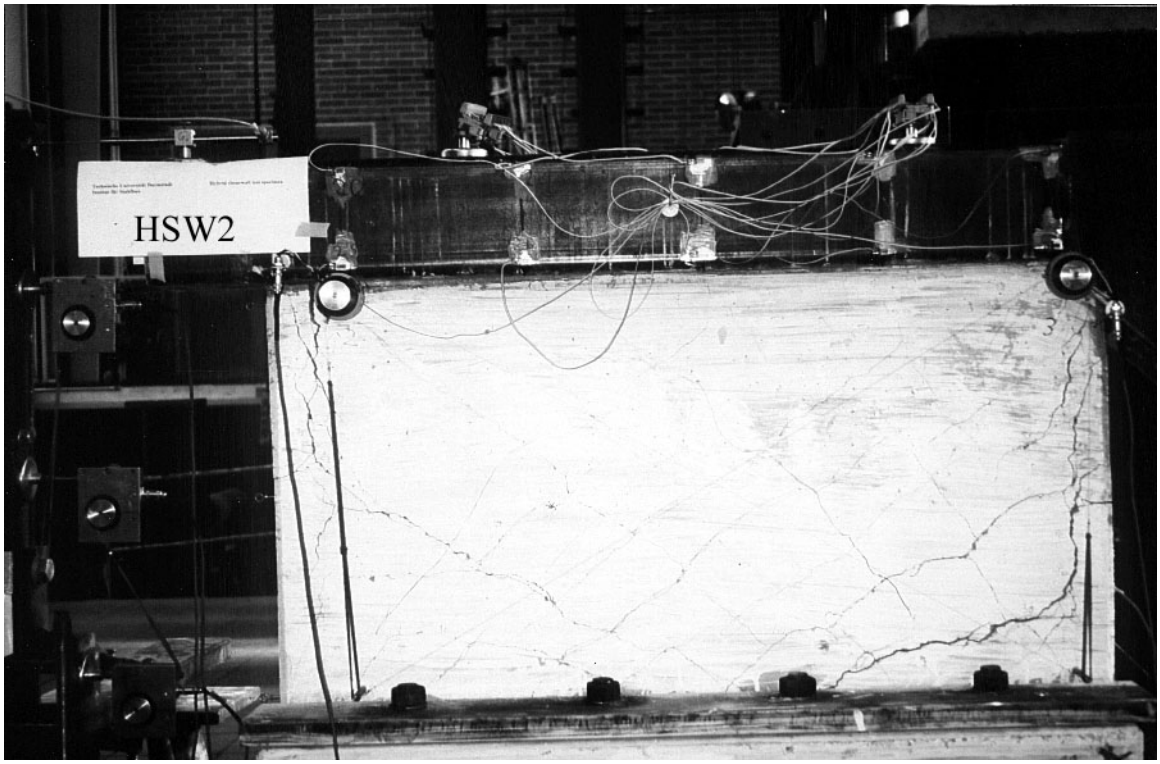

Figure 4.11: Cracking pattern of Specimen HSW2

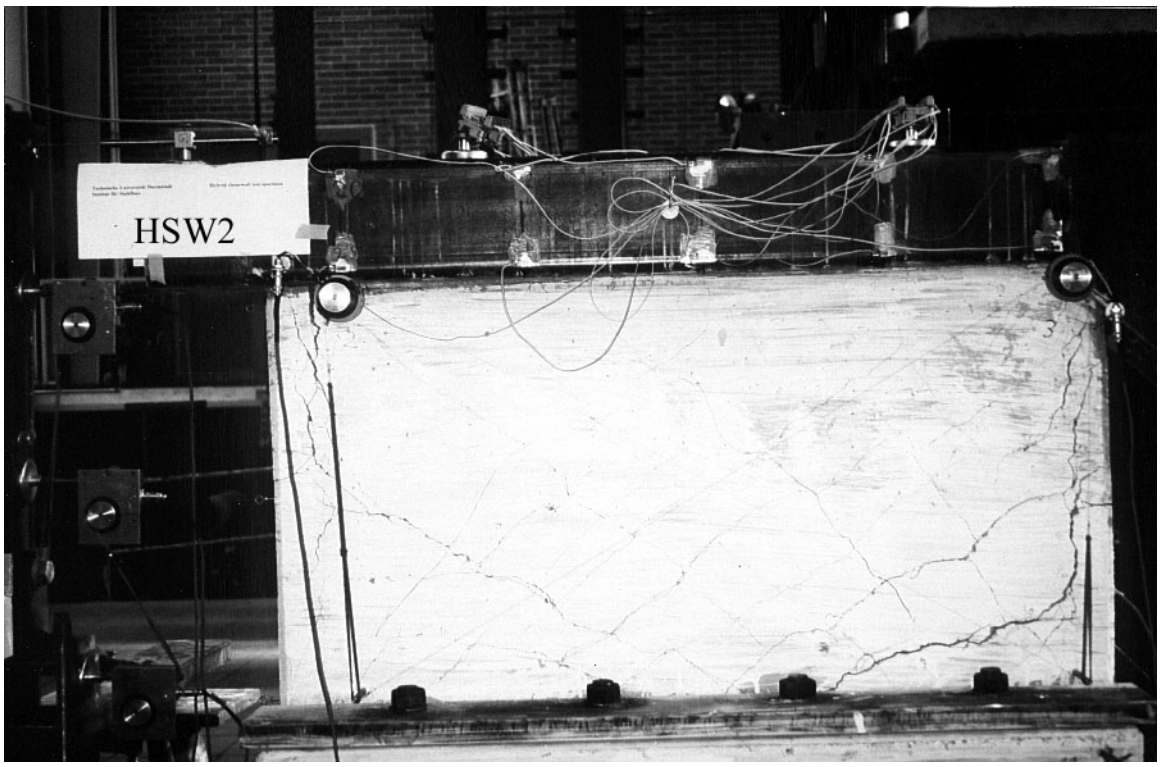

Figure 4.12: Cracking pattern of Specimen HSW2

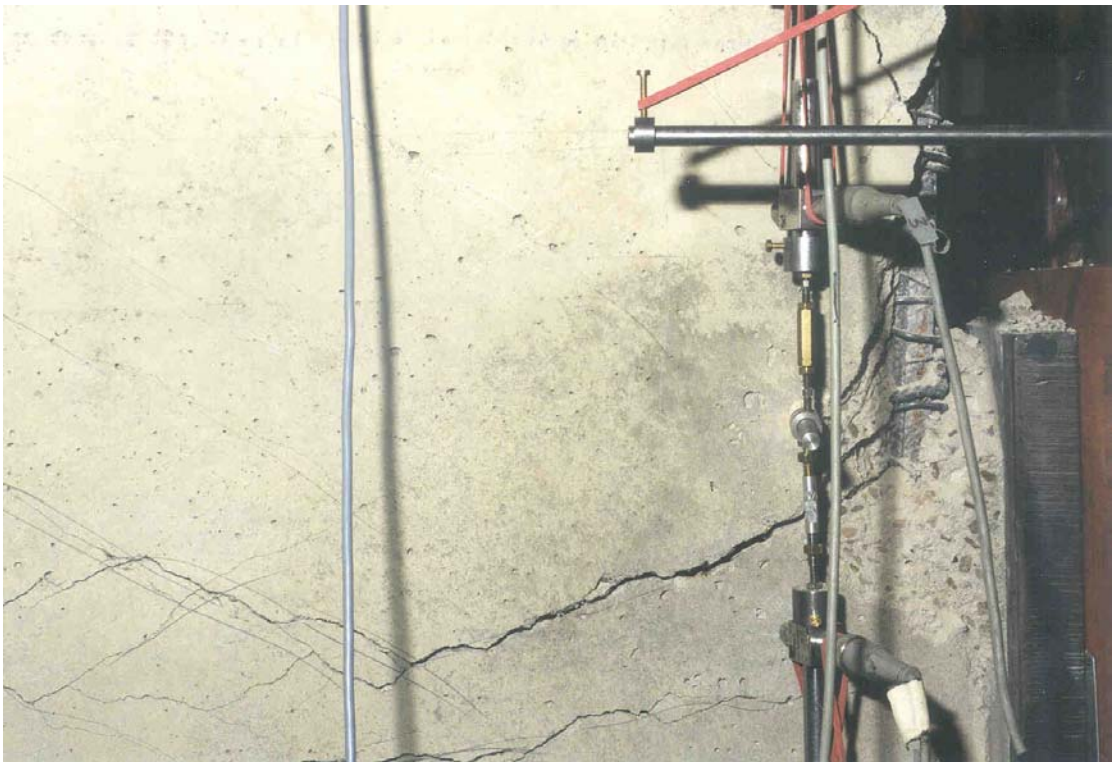

Figure 4.13: Cracking pattern of Specimen HSW2

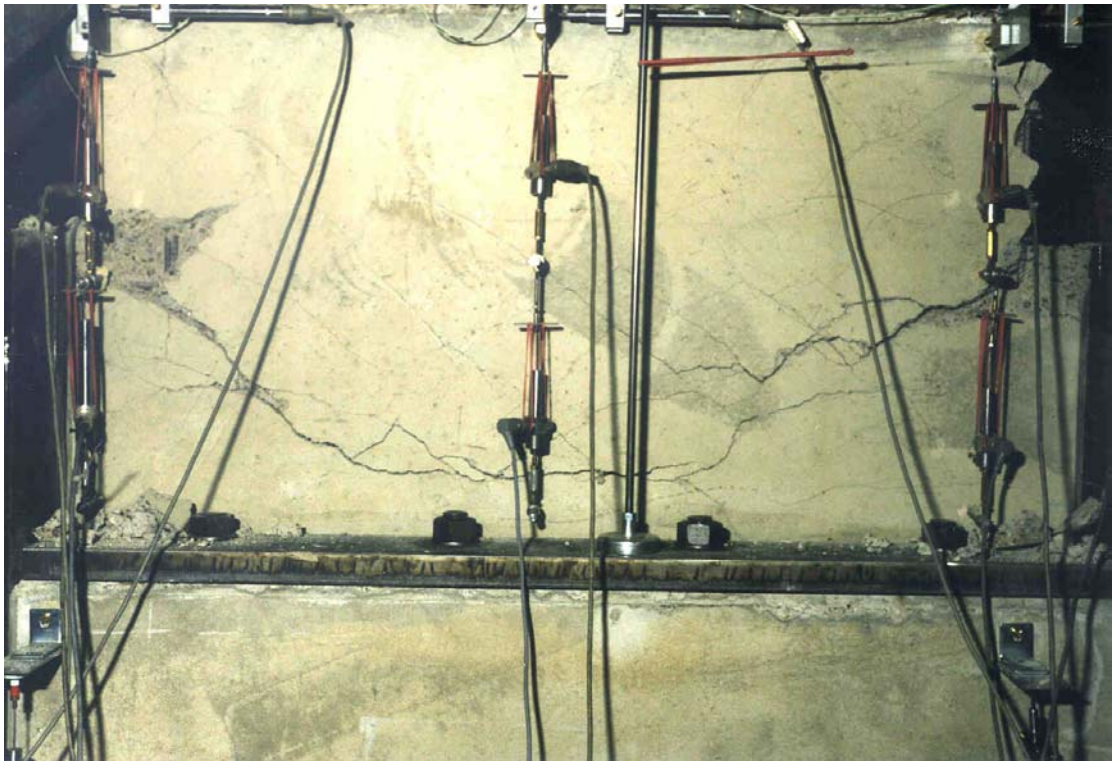

Figure 4.14: Cracking pattern of Specimen HSW2

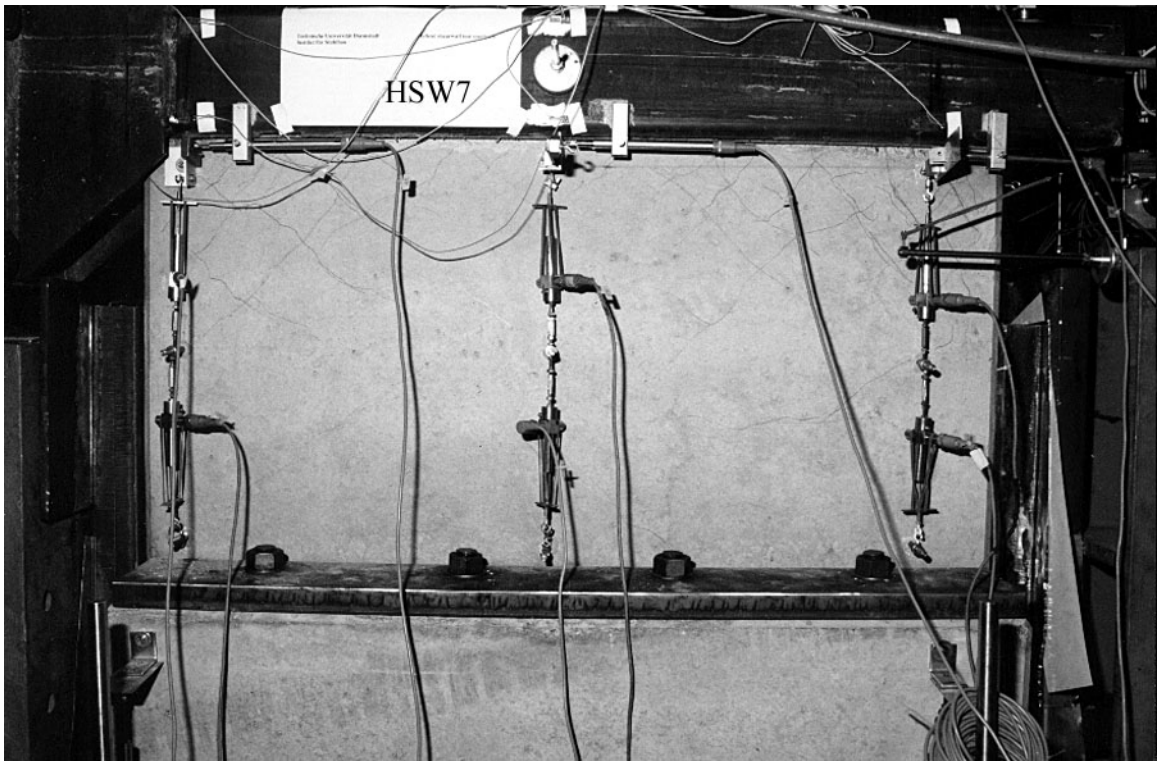

Figure 4.15: Cracking pattern of specimen HSW7, front view

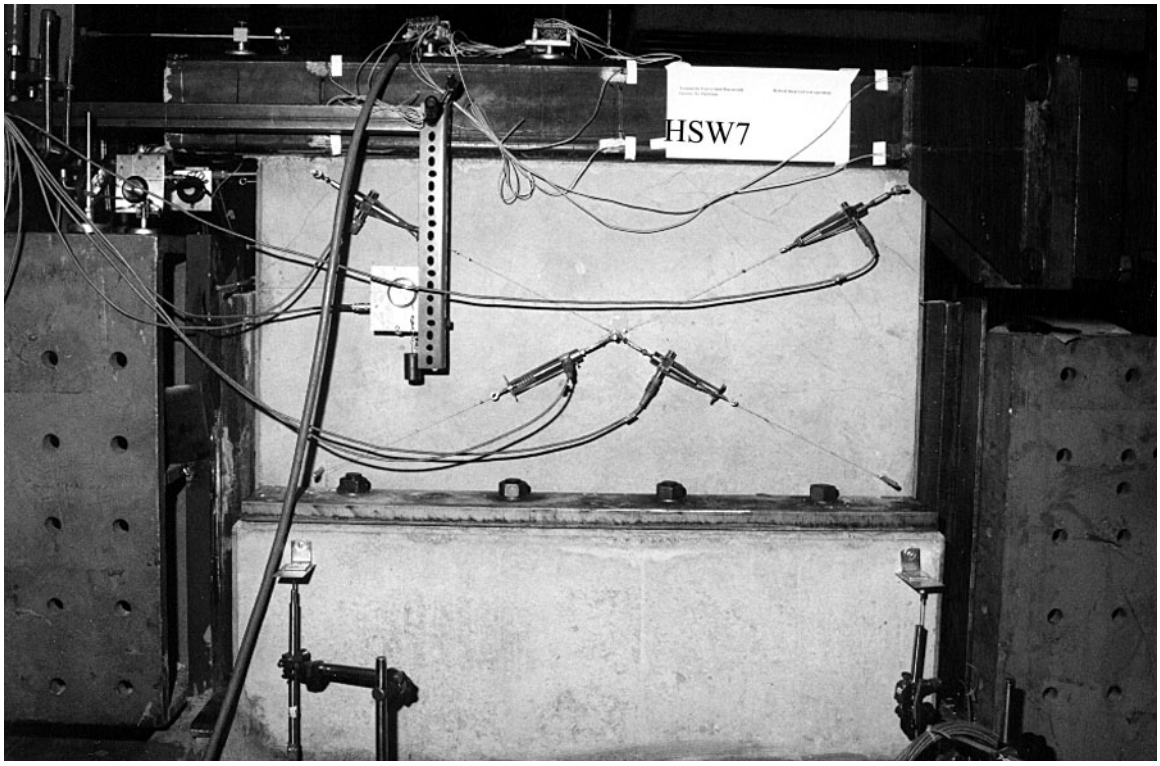

Figure 4.16: Cracking pattern of specimen HSW7, back view

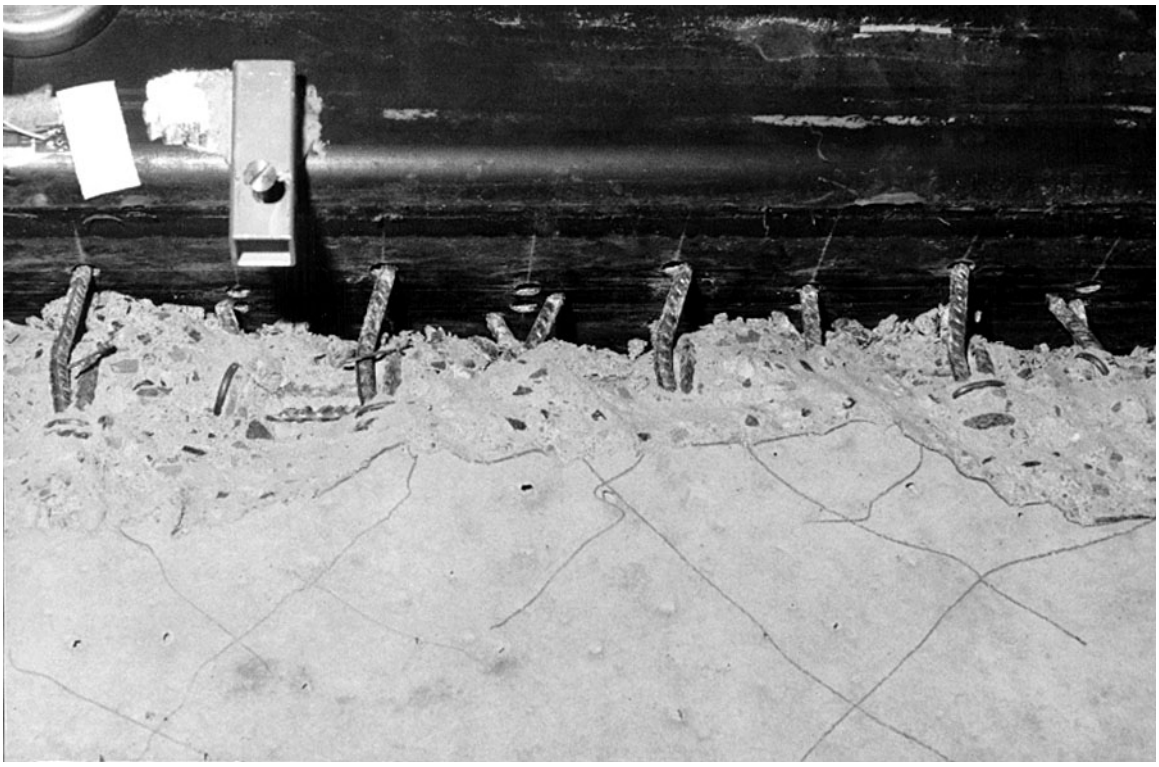

Figure 4.17: Cracking pattern of Specimen HSW7 at failure stage

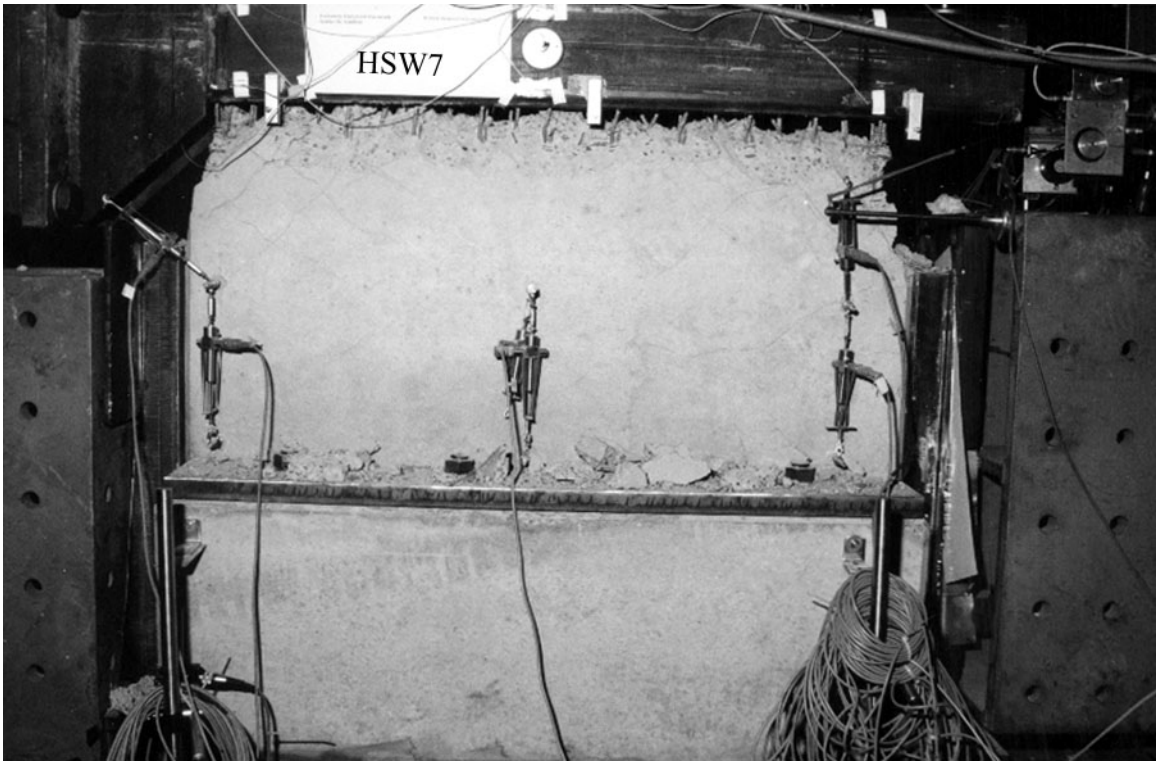

Figure 4.18: Cracking pattern of Specimen HSW7 at failure stage

4.3 Shear Force – Shear Distortion

4.3.1 Test serie 1

In principle, the shear distortion of the wall panel can be derived from several displacement measurements. In case the bending deformation of the wall is small, as in the present case of squat walls, the shear distortion can be expressed by considering the horizontal displacement measured by the linear displacement potentiometers (LVDTs) at the edge of the panel (SZ2 in Fig. 3.10). In fact, in case the longitudinal slip along the interface between the composite column and concrete shear wall panel is negliable, also the displacement test-control values could be used directly. Even in case of larger slippage between column and wall, the control displacement values can be used, provided that these values are corrected by the measured slippage.

In general, considering that the deformation of the panel is a direct result of both shear and bending distortions of the panel, the average shear strain in the wall panel can be evaluated by considering the displacement measurements recorded by the two pairs of diagonally placed LVDTs (W10 + 11, and W12 + 13 in Fig. 3.10).

The general shear and bending moment distortion of the panel is shown in Figure 4.19. Considering the panel deformations along each of the diagonals in general terms, as expressed in equations 4.1 and 4.2, the average shear distortions can be calculated by equation 4.3. In the present test setup the gage length of both diagonals is the same.

$$d_1' = \sqrt{(h - x_2)^2 + (l + \Delta_2)^2} \tag{4.1}$$

$$d_2' = \sqrt{(h + x_1)^2 + (l - \Delta_1)^2} \tag{4.2}$$

$$\gamma_{ave} = \frac{(d_1' - d_1)d_1 - (d_2' - d_2)d_2}{2hl} \tag{4.3}$$

In Figures 4.20 thr. 4.24, the average shear strains have been calculated by the above formula and are presented graphically versus the cyclic displacement-controlled forces. In fact, because of the limited slippage along the interface and the squat nature of the wall (negliable bending distortions), the results are in close agreement with results derived directly from the test control displacements and the horizontal panel deformations recorded by SZ2.

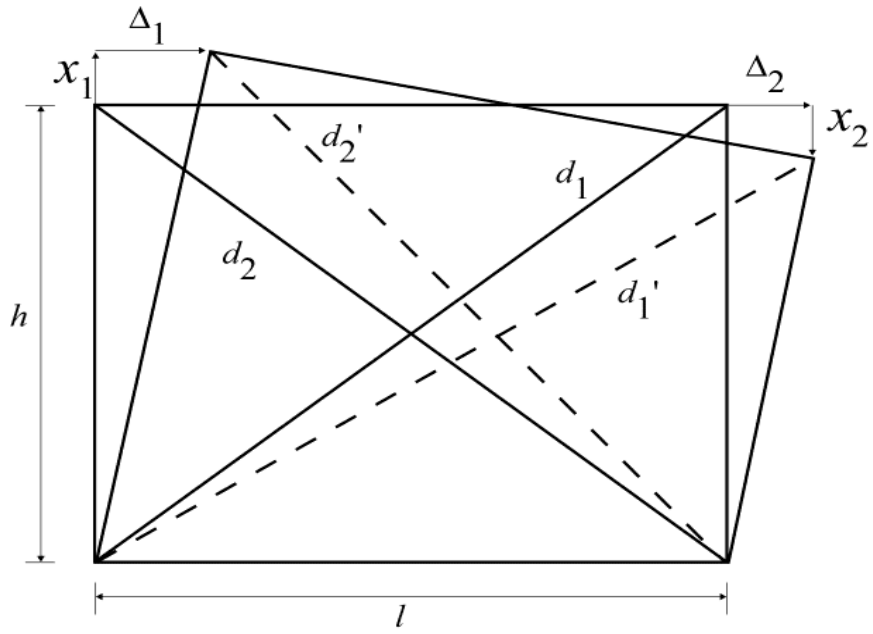

Figure 4.19: shear strain - displacement relationship

4.3.2 **Test serie 2**

In the 2nd test series, the test specimens were supported on the side to prevent an unrealistic bending failure of the wall panel. In this case the shear strain, which was to be presented graphically against the applied cyclic load, was determined by considering the shear distortion of the wall panel resulting from the difference between the test displacement and the slippage along the interface. The relationship between shear strain and test load are pre-

sented graphically in Figures 4.25 – 4.29. The shear strain values under maximum loads are similar to those observed in the 1st test series. This is not surprising as the shear resistance of the panels – because of the same mesh reinforcement for all specimens – should basically lead to the same shear resistance and associated shear distortion at failure.

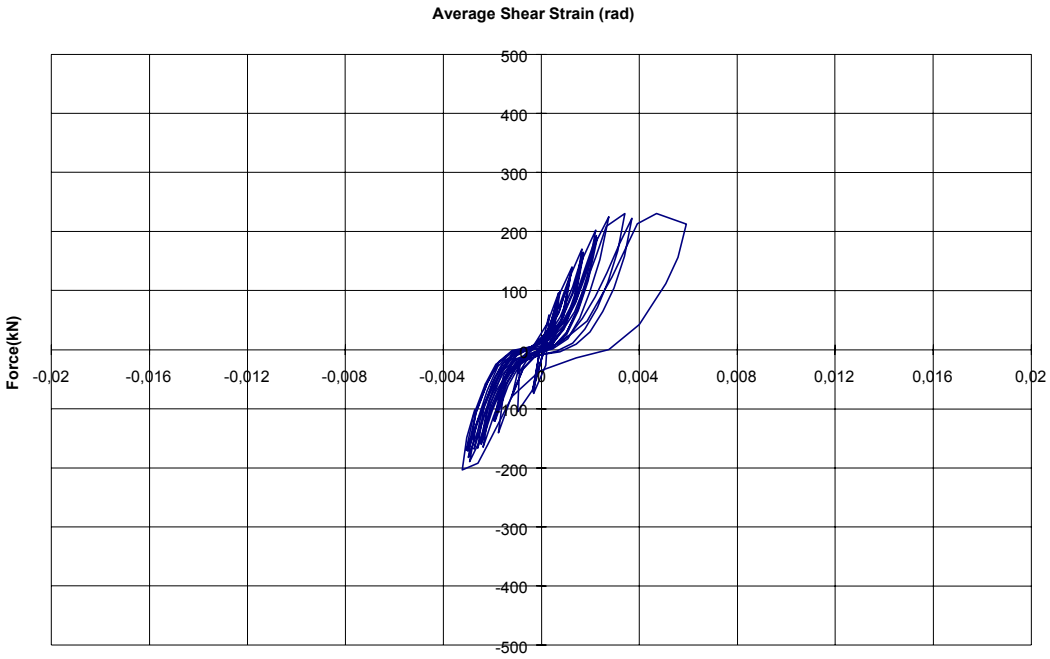

Figure 4.20: Applied Force - Average Shear Strain (rad) for HSW-1

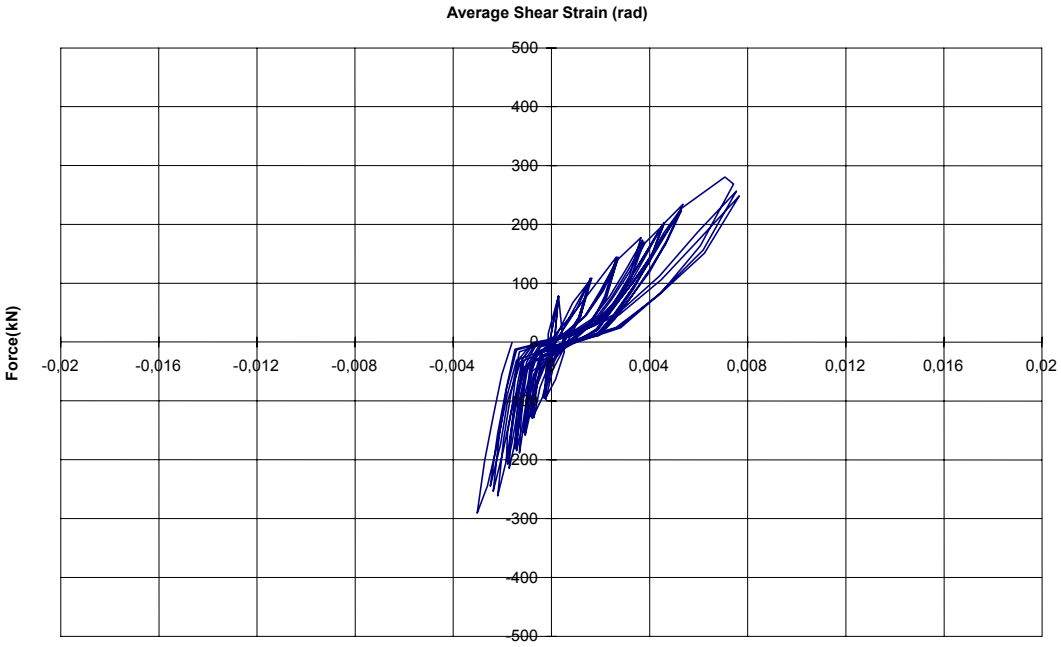

Figure 4.21: Applied Force - Average Shear Strain (rad) for HSW-2

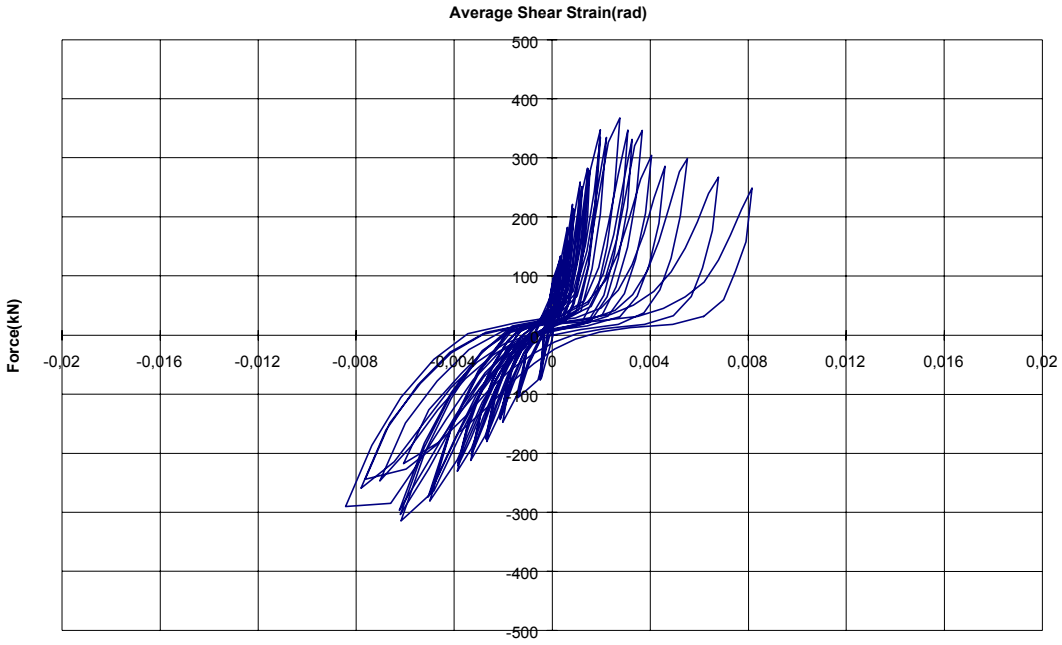

Figure 4.22: Applied Force - Average Shear Strain (rad) for HSW-3

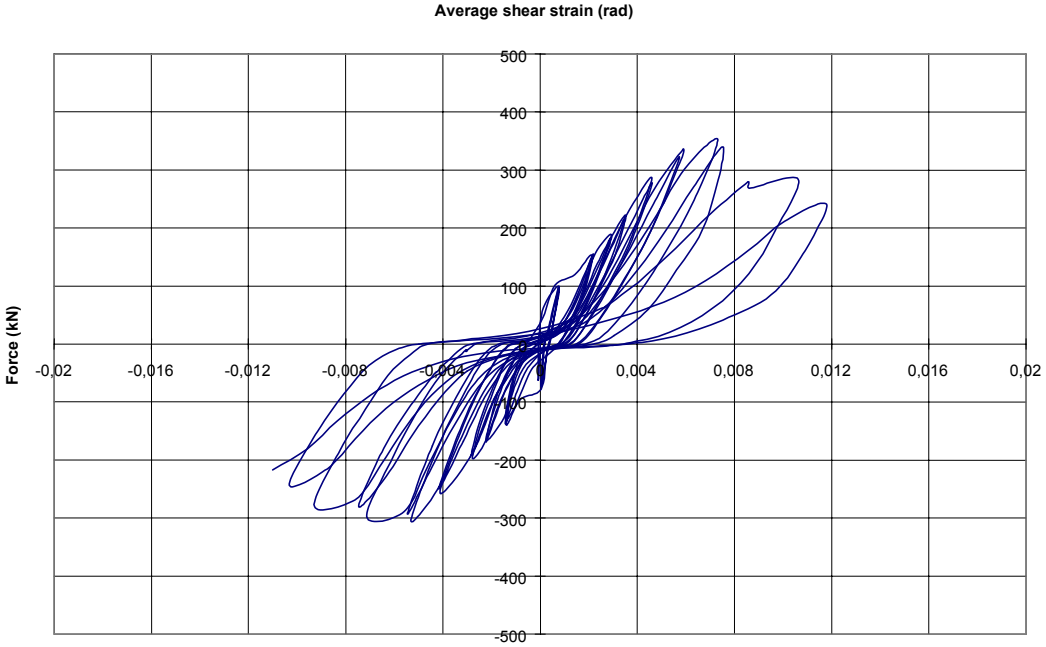

Figure 4.23: Applied Force vs. Average Shear Strain (rad) for HSW-4

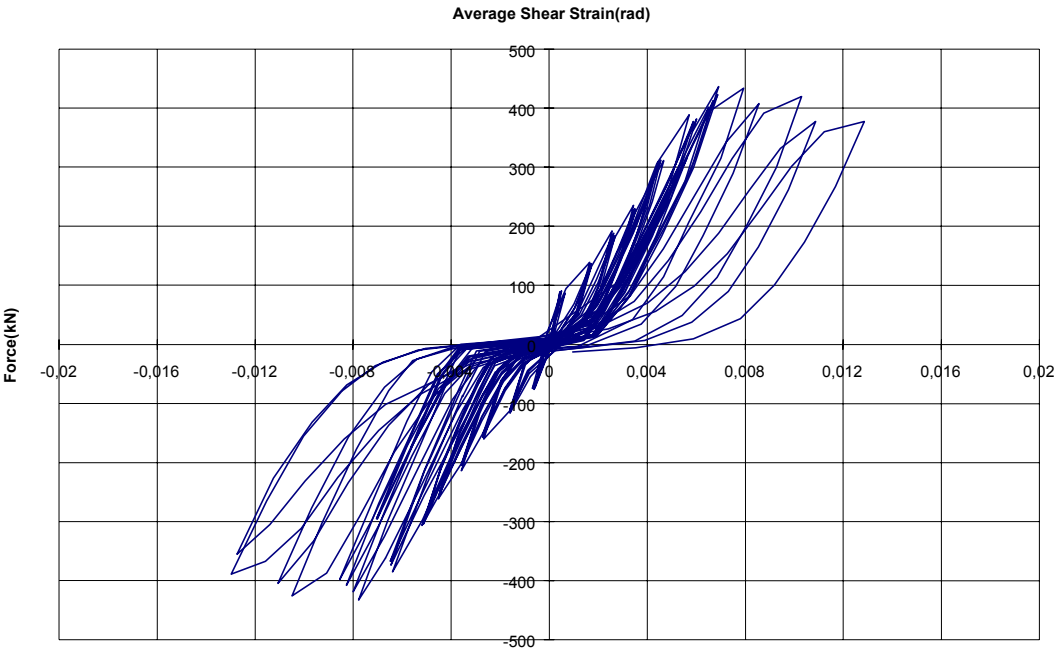

Figure 4.24: Applied Force - Average Shear Strain (rad) for HSW-5

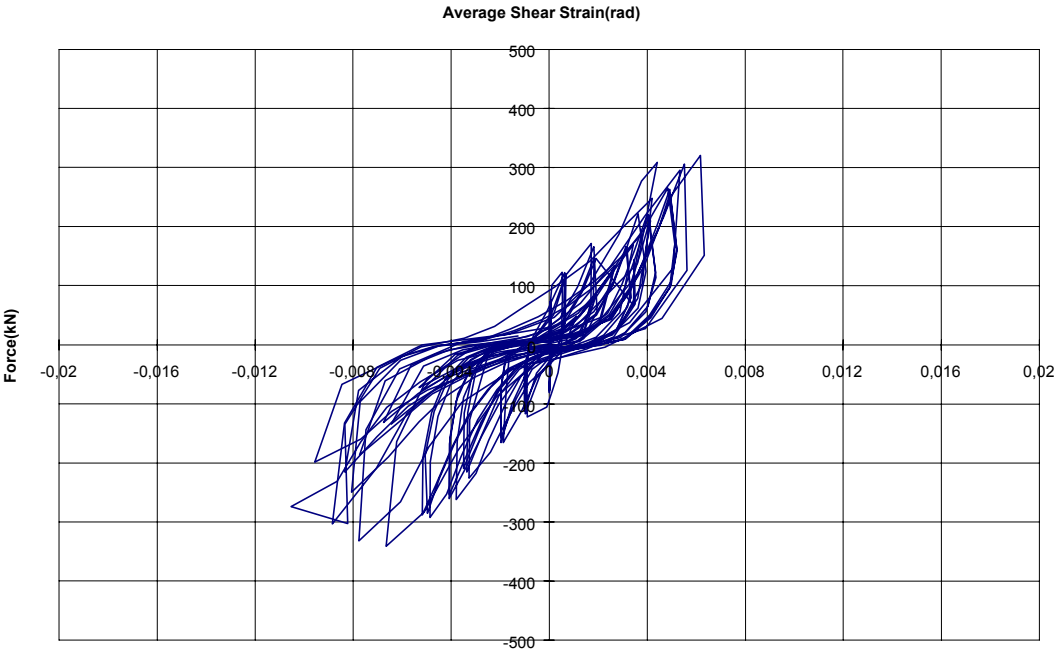

Figure 4.25: Applied Force - Average Shear Strain (rad) for HSW-6

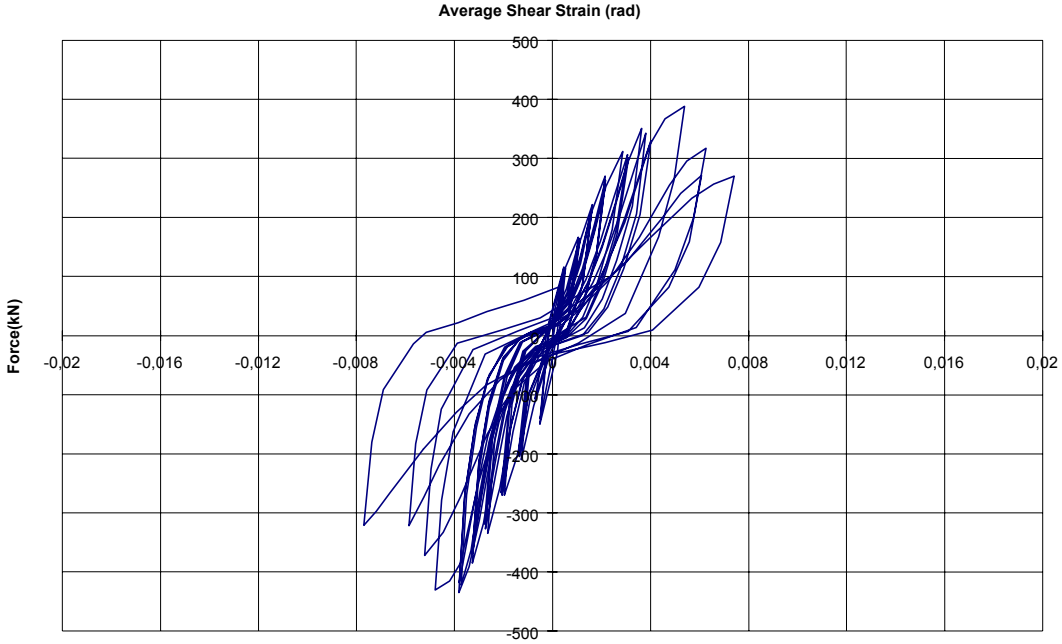

Figure 4.26: Applied Force - Average Shear Strain (rad) for HSW-7

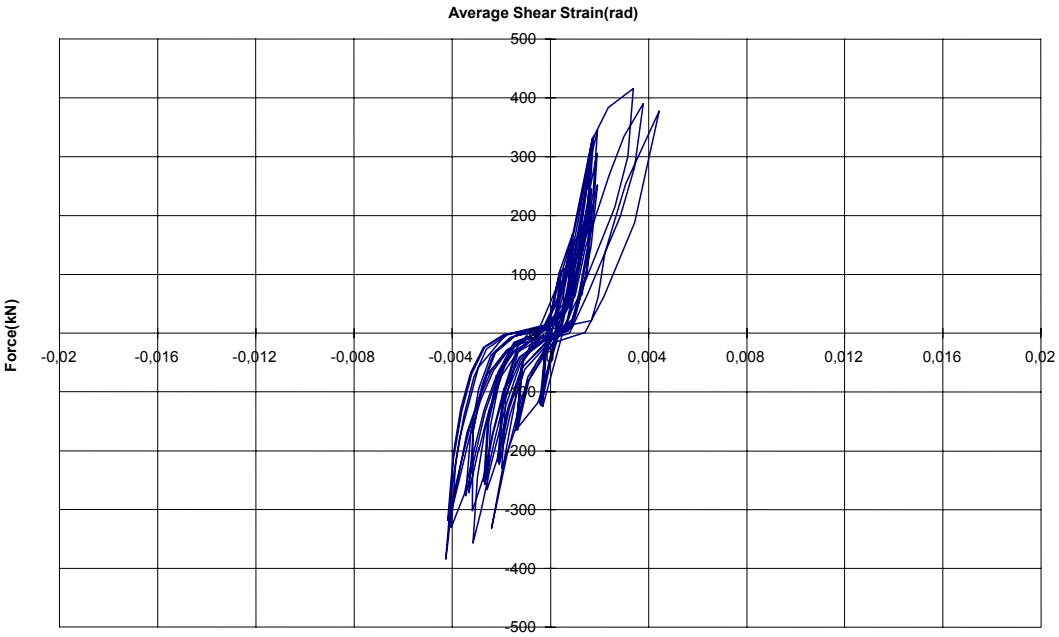

Figure 4.27: Applied Force - Average Shear Strain (rad) for HSW-8

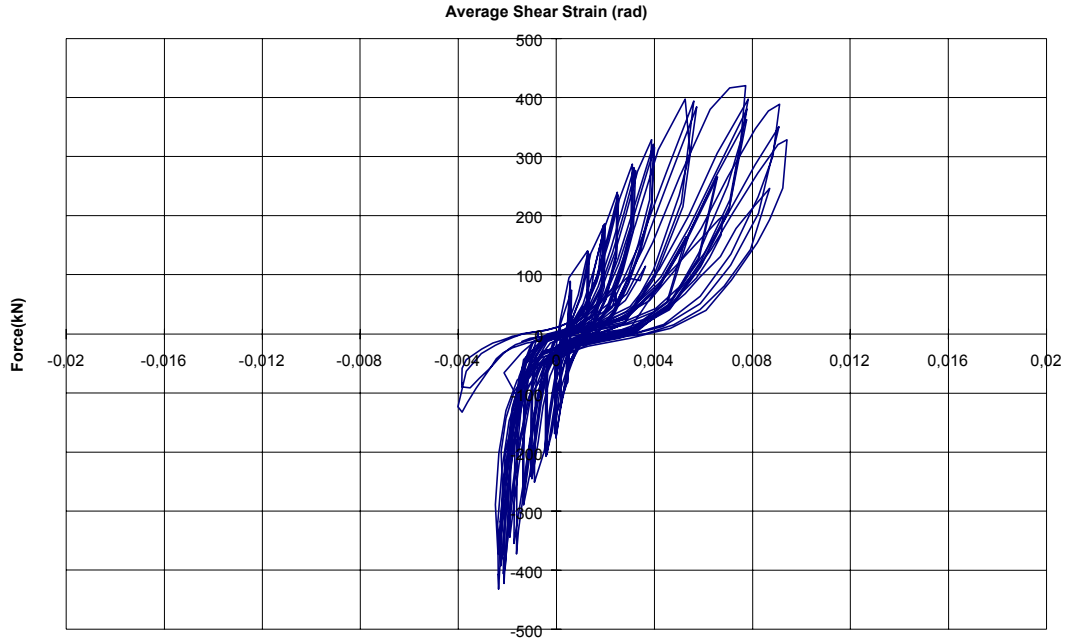

Figure 4.28: Applied Force - Average Shear Strain (rad) for HSW-9

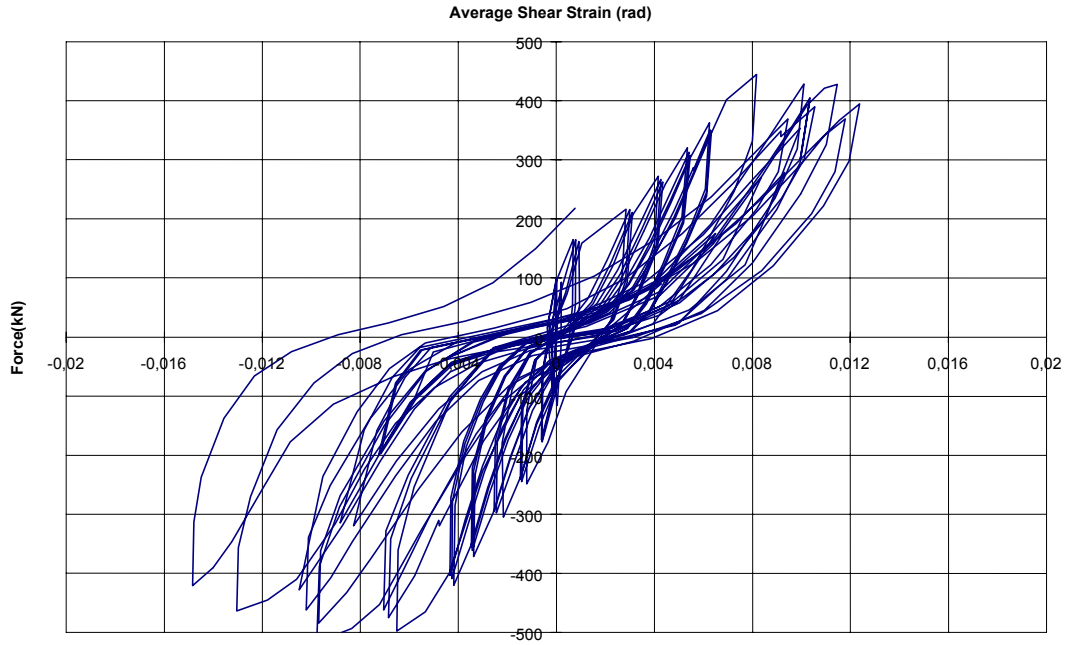

Figure 4.29: Applied Force - Average Shear Strain (rad) for HSW-10

4.4 Force – Slip relationship

4.4.1 Test serie 1

The slip of the column relative to the RC wall panel has been recorded at three locations along the length of the column member. In as far as in both test series the recorded slip displacements at these locations were virtually the same under increasing loads (reflecting a rather uniform load transfer), the slip recorded at the middle section was used in preparing the graphs showing the force-slip relationship.

For the first series of tests the force-slip graphs for the 5 specimens of Series 1 are presented in Figures 4.30 thr. 4.34. Considering that, for Specimens HSW1 thr. 4, the slip values under maximum load were only 0.3 to 0.5 mm (Figs. 4.30 – 4.33) as compared to total test displacements of +/- 4 to 6 mm at maximum load (Figs. 4.1 – 4.4), it is obvious that the concrete panel sustained considerable shear distortion. In as far as the tests were to evaluate the efficiency of different interface connection designs, the results of limited slip and significant shear panel deformations – resulting in shear cracking and ultimate bending failure of the panel – did not allow an assessment of the possible interface connection design solutions. Hence, it was decided for the specimens to be tested in Series 2, to effectively strengthen the panel by supporting the panel up to its mid-height. Considering that in Specimen HSW5 the anchorage bars were welded to the steel tubular column wall, the slip should of course be virtually nil as supported by the results shown in Fig. 4.34.

4.4.2 Test serie 2

Similar as for the test specimens tested in Series 1, also in the second test series, the force applied to the specific test specimen has been presented in relation to the slip of the edge member column relative to the shear wall, as measured by LVDT W15 (see Figure 3.10).

The results are presented in Figures 4.35-4.39. The results clearly show that the specimens with straight anchorage bars (HSW6, 7 and 8) exhibited considerable slippage along the column-wall interface. On the otherhand, the specimens HSW8 and 9, with diagonally oriented achorage bars, showed only a limited amount of slippage.

In these tests, response of the specimens changed as the number of cycle of the loading and level of loading increased. This is illustrated in Figure 4.40, which shows typical force - slip curves at different stages of loading. Response to succeeding cycles of loading is characterized by a low shear stiffness at a low value and a gradual increase in shear stiffness with increase in shear in both positive and negative directions. As the number of load cycles increases, the shear stiffness at low shears decreases and the increase in stiffness with increase in shear becomes greater. This causes the shear-slip curve for a complete loading cycle to assume a progressively more pinched shape as the number of loading cycles increases. For the specimens with failure at IFC, the max slip of +/- 3.5 mm with the spalling of concrete adjacent to IFC is observed. The amount of the slip is proportional to load carrying capacity and correspondingly amount and distribution of reinforcing bars at IFC. The slip, measured against a 7 cm gage length, reaches for the first three specimens, with straight anchor bars and welded shear studs (in Specimen 8 only), displacements of close to +/- 3.5 mm. For the specimens with diagonal anchorage bars, the slip reaches maximum values of between 0.5 and 1.5 mm. In the case of the diagonal reinforcement the shear transfer strength was about 25 % greater than in the case of straight reinforcement. A plot of maximum envelop of the force - slip relationships are also given in Figures 4.41 - 4.45. These envelop curves are used to develope an idealized cyclic force - slip relationship in the next chapter.

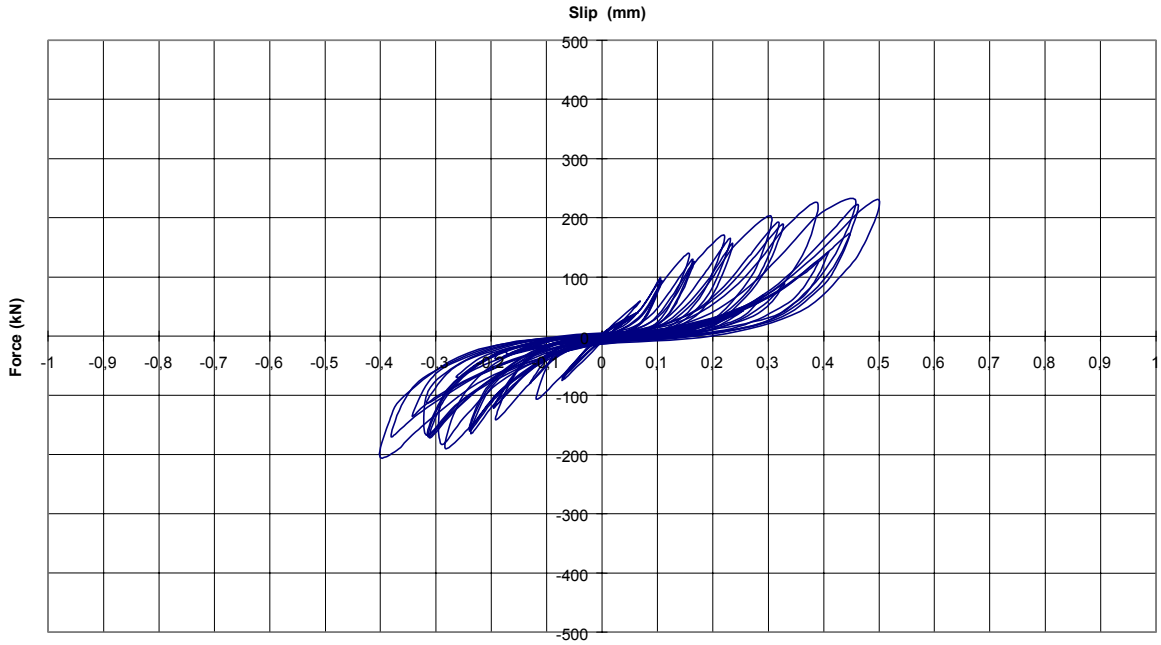

Figure 4.30: Force - slip diagram for HSW-1

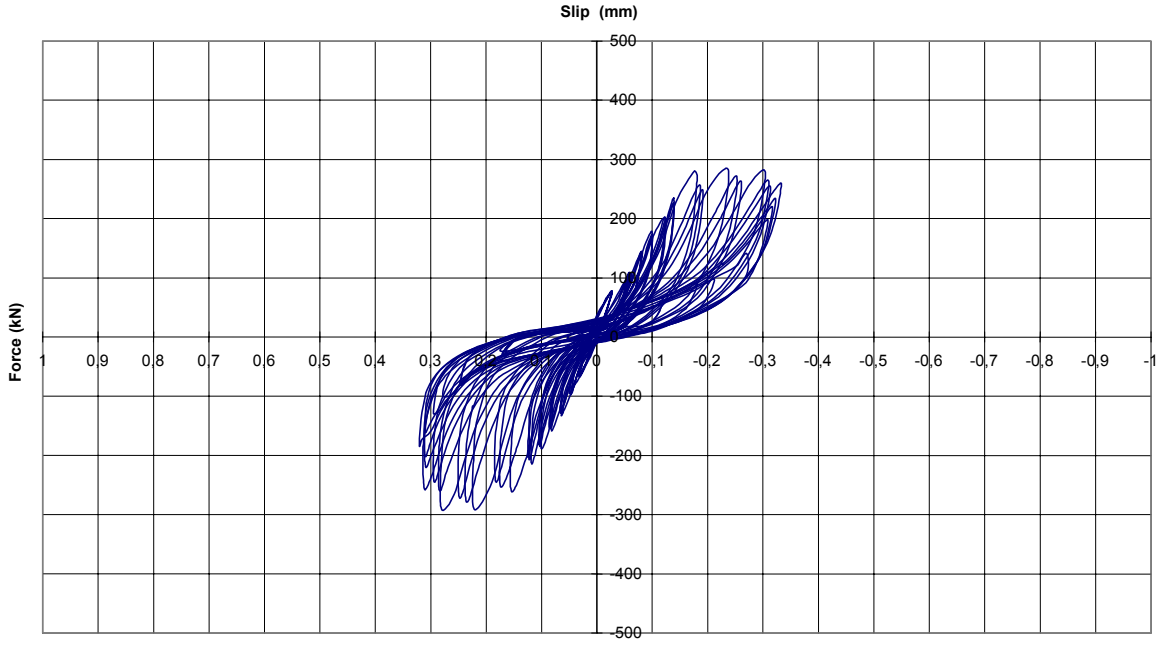

Figure 4.31: Force - slip diagram for HSW-2

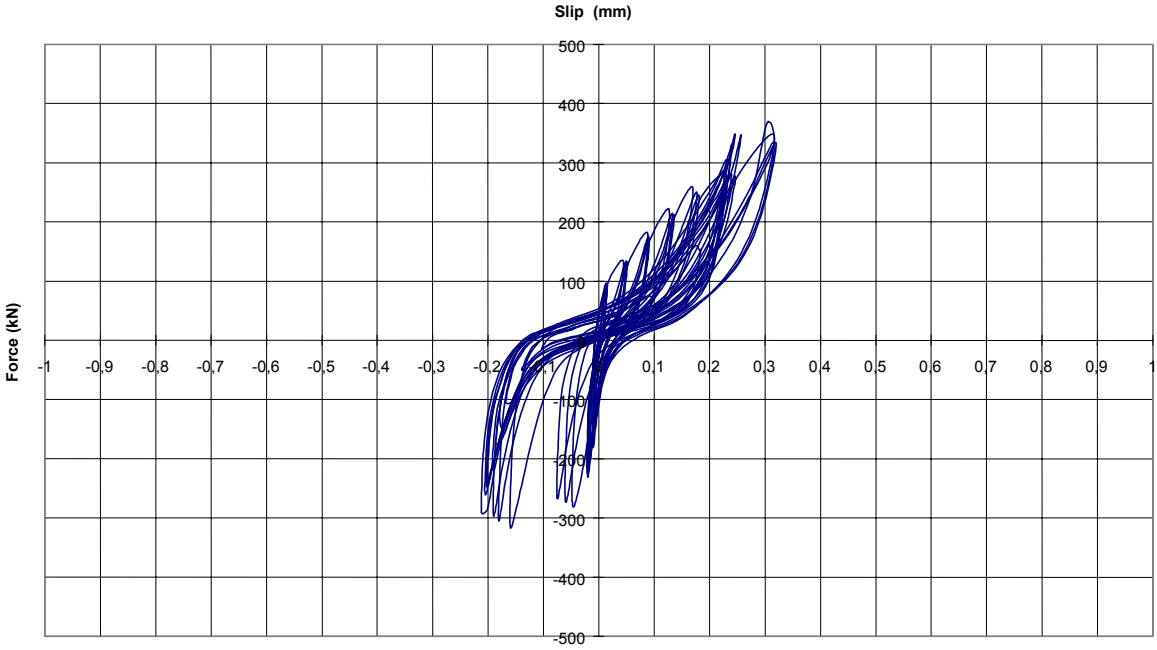

Figure 4.32: Force - slip diagram for HSW-3

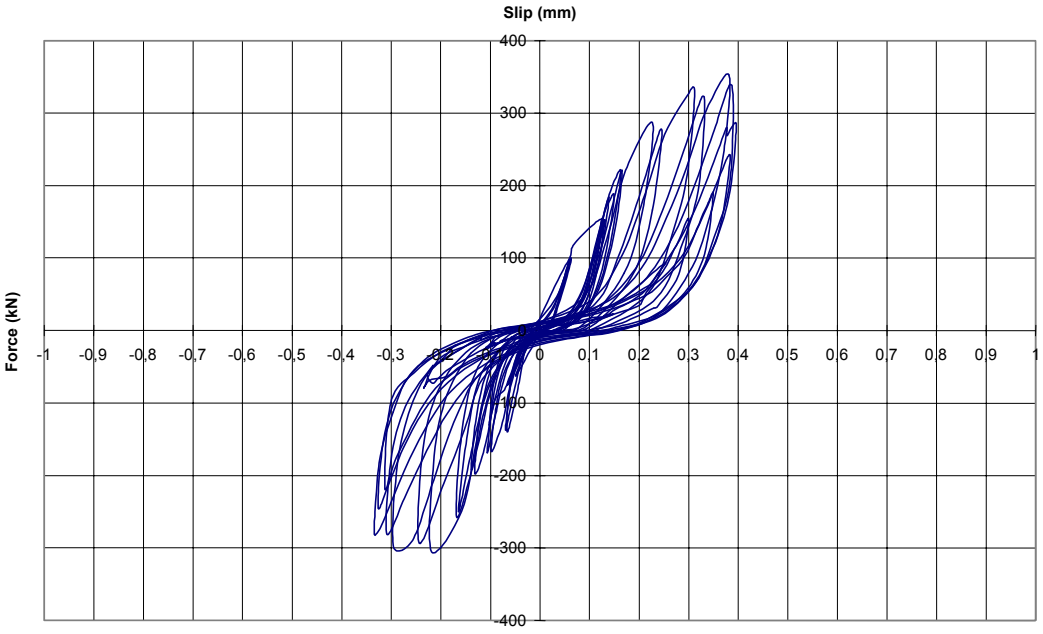

Figure 4.33: Force Slip diagram for HSW-4

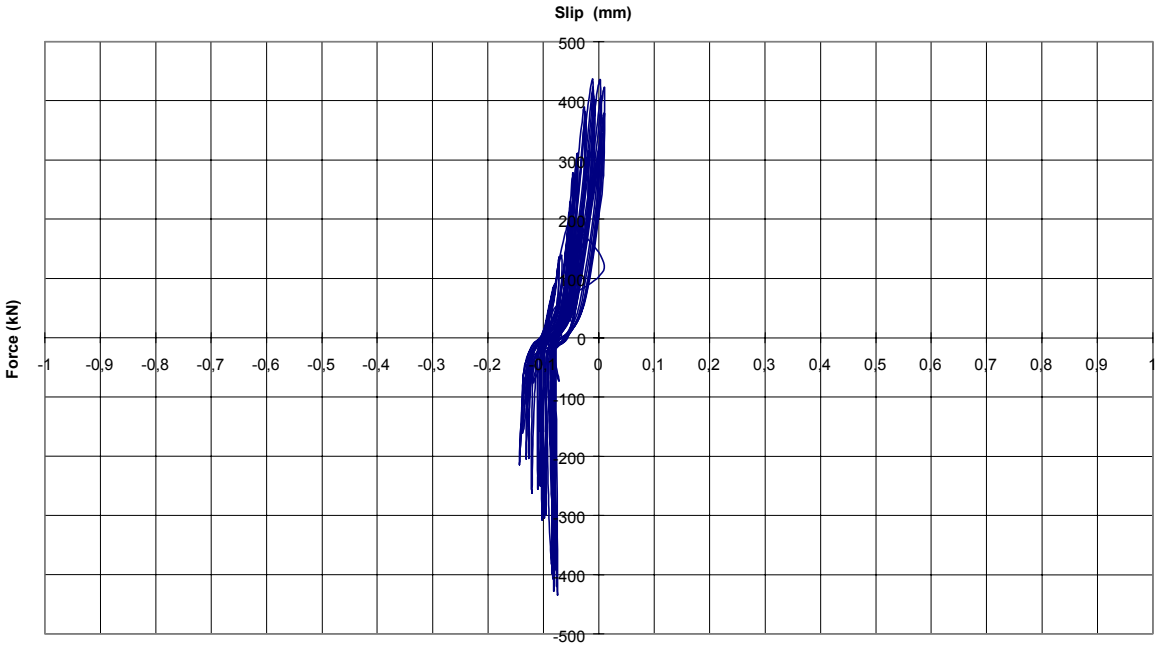

Figure 4.34: Force - Slip diagram for HSW-5

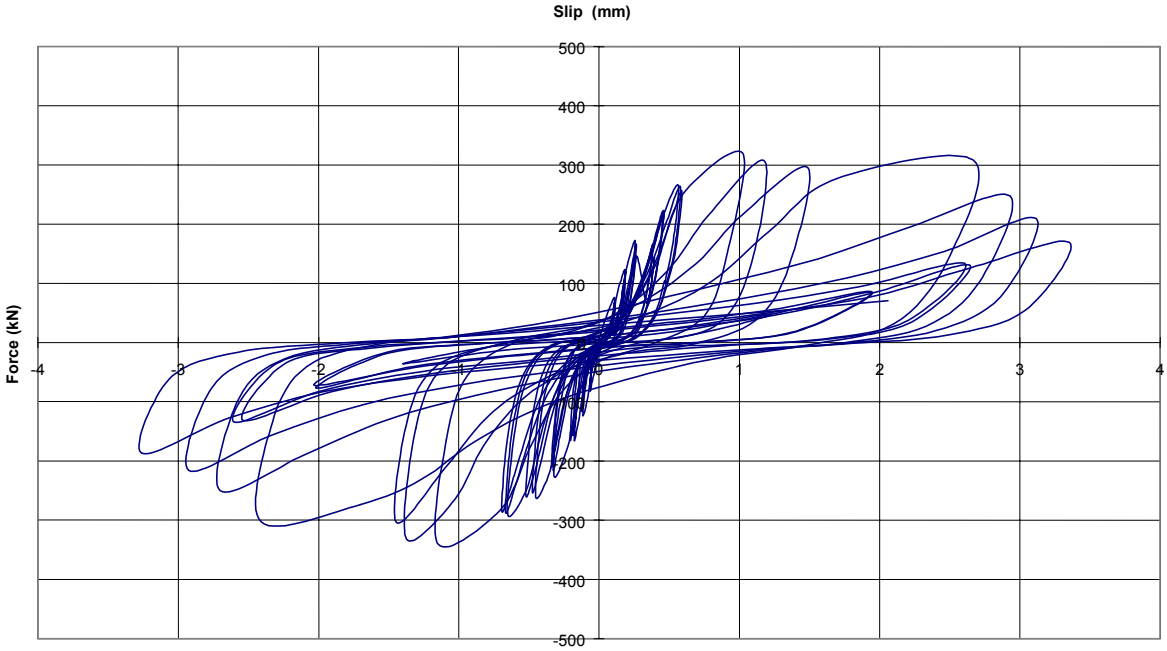

Figure 4.35: Force - slip diagram for HSW-6

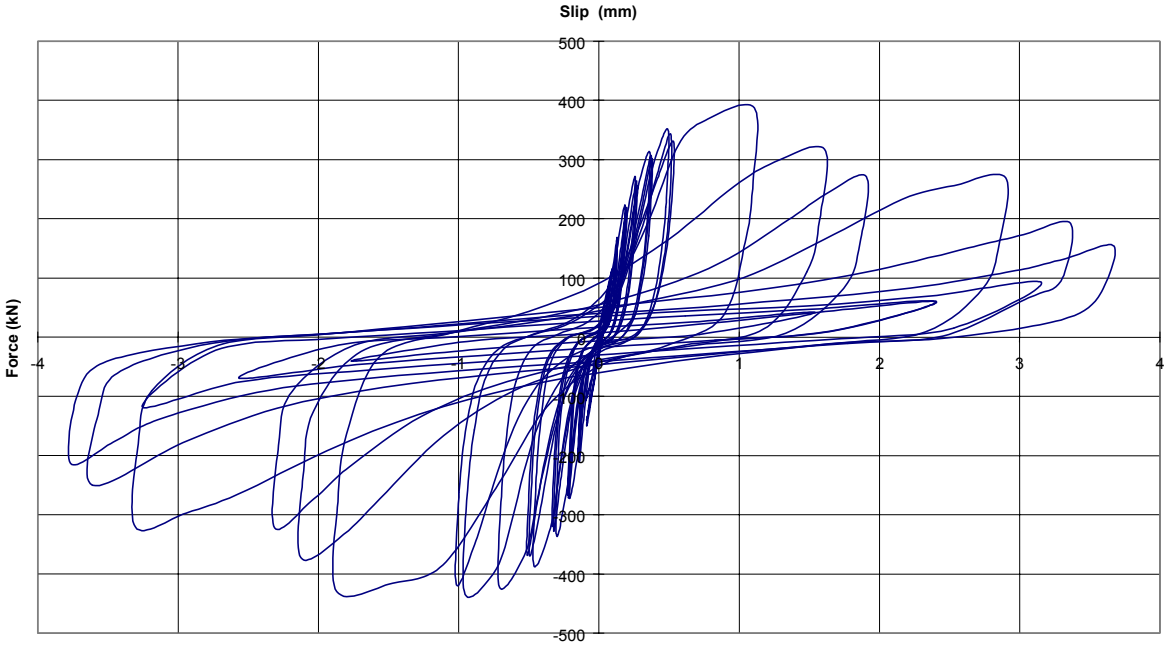

Figure 4.36: Force - slip diagram for HSW-7

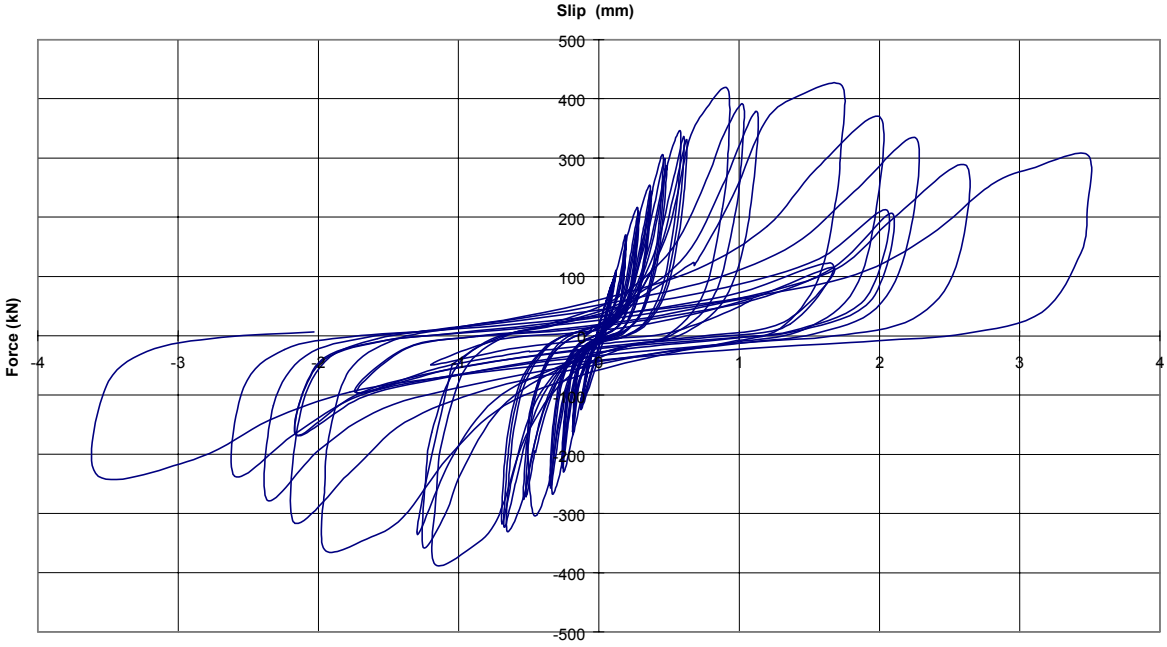

Figure 4.37: Force - Slip diagram for HSW-8

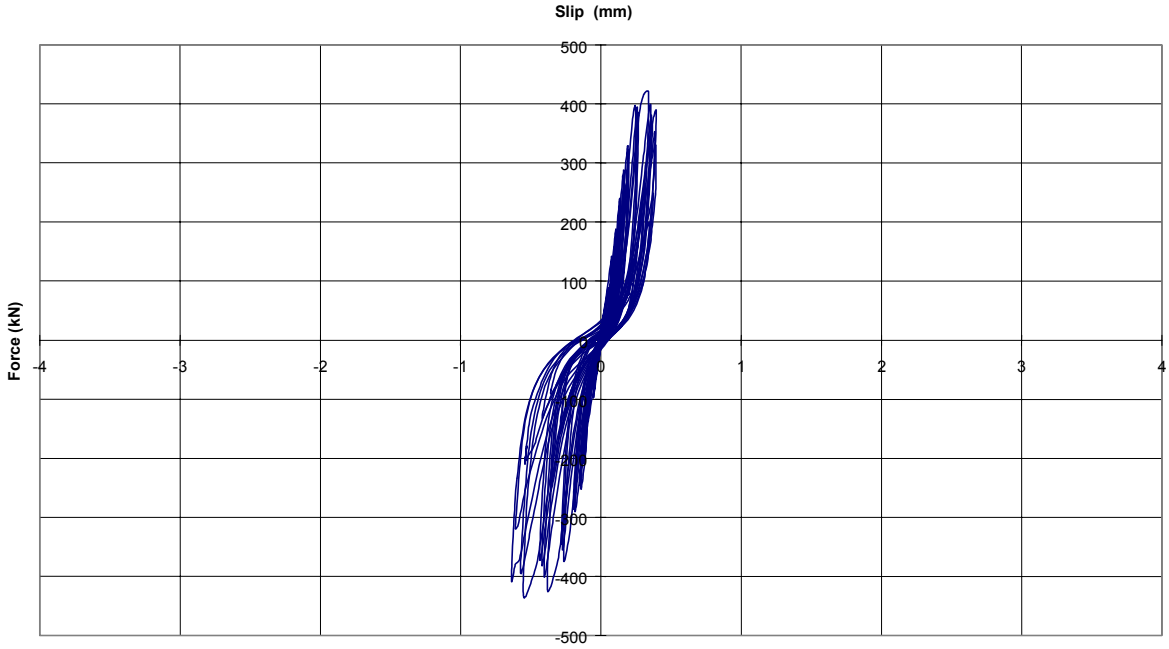

Figure 4.38: Force - Slip diagram for HSW-9

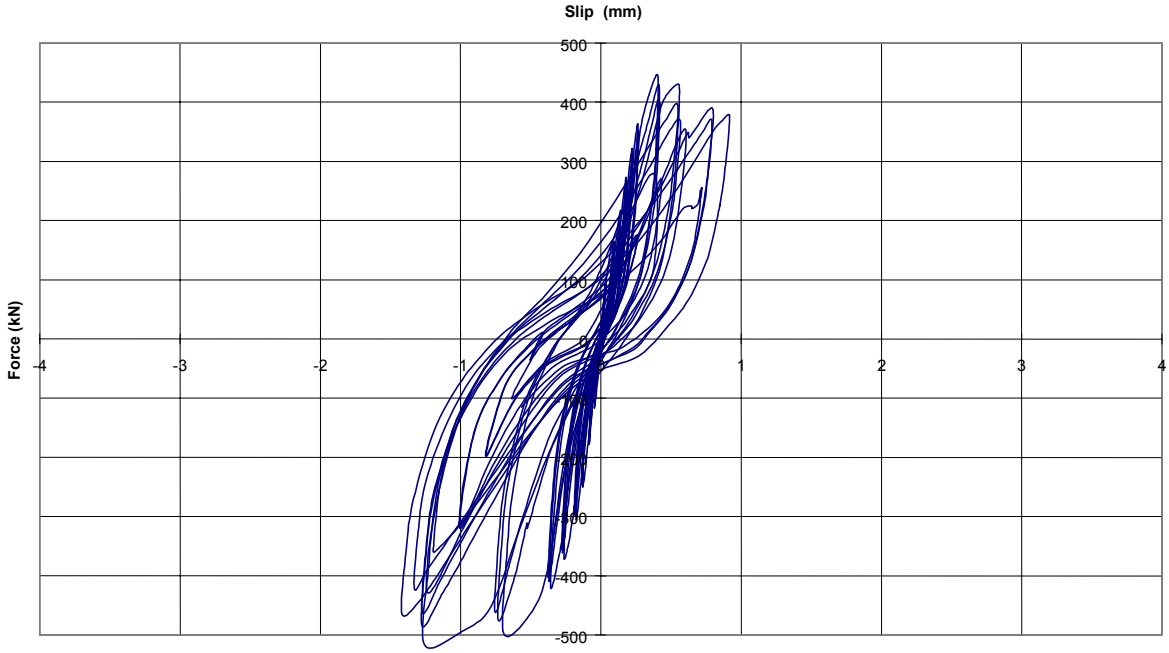

Figure 4.39: Force - Slip diagram for HSW-10

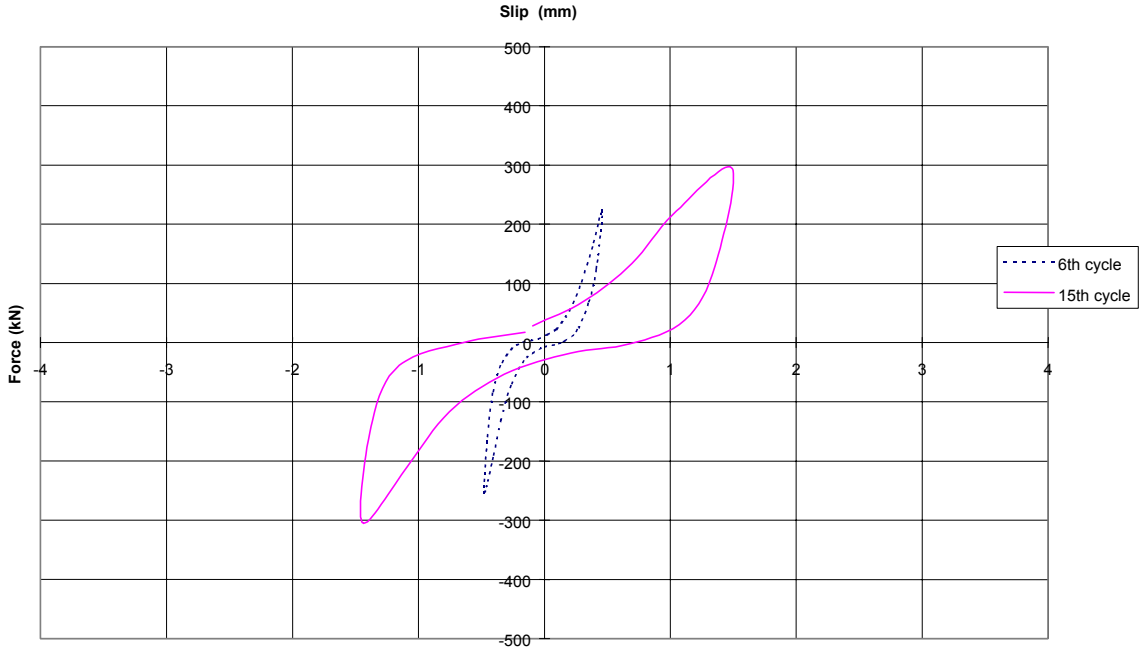

Figure 4.40: Force - slip diagrams for HSW-6 at different cycles

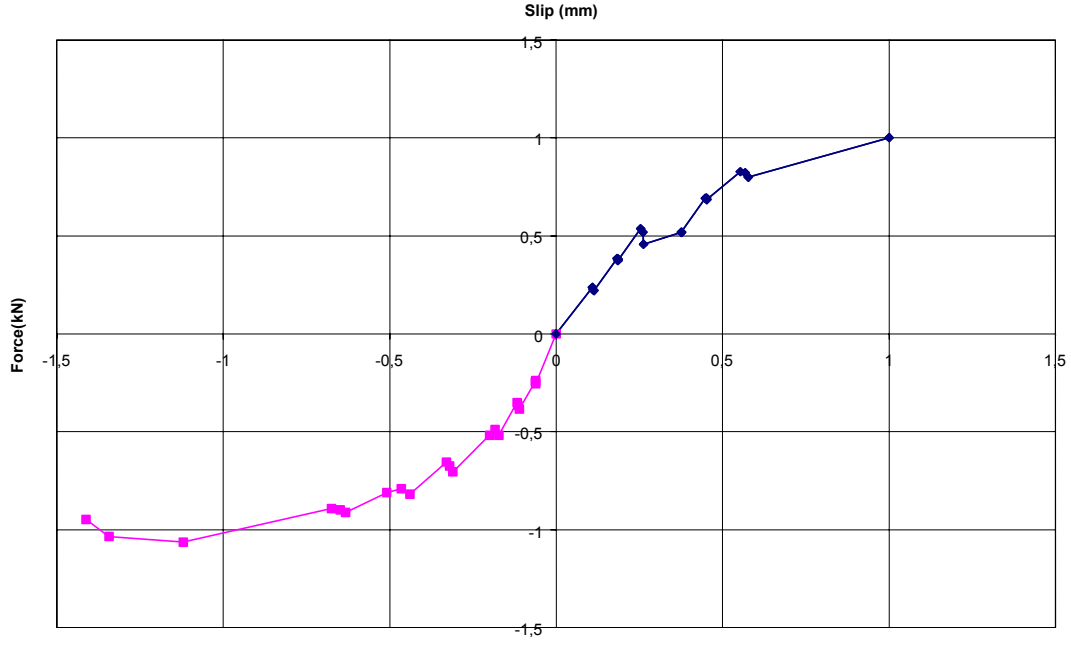

Figure 4.41: Normalized force - slip envelope for HSW6

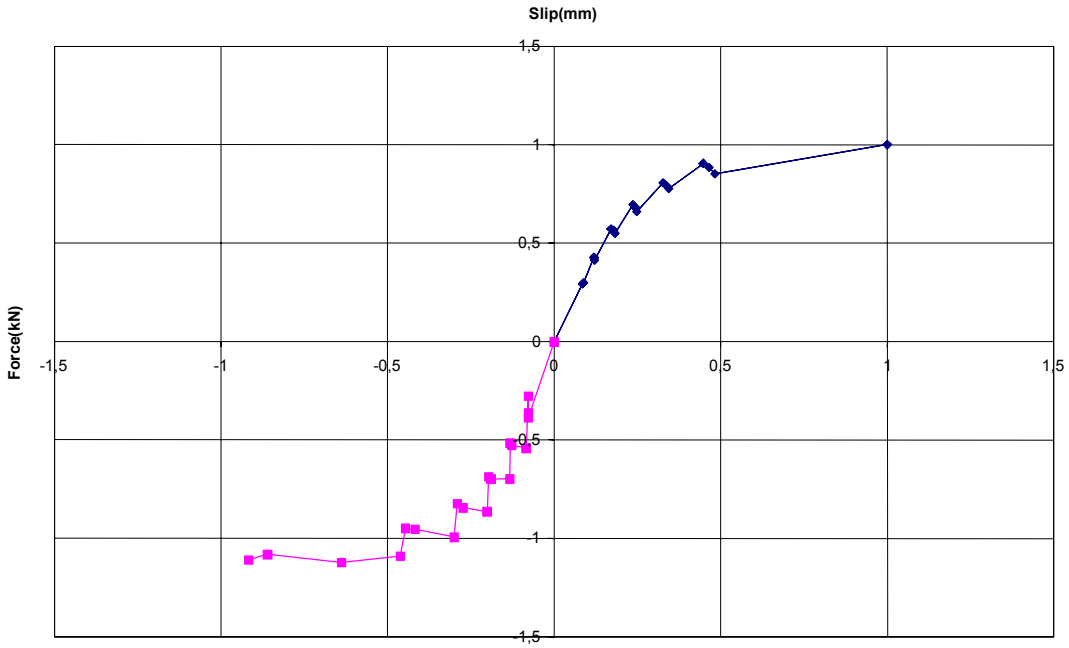

Figure 4.42: Normalized force - slip envelope for HSW7

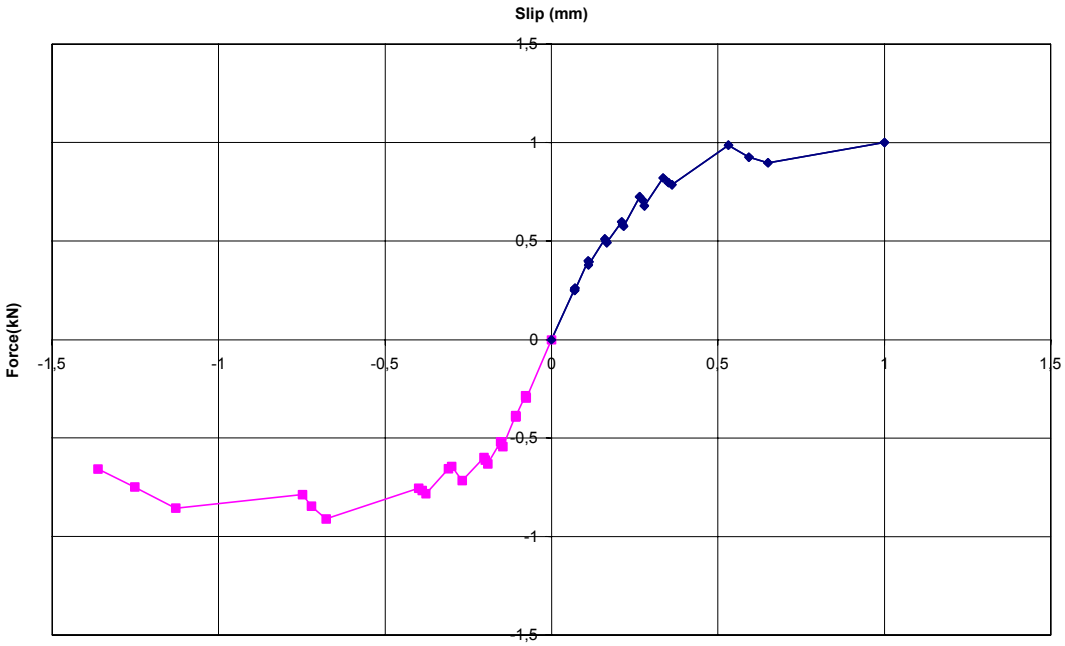

Figure 4.43: Normalized force - slip envelope for HSW8

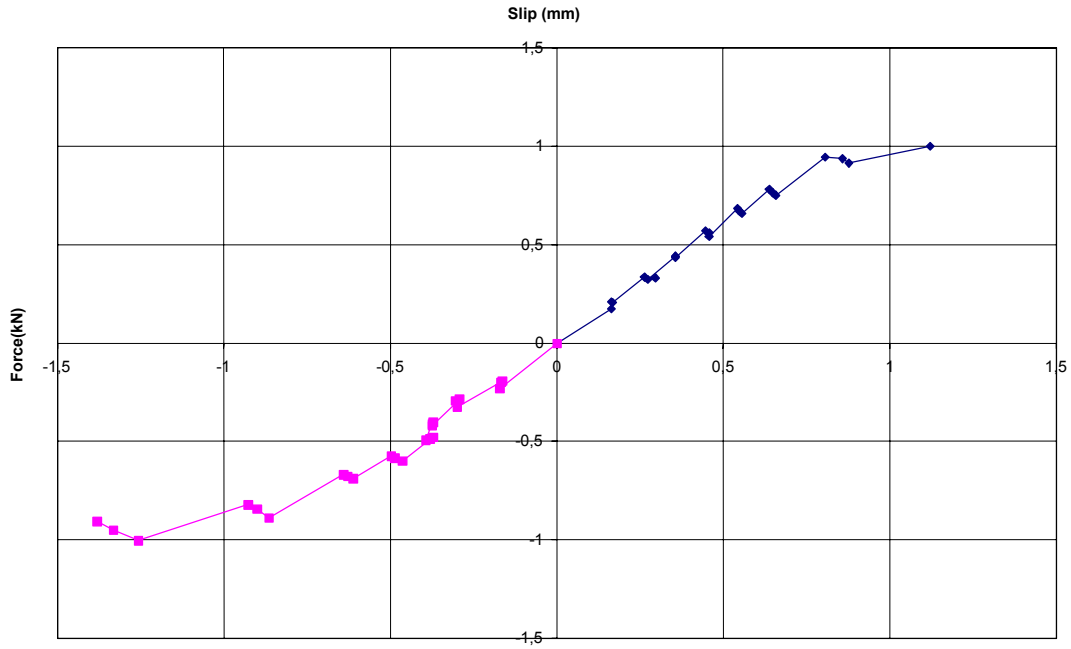

Figure 4.44: Normalized force - slip envelope for HSW9

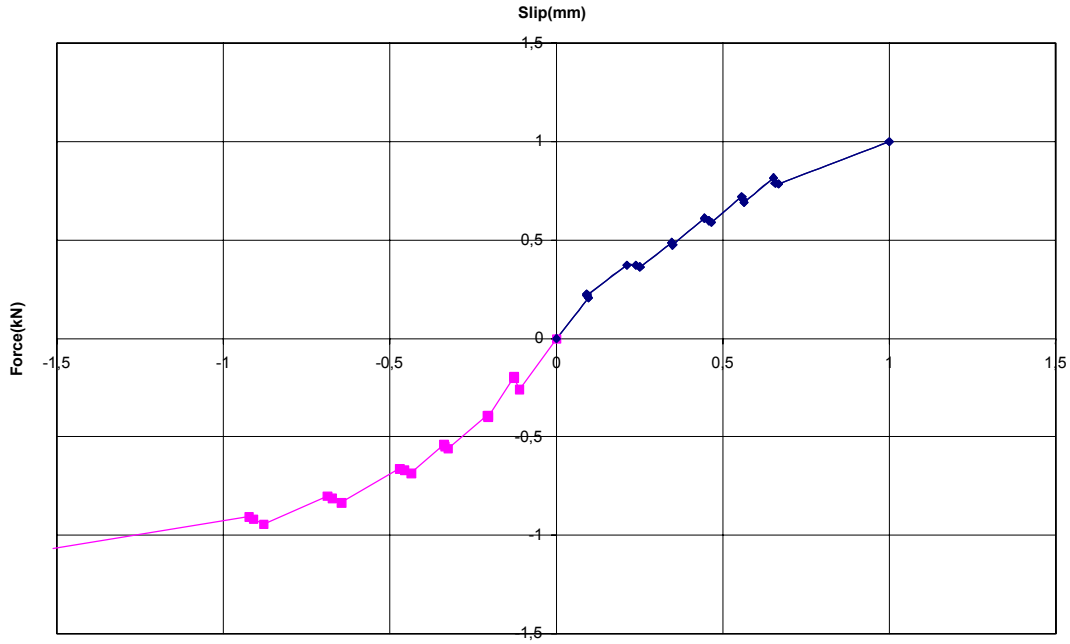

Figure 4.45: Normalized force - slip envelope for HSW10

5 TEST EVALUATION AND CHARACTERIZATION OF CYCLIC FORCE – SLIP RELATION

5.1 General

In order to describe analytically the behavior of the hybrid shear wall with composite edge member columns, an understanding of the interface behavior between edge member and shear wall panel is essential. Hence, in the experimental studies a representative portion of the hybrid wall has been investigated under cyclic alternating, displacement controlled, shear loads acting parallel to the edge-member/wall interface. In principle, the experimental results provide guidance in developing numerical models which are capable to accurately predict the edge-member/wall interface behavior. These models are essential to describe the overall shear wall behavior under extreme seismic action not only for the type of wall investigated in this study, but also, in general, for walls with different edge-member and wall design configurations. In this chapter, empirical derived force-slip curves describing the interface behavior are derived from the available test results and are used to develop a force-slip relationship (describing the interface dowel action as a multi-linear spring) for the type of edge-member/wall design here investigated.

5.2 Idealized cyclic nonlinear Force–Slip Relationships

In principle, an idealized force-slip hysteresis is required for hybrid shear walls in order to perform an inelastic response analysis of the building subjected to earthquake ground motions. In order to develop a hysteresis model for a typical structural element (in this case the interface force-slip behavior under shear), information of the pertinent experimental behavior is required. Using the experimental results, typically, an envelope, or primary curve, can

be generated to describe the major hysteretic characteristics including the stiffness at various stages and the ultimate strength under cyclic behavior.

In this process, it is necessary to correlate the observed experimental behavior with the pertinent geometric layout and material properties of the actual design of the test model. The force - slip envelope curves for the specimens in the second series, with both straight and diagonal reinforcing bars at the interface connection, are shown in Figures 5.1 and 5.2, respectively.

Considering the overall behavior, the initial shear transfer causes typical shear and flexural cracks in the wall. Subsequently, under increasing loads, also cracking and crushing of the concrete in the interface region occurs as a result of the dowel action. As a result, under ultimate load, the shear force at the interface is transferred entirely by the reinforcing bars. In Section 2.3.4.3 an expression for the dowel force capacity, based on the shear friction theory, has been given. Experimental investigations [21,28,29,30] have shown that the interface resistance depends mainly on the bar size, bar yield strength, the concrete strength, concrete cover and spacing of the bars. For the concrete walls studied in this investigation, the variables considered in this study are bar size and arrangement of the reinforcement.

In order to develop a multi-linear force-slip relation at the interface connection, for use in the analytical model, the experimental force-displacement curves have been normalized to the reference values F_R (load) and S_R (slip). Normalization of the force-slip relationship describing basic response is done with the aim of having an-easy-to-handle interpolated curve (formula) for practical use. Having the key properties, namely; initial stiffness, K and maximum shear force capacity, F_{max} at IFC, the full shape of the mathematical model for force/slip relation up to the ultimate load is defined.

The reference load has been defined as $F_R = F_{max}$, with F_{max} being the calculated shear strength according to Eqs. 2.26 or 2.37 for, respectively, a straight-bar or diagonal-bar interface-reinforcing arrangement.

The reference slip S_R, is expressed as $S_R = F_{max} / K$, where K is the initial stiffness for the straight and diagonal-bar reinforcing arrangements, respectively, defined as:

$$K = \lambda(n_s d_s + n_{st} d_{st}) \quad 5.1$$

$$K = \lambda(n_d d_d / \sin \alpha) \quad 5.2$$

Where, λ in kN/m^2 , is defined as:

$$\lambda = E_S (E_C / E_S)^n \text{ and} \quad 5.3$$

$n_s d_s, n_d d_d, n_{st} d_{st}$ are the number and diameters of the straight or diagonal bars, or the shear studs, respectively, and α is the angle of inclination of diagonal bars with the edge member.

Using Eq. 5.3, the exponent n for every test specimen is determined by considering the experimental initial stiffness K and the pertinent reinforcing layout, together with the Young's moduli of steel and concrete. Averaging the values for n for the specimen with straight bars and the diagonal bars, resulted in values of n =2.2 and n = 1.85, respectively. The initial stiffness is, therefore, proportional to the reinforcing bar diameter, the stiffness of the steel and the interaction between the stiffness of two materials namely, the concrete and steel.

Using initial stiffness values K for determining S_R, the experimental force-slip curves are normalized to a

$\overline{F}$ - $\overline{S}$ relationship according to:

$\overline{F} = F / F_R$ and $\overline{S} = S / S_R$

The resulting curves of the normalization process for the specimen with straight-bar and diagonal-bar reinforcements, are shown in Figs. 5.3 and 5.4, respectively. These curves form the basis of the pertinent generalized force-slip envelope curve.

A possible generalized force - slip envelope curve for the connection interface, describing in effect the connection spring element for use in a numerical analysis, can be expressed by a tangent hyperbolic function, as follows:

$$\overline{F} = (\tanh \overline{S})/(1 + (a.\overline{S}^2)/(1 + \overline{S}^4)) \qquad 5.4$$

For a best fit with the test results, a value for the constant a, between zero and 0.3 is suggested in this equation.

The generalized curves based on Eq. 5.4 are shown for straight and diagonal reinforcement layouts in Figures 5.5 and 5.6, respectively, together with the pertinent normalized test data. By expressing the response at IFC in the form of nonlinear force/slip curves, the whole range of loading is covered up to the ultimate load.

For use as a mathematical model to define the shear-force/slip relationship of the connection element in the nonlinear finite element analysis of the hybrid shear-wall behavior, Eq. 5.4 can be approximated as a multi-linear model as shown in Figure 5.7 and 5.8 for the different reinforcing arrangements. These curves were used in the numerical studies presented in the next chapter.

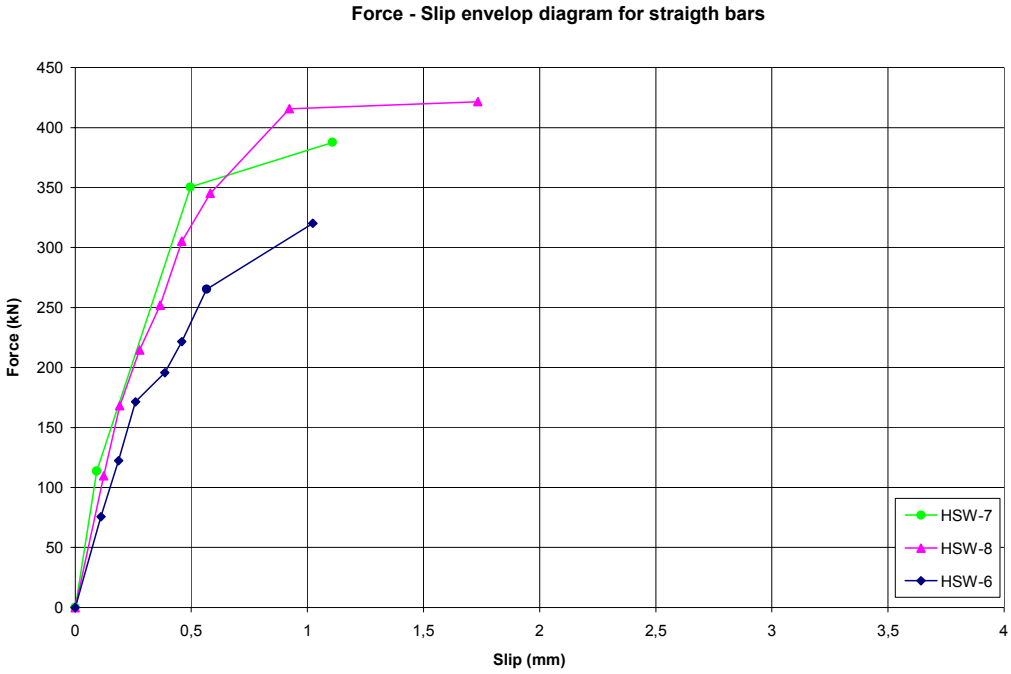

Figure 5.1: Force - slip envelope curve for specimen with straight bars at IFC

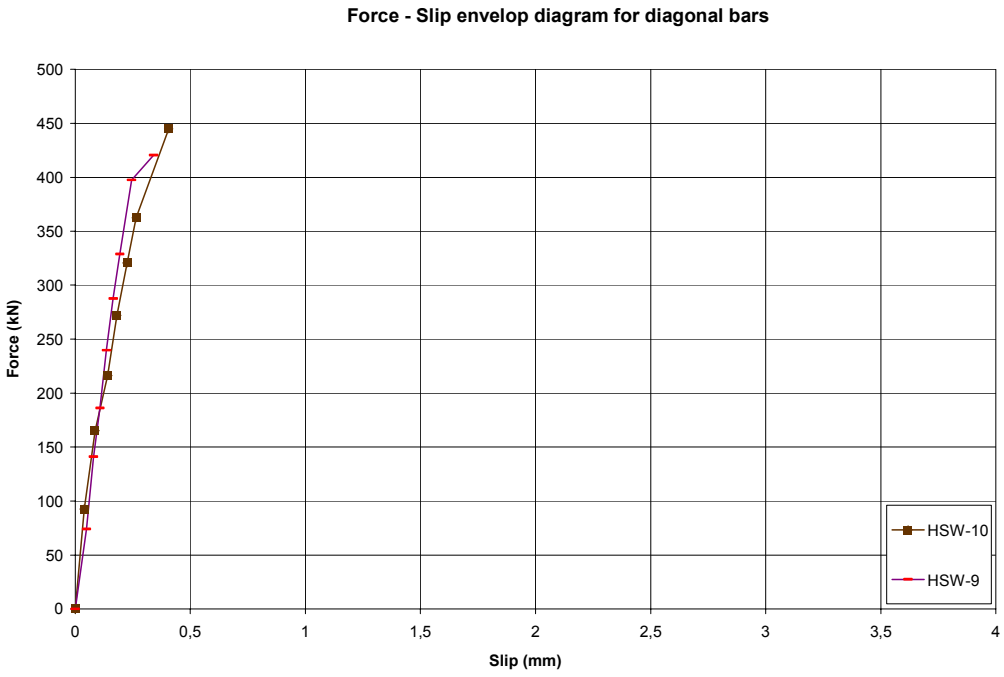

Figure 5.2: Force - slip envelope curve for specimen with diagonal bars at IFC

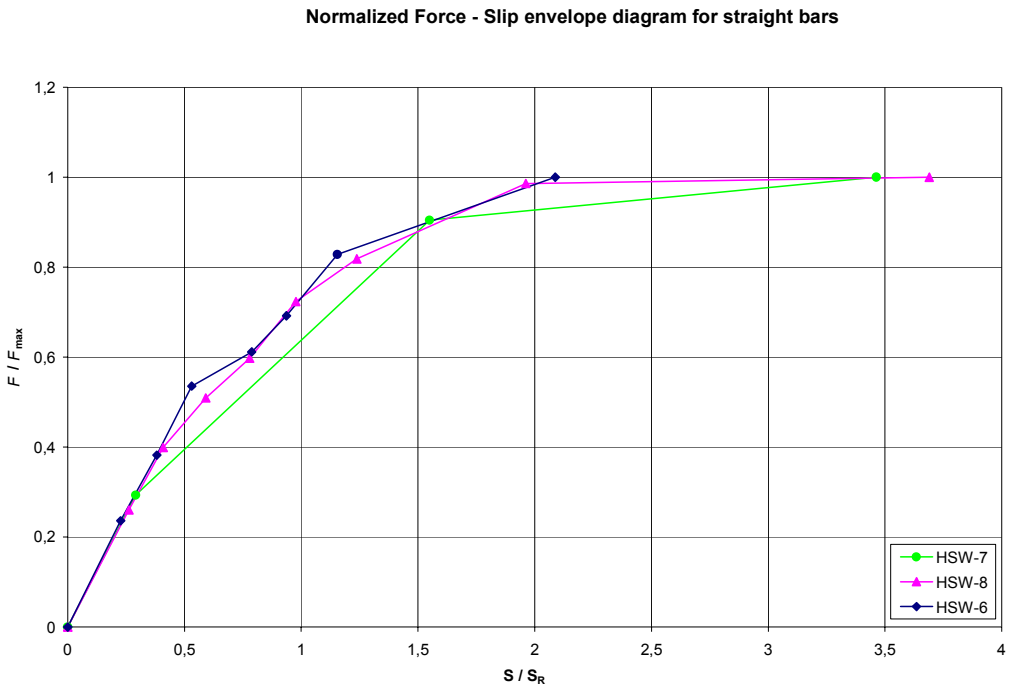

Figure 5.3: Normalized force - Slip envelope curve for straight bars

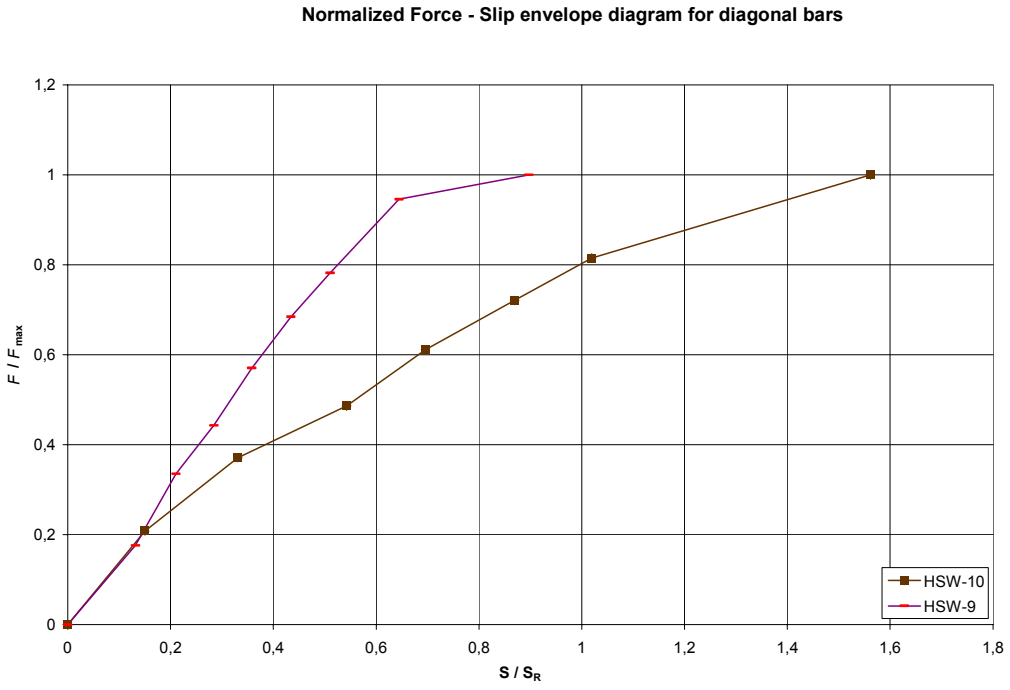

Figure 5.4: Normalized force - Slip envelope curve for diagonal bars

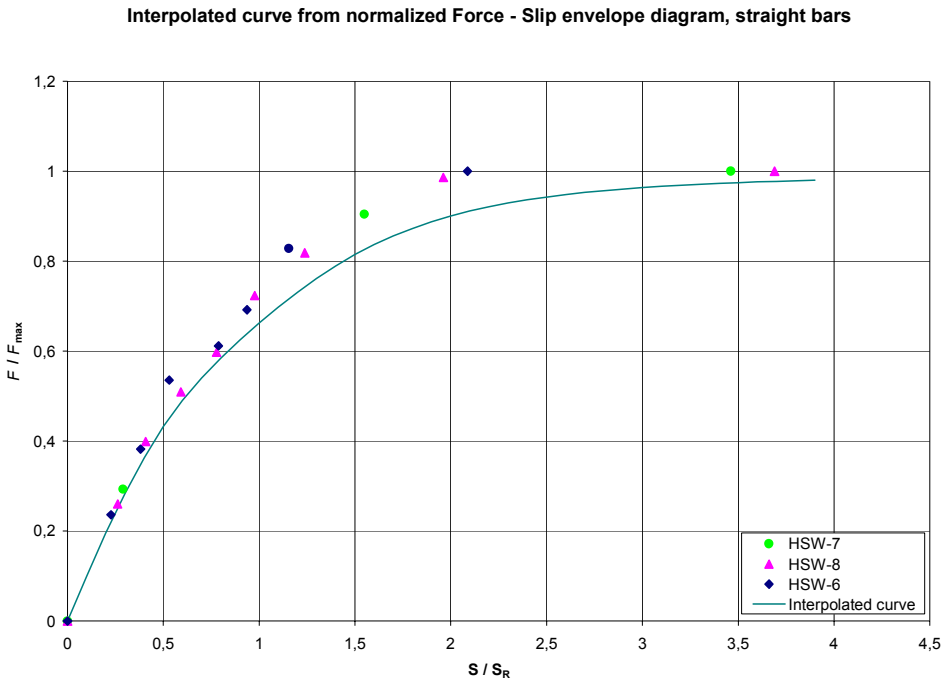

Figure 5.5: Interpolation curve based on Eq. 5.4

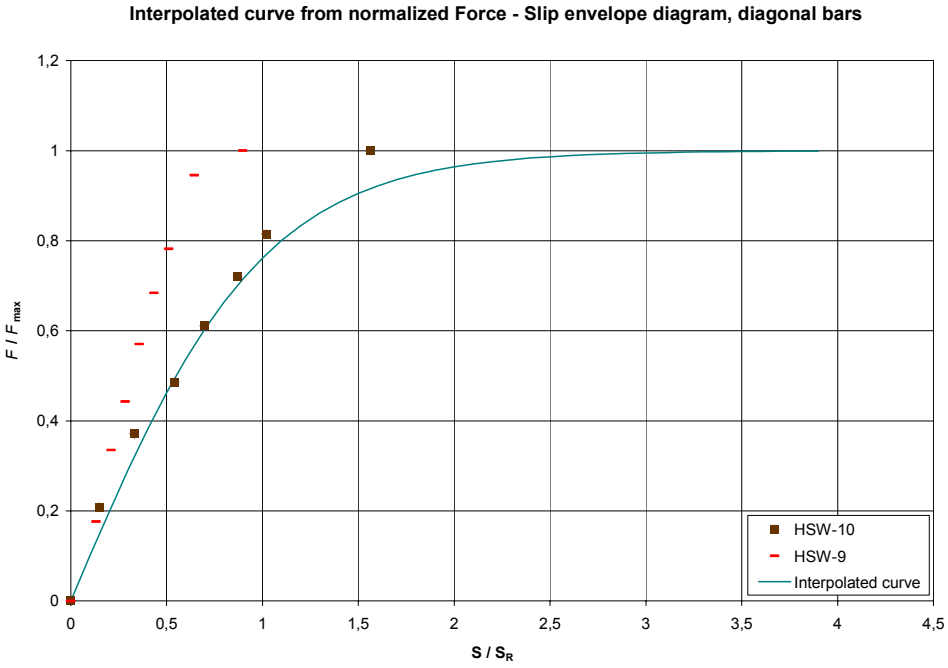

Figure 5.6: Interpolation curve based on Eq. 5.4

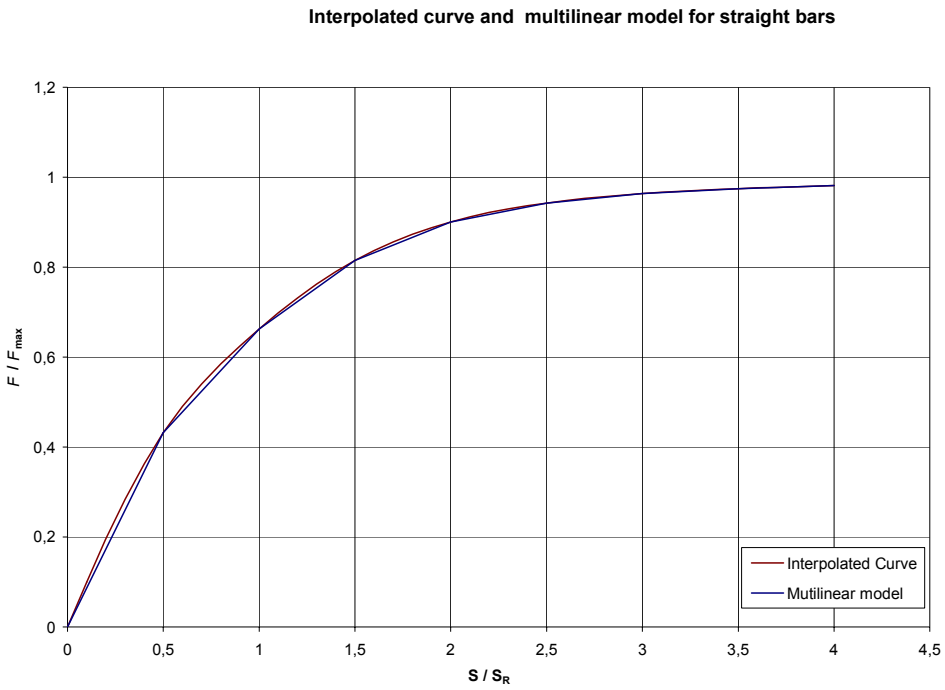

Figure 5.7: Interpolation curve and primary multilinear model for straight bars

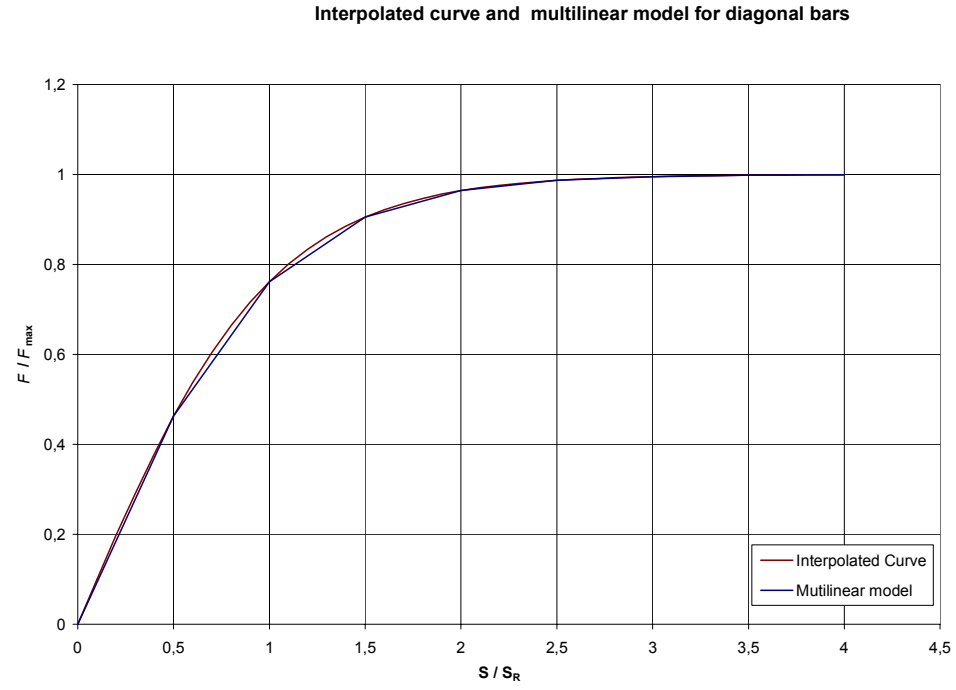

Figure 5.8: Interpolation curve and primary multilinear model for diagonal bars

6 ANALYTICAL MODEL OF TEST SPECIMENS

6.1 General

The accurate prediction of the behavior of the structure during earthquake excitation depends on the development of reliable analytical models of the critical regions. Analytical models for RC structures have generally been based on replacing the reinforced concrete composite continuum by an assembly of finite elements representing the concrete and the steel reinforcement. These models should be able to reflect the behavior of concrete in tension and compression, the response of the reinforcing bars and their interaction with the concrete. Hence, a realistic stress-strain relationship for both concrete and steel bars and a failure theory are required to obtain basic information through an analytical model of the structure.

Several approaches for defining the stress-strain behavior of the concrete under various stress states are available, namely, nonlinear elasticity, plasticity based model, plastic fracturing theory and endochronic theory of plasticity, etc [13,14]. However, by using the finite element method and performing a nonlinear analysis with appropriate constitutive relations, deformational and failure characteristics of reinforced concrete structures can be accurately predicted.

Basically, the nonlinear response is caused by two major material effects, cracking of the concrete and plasticity of the reinforcement and of the compression concrete. Other time–independent effects arise from the nonlinear action of the individual constituents of reinforced concrete, such as bond slip between steel and concrete, aggregate interlock of a cracked concrete and dowel action of reinforcing steel. The time–dependent effects such as creep, shrinkage, and temperature change also contribute to the nonlinear response. In this study, only the time-independent material nonlinearities (cracking and plasticity) will be considered in the nonlinear analysis of the specimens.

The implementation of nonlinear constitutive relations in finite element analysis codes is generally undertaken in one of two ways. In the first case the material behavior is programmed independently of the elements. Using this approach the choice of elements for a particular structural system is not limited and best practice modelling techniques can be used in identifying an appropriate element type to which any of the nonlinear material properties are assigned. This is the most adaptable approach and does not limit the analyst to specific element types in configuring the problem of interest. In spite of this, however, following the second approach, certain software developers provide specific nonlinear material capabilities only for dedicated element types. In order to achieve the analytical objective of this study, ANSYS 5.7 [2], a nonlinear three dimensional finite element computer program, was used to simulate the response of the test specimens. ANSYS provides a dedicated three-dimensional eight node solid isoparametric element, Solid65, to model the nonlinear response of brittle materials based on a constitutive model for the triaxial behaviour of concrete after Williams and Warnke [46]. This model makes no attempt to include the prediction of cyclic response because the model is intended for application to monotonic loading cases.

In the following sections, the basic failure criteria of concrete, material model for both concrete and steel and the analytical modelling of the hybrid shearwall test specimen using the ANSYS 5.7 computer program are described.

6.2 Failure Criteria of Concrete

Concrete is a nonlinear, inelastic and nonhomogeneous material with a very complex physical behavior, having a high compressive strength and low tensile strength. The load carrying capacity of concrete under multiaxial stress conditions is a function of the state of stress, and can be properly predicted by using an appropriate failure criteria. Most failure criteria are given as a hypothesis whose application to different materials should be evaluated from tests. Several failure criteria have been formulated for concrete under a general

stress state using various mathematical models with one to five parameters. Criteria such as yielding, initiation of cracking and ultimate load carrying capacity, etc. have been used in formulating the failure criteria. Simpler failure models, suitable for manual calculations, employ only one or two parameters. In computer applications failure models are mostly considering three, four or five parameters to define the failure criteria.

Considering a multi axial stress condition for an isotropic material, failure criteria can be expressed as an invariant function of the stress conditions (i.e., principle stresses σ_1, σ_2, σ_3,) as follows:

$$f(\sigma_1, \sigma_2, \sigma_3,) = 0 \qquad 6.1$$

Furthermore, one can replace this equation in terms of three principal stress invariants I_1, J_2, J_3 as

$$f(I_1, J_2, J_3,) = 0 \qquad 6.2$$

where, I_1 is the first invariant of the stress tensor σ_{ij} and J_2 , J_3 are the second and third invariants of the deviatoric stress tensor, s_{ij} .

In order to supply both a geometrical and physical interpretation of the failure, the Haigh-Westergaard stress space has been used to define the failure surface of concrete by either $f(\xi, r, \theta)$ or $f(\sigma_{oct}, \tau_{oct}, \theta)$. The general characteristics of the failure surface of the concrete are determined from tests and can best be described by its cross sectional shapes in deviatoric planes and its meridians in meridian planes. Type of failure in concrete can be classified into tensile and compressive failure, which is characterized by brittle and ductile behavior, respectively.

The Williams and Warnke three dimensional failure criteria which considers a five-parameter failure surface model for concrete in both tension and compression has been

used in this study. This model has a conical shape, as shown in Figure 6.1, with curved meridians (second order parabolas) and a noncircular deviatoric cross sections (with ellipsoids in each quadrants) as shown in Figures 6.2a and 6.2b, respectively.

The failure surface is defined as:

$$r_f(\sigma_m,\theta)=\frac{2r_c(r_c^2-r_t^2)\cos\theta+r_c(2r_t-r_c)\left[4\left(r_c^2-r_t^2\right)\cos^2\theta+5r_t^2-4r_tr_c\right]^{1/2}}{4\left(r_c^2-r_t^2\right)\cos^2\theta+\left(r_c-2r_t\right)^2} \qquad 6.3$$

where, r_t and r_c are, respectively, the tensile and compressive meridians expressed as:

$$r_t=a_0+a_1\frac{\sigma_m}{f_c}+a_2\left(\frac{\sigma_m}{f_c}\right)^2 \qquad 6.4$$

$$r_c=b_0+b_1\frac{\sigma_m}{f_c}+b_2\left(\frac{\sigma_m}{f_c}\right)^2 \qquad 6.5$$

The five parameters required to define the William-Warnke failure surface are:

The unaxial compresive strength (f_c)

The uniaxial tensile strength (f_t)

The biaxial compressive strength (f_{bc})

The high compressive stress point (f_1) on the compressive meridian

The high compressive stress point (f_2) on the tensile meridian

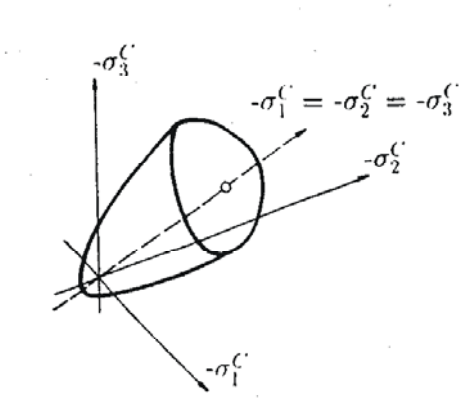

Figure 6.1: Failure surface in 3D stress space

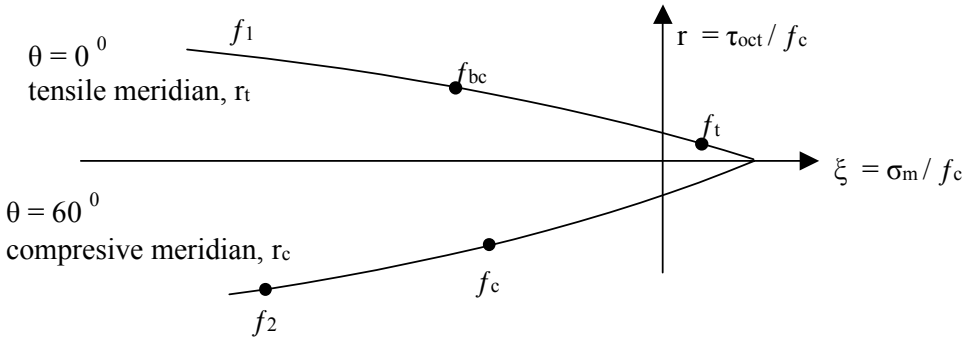

Figure 6.2a: Meridian plane

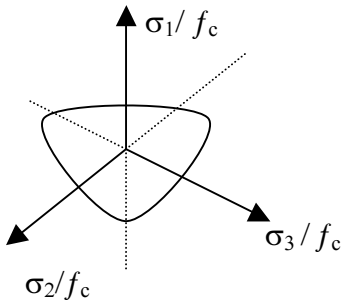

Figure 6.2b: Deviatoric plane

6.3 **Concrete Modelling**

Under loading, micro- and macrocracks occur in the concrete. The stress-strain behavior of concrete is affected by the development of these cracks. There are two main approaches for modelling the cracking of the concrete, namely, the discrete and smeared crack approach. The former one treats cracking by adapting the geometry of the structure and keeping the interior of the body linear elastic, whereas the second approach keeps the geometry fixed, and models the cracking process entirely via a constitutive law. In early studies the tension cut-off was used, assuming that after exceeding the tensile strength a complete loss of coherence occurred in the direction of the major principle stress. The performance of the smeard fixed-crack model has been improved with the introduction of tension stiffening, tension softening and degradation of shear capacity due to cracking. The fixed-crack model has been further developed to fixed multi crack and rotating crack models in order to account for the formation of cracks in other directions.

In ANSYS 5.7, the plasticity based model of concrete from Willam and Warnke has been used. The stress-strain behavior of concrete has been separated into a recoverable (elastic) and an irrecoverable (plastic) component. Each component is treated separately. The model accounts for both cracking and crushing, considering a smeared crack analogy for cracking and a plasticity algorithm to account for the possibility of concrete crushing. The tensile strength is assumed to be $0.65\sqrt{f_c}$ MPa, with f_c being the compressive strength in MPa. Since cracked concrete cannot transfer tensile stresses, the tensile strength drops suddenly after cracking. In the FE model, the actual compressive strength and modulus of elasticity of the concrete, as obtained from cube and cylinder tests, has been used. Each element has eight integration points at which cracking and crushing checks are performed. The element behaves in a linear elastic manner until either of the specified tensile or compressive strengths are exceeded. Cracking or crushing of an element is initiated once one of the element principal stresses, at an element integration point, exceeds the tensile or compressive strength of the concrete. Cracked or crushed regions are then formed perpendicular

to the relevant principal stress direction with stresses being redistributed locally. The element is thus non-linear and requires an iterative solver. In the numerical routines the formation of a crack is achieved by the modification of the stress-strain relationships of the element to introduce a plane of weakness in the requisite principal stress direction. The amount of shear transfer across a crack can be varied between full shear transfer and no shear transfer at a cracked section. The crushing algorithm follows a plasticity law in which, once the ultimate strength has been reached, any further application of load in that direction develops increasing strains at constant stress. After reaching the ultimate strain (ϵ_u) the concrete is assumed to loose its resistance completely. In case of cracking, following the formation of initial cracks, stresses tangential to the crack face may cause a second or third crack at the integration point. The concrete stress-strain relationship is represented by a parabolic curve up to the peak stress value (f_c), followed by a straight line in the softening zone as shown in Figure 6.3.

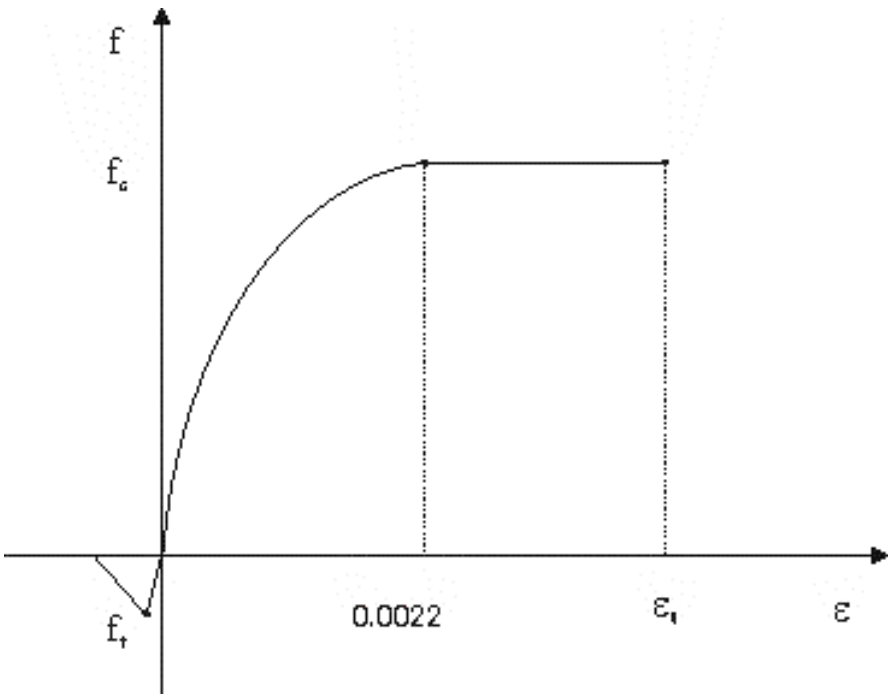

Figure 6.3: Concrete stress-strain model

6.4 **Steel Modelling**

As the reinforcing bars are long and relatively slender, they are generally assumed capable of transmitting axial forces only. Hence, a uni-axial stress-strain relationship has been adopted. The reinforcement bars may be incorporated in the finite element model according to either a discrete model (individual bars), or through a smeared model. In the discrete model, one dimensional elements carrying axial force are used. For the smeared model, the steel is assumed to be distributed over the concrete element with a particular orientation angle. In that case, a perfect bond between the concrete and reinforcing steel is assumed. The smeared modelling is more convenient from a user´s point of view, since only reinforcement ratio and steel properties of each direction need to be introduced. However, in ANSYS 5.7, the reinforcing bars can be modelled by either the smeared or discrete method. In either case, the bilinear kinematic hardening stress - strain relationship is used to simulate the behaviour of steel reinforcement. Actual material properties of the steel obtained from material tests are used in the modelling. The steel stress-strain model as shown in Figure 6.4 has been used with the following parameters:

E_e =210000 MN/m2, f_y = 500000 kN/m^2

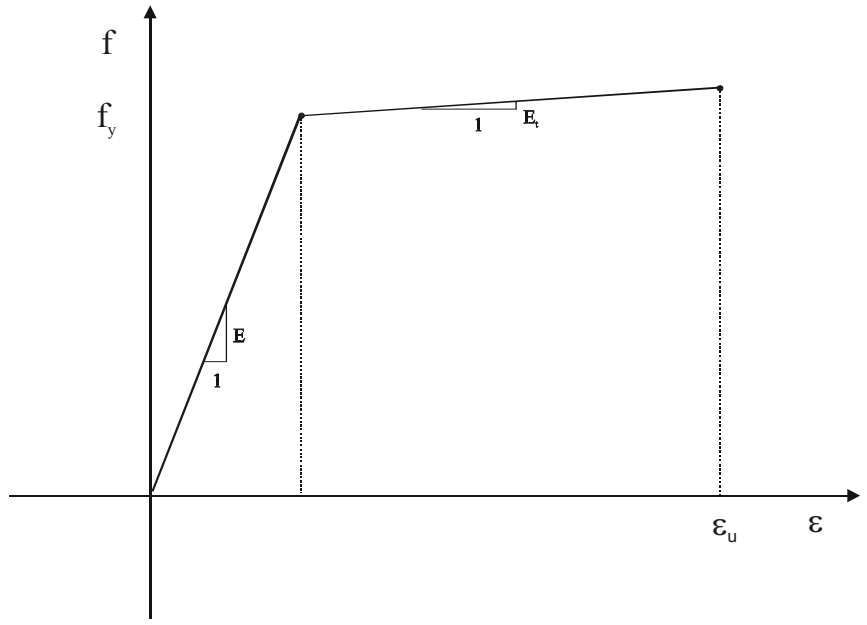

Figure 6.4: Steel stress-strain model

6.5 Geometrical modelling of test specimen

In order to perform a comparative analysis of the response of the test specimen a FE model reflecting the specimen geometry has to be developed. In principle, the concrete fixing beam and composite steel-tube edge column as well as the reinforced concrete shear wall panel can be modelled using standard ANSYS 8-noded solid elements with smeared or discrete reinforcing bars. Because of the complex force transfer (friction and dowel action) at the interface between wall panel and edge column, special consideration has been given in developing an appropriate model at the interface to capture the interface behaviour (slip).

One possibility considered has been directed to developing a spring element between wall panel and edge column. In this case, empirical (load versus slip) data have been used to describe such a spring for both the "straight" and "diagonal" interface reinforcement used in this study. Although such an approach can provide basically a good correlation between experimental and analytical results, its general validity is limited as it pertains to the specific layout tested in this investigation. Therefore, it was considered essential to develop a general model of the interface region which would be capable of capturing for any given reinforcing layout along the interface, the progressive failure and associated deformations along the interface under increasing loads. For this purpose a concrete truss model acting in conjunction with the reinforcing bars in the interface region has been developed. The correlative studies, presented in Chapter 7, clearly prove the general validity of the truss modelling procedure.

Generally, support points at the bottom of the fixing beam were restrained from translational and rotational movement in all directions. Full Newton-Raphson procedure with line search, predicator and automatic time stepping was used for the analysis. The frontal solver method was used to solve the simultaneous equations. A typical finite element mesh layout

of the wall specimen tested, without showing the interface reinforcement and connection design, is shown in figure 6.5.

6.6 Computer Model Formulation

The appropriate element layout and size (meshing) is an important aspect in finite element modelling to capture the behaviour of interest. However, a competent user must understand how elements behave in order to choose suitable types, sizes, and shapes of elements and where the mesh should be fine or coarse. It takes experience to find the "best" mesh. If the mesh is too fine, one might get singularities in the solution, stress concentrations where they should not appear, or the solver will take an extraordinarily long time to run. But if the mesh is too coarse, then the solution will not be accurate enough.

Three dimensional finite element models (FEM) representing the test specimen geometry were generated to analytically predict the response of the tested specimen under the pertinent load condition. In fact, four different models representing the two basic specimens with straight and diagonal reinforcing bars at the interface connection have been developed and analyzed.

In order to model the concrete in the wall panel, three dimensional eight-node elements, Solid65 of ANSYS, with three translational degrees of freedom at each node, were used. Considering the two-layered reinforcing mesh (mesh-size 100 mm) and wall-thickness of 90 mm, the element dimensions selected were 50x50x40 mm. The element mesh size of 50 mm reflects a mesh density of about 5% of the overall wall dimension. The mesh reinforcing bars, with only uniaxial stiffness, are assumed to be smeared throughout the element. The element is capable to capture both cracks due to tensile stresses (cracking in tension) and cracks due to excessive compressive stresses (crushing in compression). Cracking is modelled through an adjustment of the material properties which effectively treat the cracking as smeared cracks rather than discrete cracks.

The fixing beam, which was anchored to the test frame, had a far greater stiffness than the wall panel and was assumed to remain elastic during the tests. Therefore, the concrete and the reinforcement in the fixing beam was modelled with 3D-eight-node elastic elements, Solid45 of ANSYS, having three translational degrees of freedom at each node.

The reinforced concrete of the concrete-filled steel-tube composite edge member has been modelled with concrete Solid65 elements and discrete reinforcing bars, connected at the element nodal points. For modelling the steel tube, four-node shell elements, Shell43 of ANSYS, with six degrees of freedom at each node, were used.

In modelling the interface connection of the test specimen, with both straight and diagonal interface reinforcement, two different interface models have been used. In first instance, a model with non-linear springs, interconnecting the common interface nodal points of the wall panel and steel tube have been used. Specifically, a non-linear spring element, Combin39 of ANSYS, with 6 degrees of freedom was selected. The non-linear spring-characteristics for both types of specimen were taken from the empirically derived load-displacement curves measured at the interface between wall panel and edge member. In both cases the non-linear springs were modelled in a tri-linear fashion as shown in Figures 5.4-5.8. A basic layout of the test structure with selected computer elements is shown in Figure 6.6.

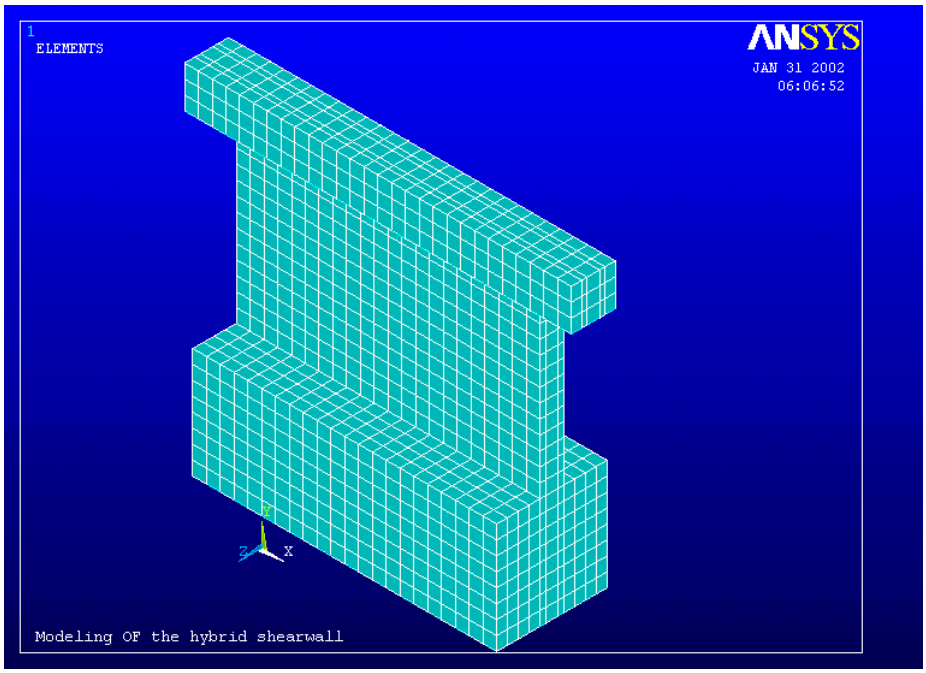

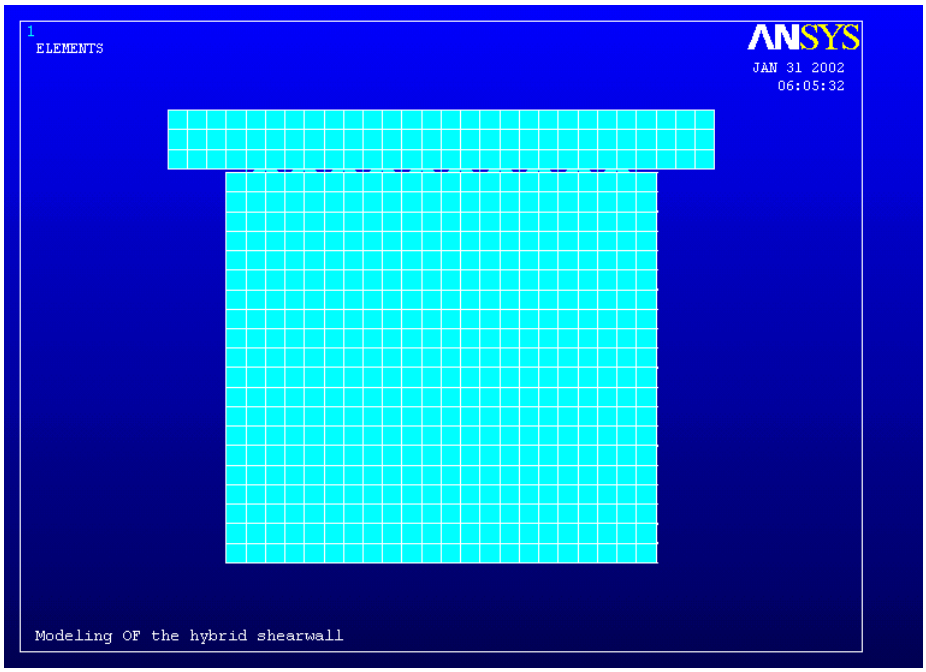

Figure 6.5: Finite element mesh layout

In second instance, a general applicable interface-truss model has been derived for comparison with the experimental test results. In that case the concrete in the entire test specimen, other than a 50 mm high zone just below the edge member, has been modelled with unreinforced concrete solid elements: Solid65 to capture the nonlinear concrete behavior of the wall panel and Solid45 for describing the linear behavior of the fixing beam. Reflecting the position of the reinforcing meshes over the thickness of the wall panel, the element thicknesses were 20 mm, 40 mm and 20 mm, respectively. The reinforcement has been modelled "externally" as discrete reinforcing bars using three-dimensional spar elements with plasticity, Link8 of ANSYS, embedded within the solid mesh. In the upper 50 mm interface connection region of the wall panel, directly adjacent to the composite edge column, a truss system was modelled with the typical reinforcing bars and diagonally arranged concrete compression- strutt elements. In general, the program considers full displacement compatibility between the reinforcement and the concrete (without bond slippage). The truss-model layouts for both the straight and diagonal reinforcing layouts are shown in Figure 6.7.

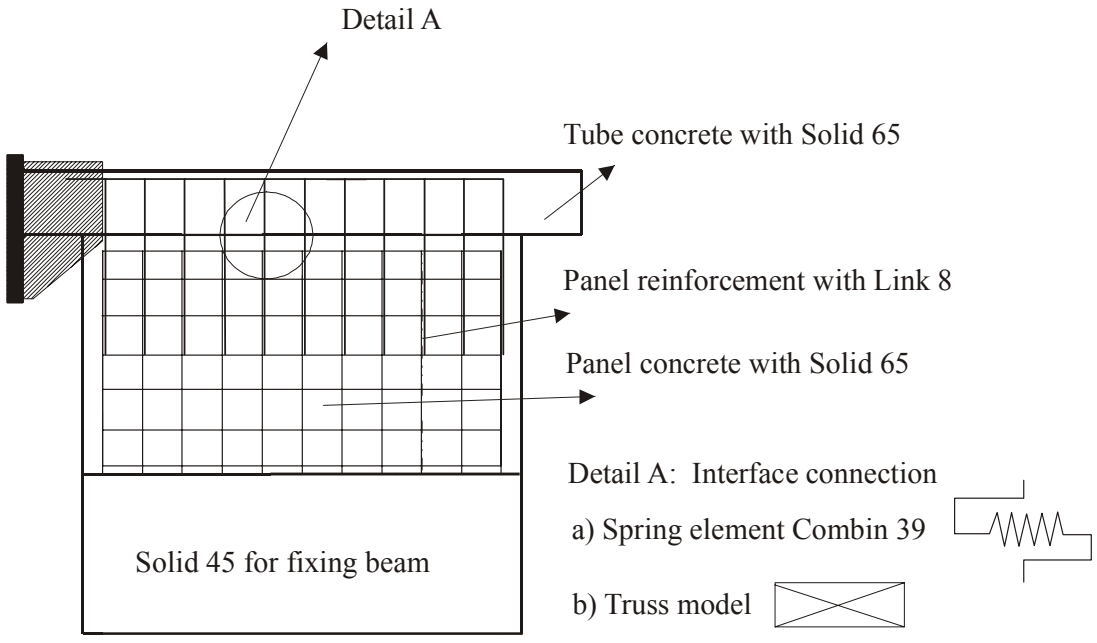

Figure 6.6: A basic layout of the test structure with selected computer elements

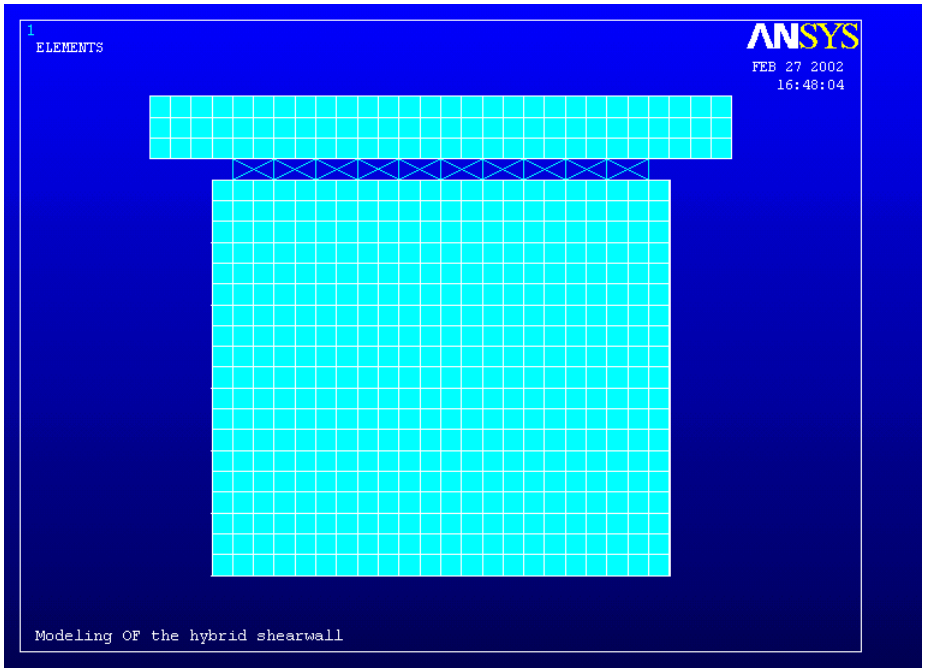

Figure 6.7: A truss-model layout for the straight reinforcing bar

6.7 **Analytical Studies**

In order to check the accuracy of the analytical models through comparison with the test results, computer models for both straight (vertical) and diagonal reinforcement in the wall-to-edge member interface region were developed as discussed in the previous section. In the analyses both types of specimen were analyzed without and with a rigid side support of the wall panel at a level 30 cm above the fixing beam. Hence, a comparison of the following test cases, as presented in Chapter 7, will be possible:

Interface type	Without side support	With side support
Specimen with vertical interface reinforcement	HSW 1	HSW 6
Specimen with diagonal interface reinforcement	HSW 2	HSW 9

In the analyses the model was subjected to controlled displacements introduced to the edge member at the interface-connection level. The analytical results are presented in Chapter 7 in direct comparison with the pertinent experimental load-displacement records.

7 COMPARISON OF ANALYTICAL AND EXPERIMENTAL RESULTS

7.1 General

In this chapter, the analytically predicted response of the hybrid shear wall specimens are compared with the experimental test results. Specifically, the analytically derived force-displacement response at the interface level is compared with the experimentally determined cyclic peak load-values for successively increased displacement levels. Also, the reduced load values due to cyclic deterioration under three repeated displacement levels are considered in this comparative assessment. The correlative studies allow an evaluation of the accuracy of the two different model concepts for the interface region presented in the previous chapter.

7.2 Interface Force – Displacement Behavior

Considering the importance of capturing the interface behavior analytically, a comparison of the numerically derived load displacement behavior under monotonic loading will be compared with the experimental cyclic results. Such a comparison will give a basic evaluation of the accuracy of the analytical model and procedures developed in this study. The development of a cyclic nonlinear computer program, capable of capturing the cyclic deterioration of the wall panel, particularly in the interface region between wall panel and edge-member, was considered outside the scope of this investigation.

For the two specimen without side supports of the wall panel, the analytical force – displacement behavior is shown in Figures 7.1 and 7.2. Specifically, these figures show, respectively, for the specimen with vertical and diagonal interface reinforcement, the mono-

tonic, step-wise increased, displacement-controlled lateral force, acting at the interface level, versus the lateral displacement of the wall at that same level. In both figures the results, using an interface-spring model as well as an interface-truss model at the „interface connection“ (IFC), are being presented. For comparison, these figures also show the experimental results covering not only the first positive cyclic peak-load values at the predetermined displacement levels but also the loads observed after subjecting the specimen to two more successive displacements of the same magnitude. In fact, the experimental results present the positive loading branch of the envelope of the cyclic alternating hysteretic load-displacement curves.

Comparing the numerical results with the experimental data, the analytical results indicate that the finite element analyses are capable of predicting the experimental behavior of the tested specimen when these had been subjected to a monotonic, displacement controlled horizontal load. In that case the cyclic deterioration would not have occurred and a more “elevated” experimental “curve”, in close agreement with the analytical results, would have resulted. It is particularly important to note that the generally applicable “truss”- type model would indeed have shown an excellent agreement with an experimental “monotonic” curve (disregarding the cyclic load deterioration at each displacement level). This gives ground to use this modelling technique with confidence, also in case of other reinforcing configurations. That also the empirically derived interface “spring model” shows good agreement, is not surprising as it has been developed using the observed test results.

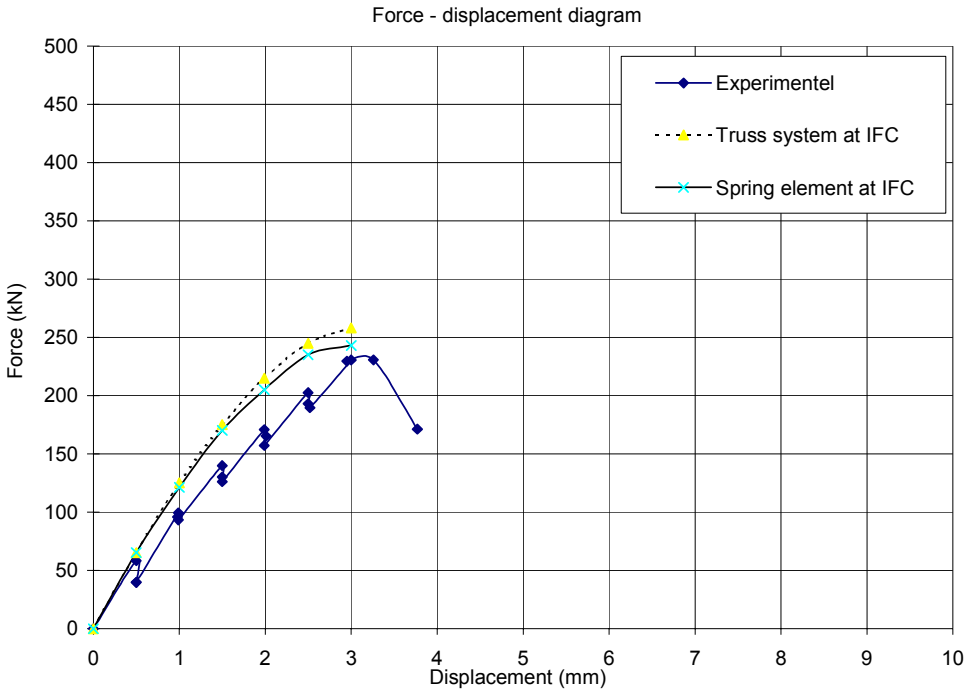

Figure 7.1: Force-displacement comparison for specimen HSW1

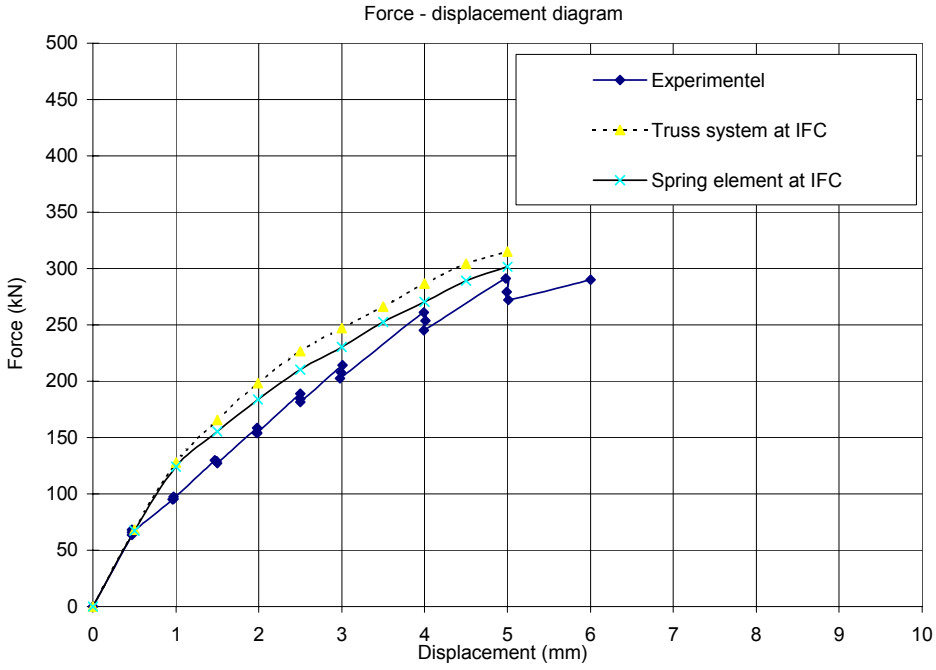

Figure 7.2: Force-displacement comparison for specimen HSW2

For the two specimen tested with side-supported walls, the analytical force – displacement behavior along the interface in comparison with the experimentally derived data for the straigt and diagonal interface bars is shown in Figures 7.3 and 7.4, respectively. The results are taken from the second series of tests, in which the test setup was altered to reduce the moment effect in the wall panel and study specifically the shear behaviour of the different interface connections. In agreement with the experimental setup, the analytical model had been formulated with the wall panel being side-supported over a length of 30 cm above the fixing beam (see Figure 3.11).

Figures 7.3 and 7.4 show, for the specimens with vertical and diagonal interface reinforcement, respectively, the monotonic, step-wise increased, displacement-controlled, lateral force, acting at the interface level, versus the corresponding lateral displacement of the wall at that same level. In both figures the results, using an interface-spring model as well as an interface truss model at the „interface connection“ (IFC), have been presented. For comparison, these figures also present the experimental results showing not only the positive cyclic peak-load values at the predetermined displacement levels but also the subsequent deteriorated loads observed after subjecting the specimen to two more successive displacements of the same magnitude. Considering the analytical and experimental results one can conclude that the numerical methods, as described in Chapter 6, are capable to capture the experimental response quite well. The basic difference between the results presented in Figures 7.3 and 7.4 is due to the deteriorating load effects resulting from the cyclically introduced displacement-controlled loads. Specifically, disregarding the deteriorating losses in load resistance and considering the experimentally derived envelope between the successive displacement steps, the “resulting” experimental curve agrees very well with the analytical results.

That the analytical models, developed for predicting the interface behavior between the edge-column and wall-panel, are indeed capable to successfully predict the load resistance under increasing displacements is also substantiated by the excellent coincidence of the

corresponding maximum loads and displacements at failure. In fact, the numerically derived maximum loads in the computer model are directly associated with the occurrence of a brittle failure (sudden crushing) of the concrete struts in the truss-like interface model. The predicted ultimate load values for the four different specimens discussed in this Chapter are 258 kN (HSW1), 315 kN (HSW2), 340 kN (HSW6) and 437 kN (HSW9), respectively. These values are within 10% of the ultimate test loads of 231 kN, 291 kN, 320 kN and 420 kN, respectively.

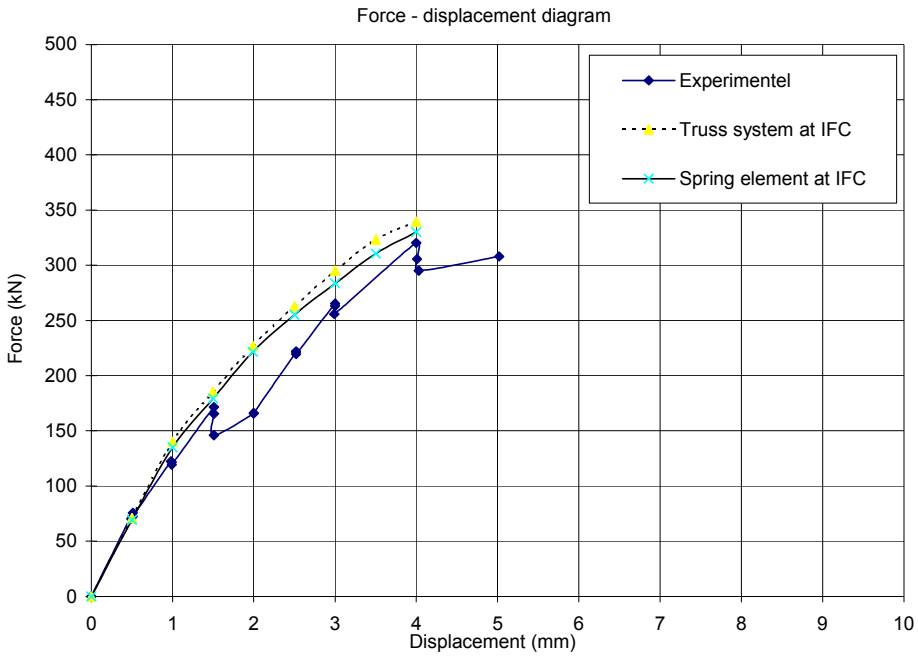

Figure 7.3: Force-displacement comparison for specimen HSW6

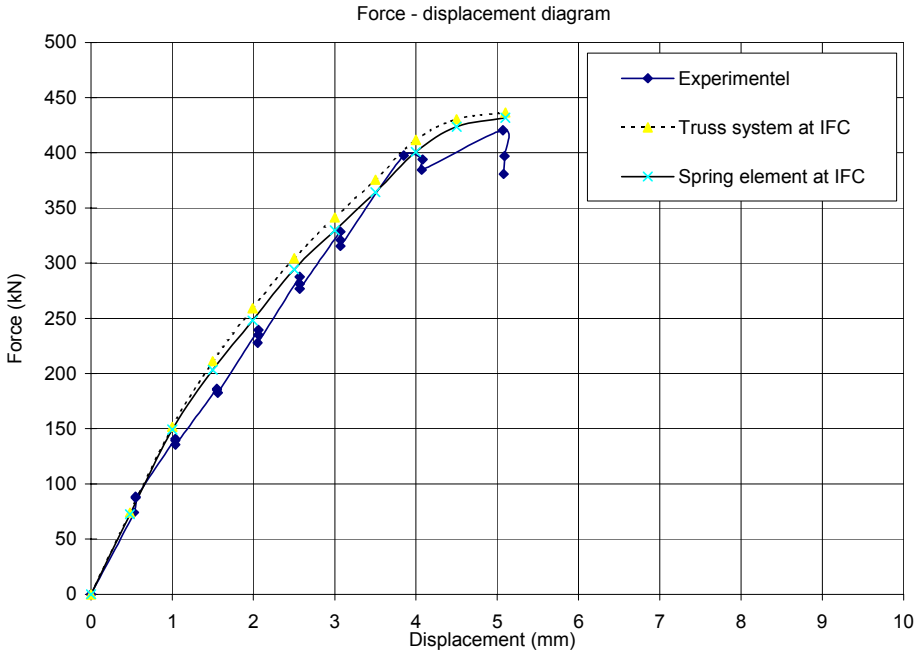

Figure 7.4: Force-displacement comparison for specimen HSW9

8 CONCLUSIONS AND RECOMMENDATIONS FOR FUTURE RESEARCH

Based on a series of alternating, displacement-controlled load tests on ten one-third scale models, to study the behavior of the interface of a hybrid shear wall system and earlier studies on moment resistant connections with hybrid columns by Bouwkamp et al [12], it can be concluded that the concept of hybrid construction in earthquake prone regions is feasible. The hybrid shear-wall system consists of typical reinforced concrete shearwalls with composite edge members or flanges. The edge members, which are formed by composite hollow steel square column sections with infilled concrete and reinforcing bars connected to typical shear wall reinforcing steel, are prefabricated with reinforcing bars extending through the wall of the column for connection to the shear wall reinforcing steel. The remainder of the building is constructed like a typical reinforced concrete structure.

In this study, ten different anchorage bar arrangements to evaluate the column-shearwall interface behaviour under cyclic shear forces acting along the interface between column and wall panel have been developed. Five test specimens had straight (horizontal) column anchorage bars and four specimen had diagonally oriented anchorage bars passing through holes in the tube wall. A tenth specimen had horizontal anchorage bars welded to the wall of the tubular column. In all cases the column reinforcing bars were connected to the wall reinforcement through overlapping.

Results showed that the diagonally arranged bars at the column-wall interface, performed better under cyclically induced alternating interface shear-loads than the interface connections with horizontal anchorage bars. In the latter case dowel action of the bars at the direct interface causes significant slip between column and wall. In fact, an alternative design with horizontal anchorage bars welded to the column wall exhibited the least slip between edge member and wall. For developing a rather stiff integrated behavior of the hybrid shear wall with the edge column member, either diagonally arranged anchor bars extending from

the column or welded horizontal stirrups to be connected (lapped) to the shear wall reinforcement are recommended. However, in case a softer interface connection between edge column and shear wall should be desired, a design using straight bars, extending through the wall of the edge member column and connected (lapped) to the wall reinforcement may be considered.

Finite element models of the test specimens, using available ANSYS Solid 8-noded elements capable to capture the integrated concrete and reinforcing steel behavior in the wall panels have been developed. Special models have been developed to capture the interface behavior between edge column and shear wall. Specifically, using the experimental test results, a spring element idealizing the force-displacement relationship at the interface, has been introduced. Also, a more generally applicable truss-like model capable of capturing the interface behavior between edge column and wall has been developed. In this model concrete struts in combination with the horizontal and vertical reinforcement in the wall near the edge column allow a general description of the composite behavior in the wall interface region. A comparison between experimental and numerical results show an excellent agreement and clearly support the validity of the truss model developed in this study for predicting the non-linear response of the hybrid wall system under earthquake load conditions.

With the numerical model capability developed in this study, it is possible to predict the seismic response of hybrid shear walls. Depending on the design of the edge columns and the reinforcing layout in the interface regions between edge columns and shear wall over the height of the building, it is possible to develop a highly efficient ductile wall system which permits optimizing the axial stiffness of the edge member columns and interface regions in order to increase the wall ductility and allow an increase of the q factor. Future studies may focus on this design optimization process and should be supplemented with full or medium-size model studies of entire hybrid shear walls or portions thereof.

REFERENCES

[1] ACI 318-89, 1989, Building code requirements for reinforced concrete, Detroit, Michigan: American Concrete Institute, USA.

[2] ANSYS, 2001, User's - Theory Manual for Revision 5.7, Swanson analysis system's Inc., USA.

[3] Architectural Institute of Japan, 1987, AIJ standard for structural calculation of steel reinforced concrete structures. Revised 1991.

[4] Ashadi H. W., 1997, A Hybrid Composite-Concrete Structure Earthquake Resistant System , Dissertation, Technische Universität Darmstadt.

[5] Bazant Z. P., 1976, Instability, Ductility and Size Effect in Strain Softening Concrete, Journal of Engineering Mechanics, ASCE, Vol. 102(2), pp. 331-344.

[6] Bazant Z. P., Belytschko T. B., Chang, T.-P., 1984, Continuum Theory for Strain Softening, Journal of Engineering Mechanics, ASCE, Vol. 110, pp. 1666-1692.

[7] Bazant Z. P., Prat P., 1988, Microplane model for brittle plastic materials. I: Theory, II: Verification, Journal of Engineering Mechanics, ASCE, Vol. 114, pp. 1672-1702.

[8] Belytschko T., Liu W. K., Moran B., 2000, Nonlinear Finite Elements for Continua and Structures, John Wiley & Sons, New York, USA.

[9] Bergmann R., 1981, Traglastberechnung von Verbundstützen, Mitteilung Nr. 81-2, Technisch-wissenschaftliche Mitteilungen Institut für Konstruktiven Ingeunieurbau Ruhr-Universität Bochum.

[10] Betten J., 1993, Kontinuumsmechanik, Springer-Verlag, Berlin.

[11] Boresi A. P., Chong K. P., 1987, Elasticity in Engineering Mechanics, Elsevier Science Publishers, England.

[12] Bouwkamp J.G., Ashadi H.W.,1992, A seismic hybrid composite structural frame system for buildings. International symposium on Earthquake disaster prevention, Mexico City, Mexico.

[13] Chen W. F., 1982, Plasticity in Reinforced Concrete, McGraw-Hill Book Company Inc., USA.

[14] Chen W.F. & Han,D.J., 1988, Plasticity for Structural Engineers, Springer-Verlag, New York Inc. USA.

[15] Comite International pour le development et etude de la construction tubulaire, 1970, Concrete filled hollow section steel columns, British edition, London.

[16] Darwin D., Pecknold D. A., 1976, Analysis of RC Shear Panels under Cyclic Loading, Journal of the Structural Devision, ASCE,Vol. 102, No. ST2, pp. 355-369,USA.

[17] European Committee for standardization, 1992, Eurocode-4,common unified rules for composite steel and concrete structures, ECSC-EEC-EAEC, Brussels:Luxembourg.

[18] European Committee for standardization, 2000, Draft No. 1, Eurocode-8, Design Structures for Earthquake resistance, Brussels.

[19] European Committee for standardization,1994, Design provision of earthquake resistance structures, Central European Norm.

[20] Fajfar Peter, Krawinkler Helmut, 1992, Nonliear Seismic Anylysis and Design of Reinforced Concrete Building, Elsevier Applied Science, London, England.

[21] Finite Element Analysis of Reinforced Concrete, 1982, State of the Art Report, American Soceity of Civil Engineers, New York, USA.

[221] Ghosh S. K.,1991, Earthquake-Resistant Concrete Structures, Inelastic Response and Design, American Concrete Institute, SP-127, USA.

[23] Hsu T. C. C., Mau S. T., 1992, Concrete Shear in Earthquake, Elsevier Science Publisher Ltd. England.

[24] Jacob Lubiner, 1990, Plasticity Theory. Macmillan Publishing Company, United States of America.

[25] Kahn A. S., Huang S.,1995, Continuum Theory of Plasticity, John Wiley & Son, New York, USA.

[26] Krätzig W. B., Niemann H. J., 1996, Dynamic of civil Engineering Structures, A.A. Balkema, Rotterdam, Netherlands.

[27] Lemaitre J., Chaboche J., 1990, Mechanics of Solid Materials, Cambridge University Press, Cambridge, Great Britain.

[28] Mattock Alan H., 1981, Cyclic Shear Transfer and Type of Interface, ASCE, Vol. 107, No. ST10, pp. 1945-1964.

[29] Mattock Alan H., Hawkin Neil M., 1972, Shear Transfer in Reinforced Concrete – Recent Research, PCI Journal.

[30] Meyer C., Okamura H., 1985, Finite Element Analysis of Reinforced Concrete Structure, Proceedings of Seminar - State of the Art Report, American Soceity of Civil Engineers, New York, USA.

[31] Meyer C., 1987, Finite Element Idealization for Linear Elastic Static and Dynamic Analysis of Structures in Engineering Practice, American Soceity of Civil Engineers, New York, USA.

[32] Ottosen N. S., 1977, A Failue Criterion for Concrete, Journal of Engineering Mechanics, ASCE, Vol. 103, pp. 527-535.

[33] Ozcebe G., Saatcioglu M., 1989, Hysteretic Shear Model for Reinforced Concrete Members, Journal of Structural Engineering, ASCE, Vol. 115, No. 1, pp. 132-147.

[34] Paulay, T., Bachmann H., Moser K., 1990, Erdbebenbemessung von Stahlbetonhochbauten, Birkhäuser Verlag, Basel:Switzerland.

[35] Paz Mario, 1991, Structural Dynamics, Theory and Computation, Van Nostrand Reinhold, New York, USA.

[36] Pradhan A. P., Bouwkamp J. G., 1992, Hybrid Shearwall, Proc. of 12th WCEE, Madrid, Spain

[37] Roik K., 1989, Experimentelle und theoretische Untersuchungen zum plastischen Verhalten von Verbundstützen bei großen Deformation, Stahlbau 58, H. 11, 1989, pp. 321-330.

[38] SAP2000, 1996, Analysis Reference Vol. 1 & 2, Computer and Structures Inc., Berkely, California, USA.

[39] Shirali N. M., 1989, Seismic shear strength of reinforced masonry piers, M. Sc.Thesis, Middle East Technical University, Ankara, Turkey.

[40] Shirali N. M., Bouwkamp J. G., 1998, Hybrid shearwall system – Shear strength at interface connection, Proc. of 11th European Conference on Earthquake Engineering, European Association of Earthquake Engineer, Paris: France.

[41] Srinivasan C.N., Behavior of concrete in-filled tubular columns, AICAP-CEB symposium , CEB, Bulletin d'Information, No. 131, Rome, Italy.

[42] Sucuoglu H., Shirali N. M., 1989, Seismic shear strength of reinforced masonry piers, Proc. of 8th European Conference on Earthquake Engineering, European Association of Earthquake Engineer, Moscow: Russia.

[43] Takeda T., Sozen M. A., Nielsen N. N., 1970, Reinforced concrete response to simulated earthquakes. Journal of Structural Division ASCE, Vol. 96, No. ST 12, Dec.:2557-2573.

[44] Uniform Building Code, 1994, Structural Engineering Design Provisions, International Conference of Building Officials, USA.

[45] Valenas J. M., Bertero V. V., Popov E. P., August 1979, Hysteretic behavior of reinforced concrete structural walls, Report No. UCB/EERC-79/20, University of California . Berkeley, California, USA.

[46] Willam K. J., Warnke E., 1974, Constitutive Model for Triaxial Behavior of Concrete, Proc. Concrete Structures Subjected to Triaxial Stresses, International Association for Bridge and Structural Engineers, Section III, pp. 1-30, Bergamo, Italy.

[47] Wight J. K., 1985, Earthquake Effects on Reinforced Concrete Structures, U.S. – Japan research, American Concrete Institute, SP-84, USA.

LEBENSLAUF

Zur Person: N. Mohammad Shirali

Geboren in Bander-e-turkman, Iran

Familienstand: ledig

Staatsangehörigkeit: Iran

Studium und berufliche Tätigkeit**:**

1979 - 1985 : Ingenieursstudium an der Middle East Technical University in Ankara mit Abschluss des „Bachelors of Science in Civil Engineering“.

1985 - 1986 : Tätigkeit im Ingenieurbüro Enka in Ankara als Statiker.

1986 - 1989 : Ingenieursstudium an der Middle East Technical University in Ankara mit Abschluß des „Master of Science in Civil Engineering”.

1990 – 1997 : Wissenschaftlicher Mitarbeiter bei Prof. Ir. J. G. Bouwkamp im Institut für Stahlbau und Werkstoffmechanik der TU Darmstadt.

1992 - 1997 : Freier Mitarbeiter (als Statiker) im Ingenieurbüro Bouwkamp, Fehling und Partner, Landskronstraße 31, 64285 Darmstadt.

1998 - 2002 : Wissenschaftlicher Mitarbeiter bei Prof. Dr. J. Lange, Institut für Stahlbau und Werkstoffmechanik der TU Darmstadt.

Seit 2002 : PWW, Ingenieurbüro für Bauwesen, Ingelheimerstraße 3 64295 Darmstadt